Lake Lisan and the Dead Sea: Their Level Changes and the Geomorphology of their Terraces

Dissertation
zur Erlangungen des Gerades eines
Doktors der Naturwissenschaften
(Dr. rer. nat.)
am Fachbereich Material- und Geowissenschaften
der Technischen Universität Darmstadt (D17)

Vorgelegt von
M.Sc. Shahrazad Abu Ghazleh
aus Amman (Jordanien)

Darmstadt
2011

Eingereicht am: **13.12.2010**
Tag der mündlichen Prüfung: **9.02.2011**

Gutachter: Prof. Dr. Stephan Kempe
Gutachter: Prof. Dr. Andreas Hoppe
Co-Supervisor: Prof. Dr. Abdulkader Abed

To my parents

To my husband

To my daughter Sanabil

Contents

ACKNOWLEDGEMENTS

First of all, I would like to extend my deepest gratitude to my supervisor Prof. Dr. Stephan Kempe for his invaluable guidance, contributive suggestions and careful corrections that contributed significantly to the success of this study. He guided me in the fieldwork and introduced me to structural and stratigraphy geology. The thesis has also benefited from his professional experience and knowledge in the limnogeology and paleoclimtology. I am deeply indebted to him for all his help, encouragement and exceptional support during the whole time of my study.

I would like also to express my sincere thanks to my co-supervisor Prof. Dr. Abdulkader M. Abed (The University of Jordan, Amman) for his help and support during the field work in Jordan, for introducing me to Quaternary deposits in the Lisan Peninsula and Jordan Valley and particularly to the Lisan and Damya Formations, and for providing me with geological maps and other available facilities in the University of Jordan.

Many thanks go also to Prof. Dr. Ahmad Al-Malabeh (Hashemite University, Al-Zarqa') and PD Dr. Hans-Peter Harres (TU Darmstadt) who helped supervising the PhD work; Dr. Mohammad Nawasrah (NRA, Jordan) and Dr. Horst-Volker Henschel (Darmstadt) for field work support and useful discussions; Prof. Dr. Jens Hartmann and Dr. Nils Mossdorf (neè Jansen) from the University of Hamburg for their help with evaluating SRTM Data; Prof. Dr. Jozef Kazmierczak (Polish Academy of Science, Warsaw) for help with interpretation of stromatolite thin-sections; Dr. Markus Fuchs (Bayreuth) for OSL dating; Prof. Dr. Anton Eisenhauer (GEOMAR) and Prof. Dr. Augusto Mangini (Heidelberg) for U/Th dating.

I wish also to thank all professors, research associates and the administrative and technical staff in the Institute for Applied Geosciences (TU Darmstadt); particularly, Dr. Günter Landmann for his assistance in preparing the PhD proposal and sharing knowledge on Lake Lisan; Prof. Dr. Ingo Sass for providing DGPS equipment; Prof. Dr. Andreas Hoppe for providing updated articles on the Dead Sea; Rainer Brannolte for laboratory assistance; Ulrike Simons for Arc GIS assistance; Ingrid Hirsmüller, Kirsten Herrmann and Petra Kraft among many others for being always helpful and friendly.

My grateful thanks are also due to my husband Dr. Mohammad Abu Ghazleh for his unconditional support and assistance in the field work, GPS measurements and data processing.

Aerial photos of Lake Lisan and the Dead Sea were kindly provided by the BGR Hannover. The field and lab work of this study was made possible by grants from the Deutsche Akademische Austauschdienst (DAAD) and the Deutsche Forschungsgemeinschaft (DFG-Ke-287/28-1).

My family in Jordan is also acknowledged for their prayers and moral support; special thanks deserve my brother Abid Al-Latif for his help to improve the accuracy of the fit functions.

List of Publications

Based on this thesis several scientific contributions were published in international peer reviewed journals and books. Meanwhile, others are prepared for submitting. A list of these publications is given below.

a) Published articles

ABU GHAZLEH, S. & KEMPE, S., 2009: Geomorphology of Lake Lisan terraces along the eastern coast of the Dead Sea, Jordan. - Geomorphology 108: 246-263.

ABU GHAZLEH, S., HARTMANN, J., JANSEN, N. & KEMPE, S., 2009a: Water input requirements of the rapidly shrinking Dead Sea. - Naturwissenschaften 96 (5): 637-643.

ABU GHAZLEH, S., JANSEN, N., HARTMANN, J. & KEMPE, S., 2009b: Das Sterben des Toten Meeres. - Naturwissenschaftliche Rundschau 62(7): 368-370.

ABU GHAZLEH, S., KEMPE, S., HARTMANN, J. & JANSEN, N., 2010: Rapidly shrinking Dead Sea urgently needs infusion of 0.9 km^3/a from planned Red-Sea Channel: Implication for renewable energy and sustainable development. - Jordan Journal of Mechanical and Industrial Engineering 4 (1): 211-216.

ABU GHAZLEH, S., ABED, A.M. & KEMPE, S. 2011: The dramatic drop of the Dead Sea: background, rates, impacts and solutions. - In: Badescu, V. & Cathcart, R.B. (eds.), Macro-engineering Seawater in Unique Environments; Arid Lowlands and Water Bodies Rehabilitations; Springer, in press.

b) In preparation

ABU GHAZLEH, S. & KEMPE, S., in prep: Geomorphological and sedimentological evidence of high stands of Lake Lisan up to 0 m a.s.l: ~ 150 m higher than previously reported.

Abstract

Changes in the level of closed lakes such as the glacial Lake Lisan/Near East, that occupied the Jordan Rift Valley between 80 to 15 ka BP*, reflect climatic changes in evaporation and precipitation patterns. However, in an actively subsiding basin such as the Dead Sea (water level today is at -423 m relative to mean sea level), tectonic activity could also contribute to lake level recession. The retreat of Lake Lisan left behind a sequence of shoreline terraces and deposits of aragonite and gypsum. The ability to determine shore line elevations and to date them offers an excellent possibility to evaluate hydrologic changes, paleoclimatic conditions and tectonic activity of the lake basin during the Last Glacial.

By the end of the Pleistocene, Lake Lisan receded sharply and was followed by the current Dead Sea at ~10 ka BP. Both lakes experienced several rises and regressions due to climatic change. However, the most recent lowering of the Dead Sea level since the beginning of the twentieth century of more than 30 m is mainly due to the impact of upstream freshwater diversion together with mineral extraction by the salt industry in the southern Dead Sea basin. This recent level drop left behind a unique landscape of shore line terraces, allowing investigation of the recent lake regression in detail.

Therefore the dissertation aims at (1) examining the most recent changes in the Dead Sea level and shore morphology and developing a terrain model of the Dead Sea Rift Valley that allows calculating the area and volume losses of the lake for the various stages of its recession. (2) investigating geomorphological characteristics of Lake Lisan erosional terraces along the eastern side of the Dead Sea (e.g., elevation, gradient, width, length, etc.) and dating them. This investigation will help to reconstruct the lake level history and correlate the level changes with paleoclimatic conditions. Moreover, it should give additional water level data and rates of level retreat for Lake Lisan; and (3) investigating geochemical and mineralogical characteristics of the terrace stromatolites (AAS and XRD) and analyzing their stable isotope composition. This should provide indicators on the lake levels and on the lake water chemistry as well as on paleoenvironmental and paleoclimatic conditions.

* "ka BP" 1000 years before present (= 1950 AD).

The main results of this study are as follow:

1. Well-correlated and dated profiles of the modern shoreline terraces of the Dead Sea are presented for the first time. The timing and amplitude of the lake level change recorded in these terraces forms an analogue to past level changes of the paleo-Dead Sea and even to level changes of other lakes.

2. A terrain model of the Dead Sea Rift Valley was developed based on SRTM data that served as a tool to calculate the volume and area functions versus altitude of the Dead Sea. The model was further used in macro-engineering implications to calculate the water input requirements of the rapidly shrinking Dead Sea and therefore the capacity of the projected Dead Sea-Red Sea Canal. The water volume loss calculated by this study (0.47 km^3/a) and the ground water inflow to the Dead Sea (ca. 0.5 km^3/a) suggest that the RSDS should has a capacity of ~1 km^3/a in order to stop the lake level drop. However, ca. 1.3 km^3/a is required in order to fill the lake back to levels as of 30 years ago.

3. The morphological and chronological evidence presented in this study allowed generating a high resolution curve of the lake level for MIS 2 (32-10 ka BP). It can now be assumed with certainty that the lake stood as high as -150 m, removing the doubt on the highest stand found along the western coast. However, this is not the highest stand of the lake during MIS 2, much higher terraces up to -137 m were identified in the field and dated between 30 and 32 ka BP.

4. Discovery of high-level terraces of Lake Lisan > -137 m and up to 0 m along the eastern escarpment and dating of their stromatolites revealed the time and the exact elevation of the highest lake stand. This also clarified the previous doubt on the paleoenvironment conditions of the early stage of Lake Lisan as well as on the transition period from Lake Samra to Lake Lisan. The newly discovered maximal level is 150 m higher than previously reconstructed and occurred at the beginning of the last glacial period (79-76 ka BP). This allowed presenting a new curve of the lake level during the last glacial period, including new fixes on past lake level elevations as well as on the chronology of the regression and transgression cycles.

5. The new curve allows correlating the lake level with global climatic records: transgressions occurred during the warm MIS 5 and 3, while regressions occurred during the cold MIS 4, 2, and the cold Heinrich events 6, 5, 4, 3 and 2. This demonstrates a strong linkage between the paleoclimate of the Jordan valley and monsoon-affected North Africa rather than that with Europe and the North Atlantic. X-ray analysis, Mg/Ca ratios and isotope analyses of the stromatolites correlate well with transgression-regression phases of the lake. Dominance of calcite in stromatolites at -76 to 0 m and low isotope values in addition to inferred low Mg/Ca ratios of the lake water (i.e. ~2) imply a high fresh water input of the lake during the period of the highest stands. A high Mg/Ca ratio of the lake water of > 7 inferred from stromatolites at -350 m and the existence of aragonite as the sole mineral in this sample reflect low fresh water input and high evaporation rates of the lake during its regression to this low level. Low Mg/Ca ratios and low stable isotope values of stromatolites at -247 to -101 m in addition to the existence of calcite as a main mineral phase indicate wet climatic conditions that caused a lake transgression during MIS 3. The appearance of more aragonite in stromatolites at -137 to -154 m inferring a change to high Mg/Ca ratios and high stable isotope values points to a return to dry climatic conditions that caused a regression of Lake Lisan during MIS 2 between 32 and 22 ka BP.

Zusammenfassung

Spiegelschwankungen geschlossener Seen, wie z.B. des Lisan Sees im Nahen Osten (80-15 ka BP[*]), sind Ausdruck der klimatischen Veränderungen von Evaporations- und Präzipitationsmustern. Zusätzlich könnten sich in einem pull-apart-Becken, wie dem Toten Meer, tektonische Aktivität auf den Wasserspiegel (heute bei -423 m in Bezug zum mittleren Meeresspiegel) auswirken. Der Rückgang des Lisan Sees hat sowohl mächtige Sedimentablagerungen als auch Serien von Uferterrassen hinterlassen. Die Höhenbestimmung dieser Terrassen und ihre Datierung ermöglichen die Rekonstruktion des Seespiegls und gibt Informationen über Klimawechsel und tektonische Aktivitäten während des letzten Glazials.

Gegen Ende des Pleistozäns ging der Lisan See stark zurück und wurde vor etwa 10000 Jahren durch den heutigen Wasserkörper, das Tote Meer, ersetzt. Beide Seen erlebten mehrfach Trans- und Regressionen auf Grund von klimatischen Änderungen. Allerdings ist die heute zu beobachtenden Regression des Toten Meeres, die seit Beginn des 20. Jahrhunderts bereits mehr als 30 m beträgt, hauptsächlich auf die Frischwasserentnahme in den Oberläufen des Jordans und auf die Entnahme von Seewasser durch die Salzindustrie im Südteil des Toten Meer Beckens zurückzuführen. Dieser rezente Seespiegelrückgang hat ebenfalls eine einmalige Serie von Uferterrassen hinterlassen, an der man die jetzige anthropogen verursachte Regression im Detail untersuchen kann.

Diese Dissertation beschäftigt sich daher (1) mit den jüngsten Änderungen des Spiegels des Toten Meeres und dessen Ufermorphologie. Ein aus SRTM-Daten entwickeltes Geländemodell des Grabenbruches erlaubt die Ableitung von Flächen- und Volumenverlusten der verschiedenen Stadien der Regression des Sees; (2) mit der Untersuchung der Geomorphologie der Erosions-Terrassen des Lisan Sees (i.e., ihrer absoluten Höhe, ihrer Gradienten, und deren Breiten und Ausdehnung etc.) entlang des östlichen Ufers des Toten Meeres und deren Datierung. Dies dient der Rekonstruktion der Geschichte des Seespiegels und der paläoklimatischen Bedingungen; sowie (3) mit den geochemischen und mineralogischen Eigenschaften der Stromatolithe auf den Terrassen (durch AAS und XRD) und deren Signatur der stabilen Isotope.

[*] 1000 years before present (= 1950 AD).

Dies soll weitere Indikatoren für die Rekonstruktion der Seespiegel- und geochemischen Geschichte wie auch für die Rekonstruktion der Paläoumwelt und des Paläoklimas geben.

Die Untersuchungen haben fünf Hauptergebnisse erbracht:

1. Die neu-gebildeten Terrassen des jetzigen Toten Meeres (die z.T. nur einen einjährigen Seespiegelstillstand repräsentieren) konnten zum ersten Mal in ihrer Höhe eingemessen und zwischen den verschiedenen Delta-Schuttkörpern korreliert werden. Durch Korrelation mit der gemessenen Spiegelkurve (Hydrological Survey of Israel) wurden sie datiert und so die Zeiten ihrer Entstehung rekonstruiert (Abu Ghazleh et al., 2009a; Abu Ghazleh et al., 2010; 2011, Chapter 2). Morphologie und Bildungsgeschwindigkeit liefern interessante Analogien zu den älteren Terrassen des Lisan Sees und zu anderen Seen im Generellen.

2. Die Ermittlung der Volumens- und Flächenänderung als Funktion der Höhe des Gesamtbeckens aus SRTM Daten erlaubt die Berechnung der Wasserbilanz: Der mittlere Volumenverlust des Toten Meeres für die letzten 14 Jahre beträgt 0,47 km^3/a. Da der Seespiegelrückgang durch seitlichen Zufluss von Grundwasser von ca. 0,5 km^3/a gedämpft wird, müsste ein Kanal vom Roten Meer die Kapazität von ca. 1 km^3/a haben, um den Seespiegel zu stabilisieren und von mindestens 1,3 km^3/a, um den See auf eine „Betriebshöhe“ von ca. -400 m langfristig wieder aufzufüllen (Abu Ghazleh et al., 2010, 2011). Wenn auch die leer gelaufenen Grundwasserkörper wieder aufgefüllt wurden, kann langfristig ca. 1 km^3/a Wasser zugeführt und zur Energiegewinnung genutzt werden. Ein im Prinzip wirklich nachhaltiges System, denn das zugeführte Wasser verdunstet und das zugeführte Salz ersetzt das durch die Salzgewinnung im Südteil des Toten Meeres entzogene Salz.

3. Die morphologischen Parameter der im Südosten des Toten Meeres befindlichen Terrassen-Serien konnten an mehreren Profilen zum ersten Mal exakt vermessen und ihre Höhen mit einander korreliert werden (Abu Ghazleh & Kempe, 2009; Chapter 3). Damit konnte der auf der Westseite schlecht dokumentierte glaziale Hochstand von ca. -150 m bestätigt und über stromatolithische Krusten genauer datiert werden. Aber

auch dies ist nicht der Höchststand im MIS 2, sondern es wurden weitere Terrassen bis auf die Höhe von -137 m entdeckt und auf 32 und 30 ka BP datiert, die anzeigen, dass der See wenigstens kurzeitig diese Marke erreicht hat. Eine zementierte Schotter-Terrasse auf -148 m, die in einer Erosionsnische erhalten ist und das Vorkommen von Stromatolithen zeigen an, dass der See hoch $CaCO_3$-übersättigt war, d.h. das Wasser war vermutlich höher alkalisch als im heutigen See.

4. Erstmalig wurden deutliche Terrassen eines noch viel höheren Seestandes im Tayan Valley bis ca. 0 m nachgewiesen (Chapter 4). Auch diese Terrassen konnten an stromatolithischen Krusten erfolgreich U/Th-datiert werden. Sie gehören zur Frühphase des Lisan Sees um 79-76 ka BP und in den Übergang vom Samra Lake. Damit konnten neue Fixpunkte für die Seespiegelentwicklung gefunden werden und eine neue Kurve des Paläoseespiegels erzeugt werden.

5. Diese neue Seespiegelkurve erlaubt auch die Korrelation mit globalen Klimakurven: Während der warmen MIS 5 und 3 transgredierte der See, während die kälteren Abschnitte MIS 4 und 2 und die kalten Heinrich-Events 6, 5, 4, 3 und 2 mit Regressionen korrelieren. Dies zeigt die paläoklimatische Verbindung des Jordan Tales mit dem Monsun-geprägten Nord-Afrika und nicht so sehr mit dem Klima Europas und des Nord-Atlantiks. Die mineralogische Analyse und das Mg/Ca Verhältnis der Stromatolithe korrelieren ebenfalls sehr gut mit Transgression-Regression Phasen des Sees. Die Dominanz von Calcit in den Stromatolithen von -76 bis 0 m und die abgeleiteten niedrigen Mg/Ca Verhältnisse des Seewassers (i.e. ~2) implizieren einen hohen Frischwasserzufluss in den See während seines höchsten Standes. Ein hohes Mg/Ca Verhältnis des Seewassers von >7, abgeleitet aus der Analyse der Stromatolithen bei -350 m und Aragonit als einzige Mineral in dieser Probe, lässt auf einen geringen Frischwasserzufluss und hohe Evaporationsraten während der Regression schließen. Das abgeleitete niedrige Mg/Ca Verhältnis von Stromatolithen von -247 bis -101 m und die Existenz von Calcit als die Hauptmineralphase zeigen feuchte Klimabedingungen und eine Transgression auf über -137 m während des MIS 3 an. Höhere Aragonitgehalte in den Stromatolithen von -137 bis -154 m zeigt die Rückkehr zu trockeneren klimatischen Bedingungen und eine Regression des Lisan Sees zwischen 32 bis 22 ka BP (MIS 2) an.

Lake Lisan and the Dead Sea: Their Level Changes and the Geomorphology of their Terraces.

1. Introduction

1.1 Aims of the study

The levels of closed lakes such as the glacial Lake Lisan/Jordan Valley (70-15 ka BP[*]) (e. g., Haase-Schramm, 2003; Waldmann et al., 2007) are determined by changes in evaporation and precipitation. However, in an actively subsiding basin such as the Dead Sea (today at -423 m[**]), tectonic activity could also contribute to lake level recession. The retreat of Lake Lisan left behind sequences of prominent shoreline terraces and deposits of aragonite and gypsum exposed on the Lisan Peninsula and along the shores of the Dead Sea. The ability to determine shore line elevations and to date them offers excellent possibilities to evaluate hydrologic changes, palaeoclimatic conditions and tectonic activity of the lake basin during the Last Glacial.

The transition between the Pleistocene and the Holocene was accompanied by a retreat of Lake Lisan and its contraction to the hyper-saline Dead Sea at ~10 ka BP (Stein et al., 1997). The lake level was unstable during the Holocene. It experienced several rises and drops due to climatic changes. However, the most recent lowering of the lake level since the beginning of the twentieth century of more than 30 m is mainly due to the impact of upstream freshwater diversion together with mineral extraction by the salt industry in the southern Dead Sea basin. This recent level drop left behind a unique landscape of shore line terraces, allowing investigation of the recent lake regression in detail. The level drop caused also severe environmental consequences all around the lake, threatening the existence of the Dead Sea as a natural resource as well as the natural habitats of its shores and the livelihood of people.

Therefore this study aims at: (1) examining the most recent changes in the Dead Sea level and in shore morphology and developing a terrain model of the Dead Sea Rift Valley that allows calculating the area and volume losses of the lake for the various stages of its

[*] "ka BP" 1000 years before present.
[**] "-"before elevation denotes meters below sea level.

recession. This will help to determine water input requirements of the shrinking Dead Sea and the water capacity of the projected Dead Sea-Red Sea Canal; (2) investigating geomorphological characteristics of Lake Lisan erosional terraces along the eastern side of the Dead Sea (e.g., elevation, gradient, width, length, etc.) and dating them. This investigation will help to reconstruct the lake level history and correlate the level changes with palaeoclimatic conditions. Moreover, it should give additional water level data and rates of level retreat for Lake Lisan; and (3) investigating geochemical and mineralogical characteristics of the terrace stromatolites (AAS and XRD) and analysing their stable isotopic composition. This investigation should provide indicators on the lake levels and on the lake water chemistry as well as on paleoenvironment and palaeoclimatic conditions.

1.2 Formation of the Dead Sea rift

During the late Cretaceous and Paleogene, the African plate (including Arabia) started to move northward, forming the Syrian Arc Fold belt (Bowen and Jux, 1987). This epeirogenic uplift has led to the withdrawal of the Tethys Ocean from the Levant /Belad Al-Sham (Bender, 1974). By mid-Miocene, about 15 Ma[***] ago, the Arabian Plate separated from the African plate and began to move northwards, opening the Gulf of Aden and the Red Sea and forming the Dead Sea transform boundary (DST) (e.g., Abed, 2000).

The DST extends for about 1100 km from the southern tip of the Gulf of Aqaba in the south to the East Anatolian Fault in Turkey in the north (Fig. 1.1). From the northern end of the Gulf of Aqaba, the DST runs NNE along the eastern side of Wadi Araba-Dead Sea (Wadi Araba Fault) to peter out at the NE tip of the Dead Sea into the pre-existing Amman-Hallabat structure. The Jordan Valley Fault starts from the SW corner of the Dead Sea basin and runs along its western boundary and then diagonally crosses the River Jordan eastward up to the N end of the Tiberias basin (Fig. 1.1). From there, the Yamouna Fault takes the movement through the Bekka' and Ghab basins in Lebanon and Syria respectively, until it meets the East Anatolian Fault (Abed, 2000).

Either Jordan moves N along the Wadi Araba Fault, while Palestine is moving south along the Jordan Valley Fault (Quennell, 1958), or Jordan moves N faster than the northwards

[***] "Ma" million years.

movement of Palestine (Klinger et al., 2000). In both cases, the Arabian plate and the Sinai-Palestine sub-plate are pulled in two opposite directions. The tensional forces produced by stress-strain relations along the strike-slip DST created transverse faults formed in a NNE-SSW direction across the basin. This process produced several rhomb-shaped pull-apart basins including the Gulf of Aqaba, Wadi Araba, the Dead Sea, the lower Jordan valley, the upper Jordan valley, the Bekka' and the Ghab basins. The annual rate of the NNE movement along the southern DST is about 4.5 mm/a (Klinger et al., 2000), amounting to a total movement of 107 km since the Miocene (Quennell, 1958).

Due to the northwards movement of the Arabian plate relative to the Sinai-Palestine sub-plate, the strata outcropping on both sides of the Dead Sea are not the same. The rocks along the eastern shoulder are much older, involving units from the Precambrian to the Eocene, while along the western rim Precambrian and Paleozoic rocks are absent (Abed, 2000) (Figs. 1.2, 1.3).

The floor of the DS rift has been subsiding since its formation in the Miocene. The subsidence most probably is not a continuous process and it does not occur at the same rate throughout the various parts of the basin. The minimum rate of the subsidence was estimated to 0.2 mm/a or 200 m/Ma. Also, both shoulders of the DS Rift have been rising since its formation. The rate of uplift is certainly higher along the rift eastern shoulders compared with its western shoulders. One of the important consequences of the uplift is the isolation of the DS Rift from the Mediterranean since the early Pleistocene. Both geological processes, subsidence and uplift, shaped the DS Rift. Subsidence and uplift are much faster than erosion and sedimentation, thus a huge accommodation space for sediments was created, the modern Dead Sea-Jordan depression (Abed, 2000).

1.3 Sedimentation and water bodies in the Dead Sea basin

Towards the end of the Eocene, the Tethys migrated to the west. The shore line was slightly east of the present-day Mediterranean. Prior to that, and starting from the Cenomanian, a 1000 m thick sediment column - mostly carbonates - was deposited by the Tethys Ocean in and around the Dead Sea basin. The Oligocene was a time with enhanced epirogenic movements (Bender, 1974). By the Miocene, the ground was set for the formation of the Dead Sea rift. From this time onwards, the Dead Sea basin and the Jordan Valley have been the sites for successive lakes, varying in size and salinity.

From the early Miocene onwards, the Dead Sea basin was topographically lower than its surroundings. Erosion and re-deposition of the older marine strata led to the formation of the Miocene Dana Conglomerate Formation. The presence of micro fauna and the absence of evaporates suggests an open connection between the Mediterranean and this infant basin (Powell, 1988).

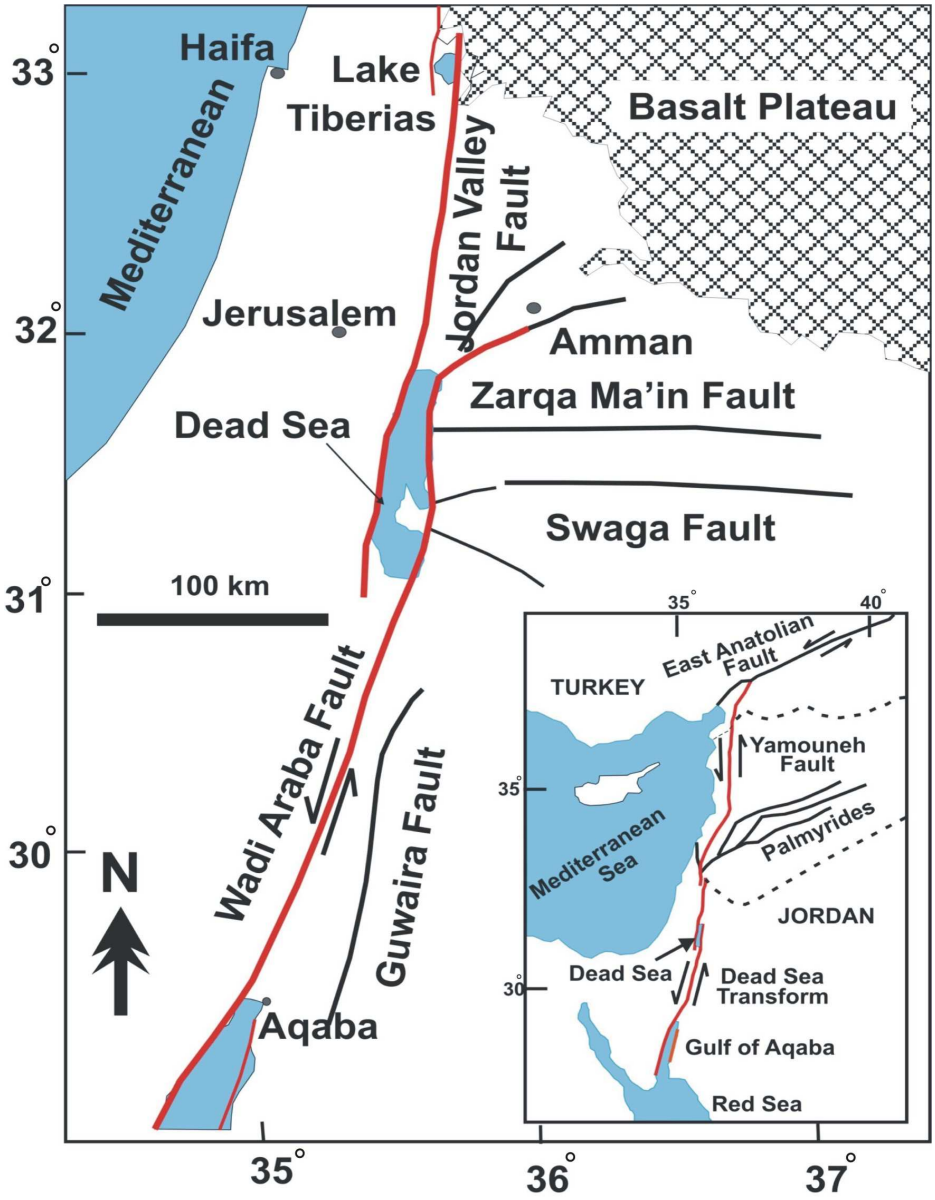

Fig. 1.1: The Dead Sea Transform Fault and associated faults in Jordan. The Wadi Araba Fault and the Jordan Valley Fault overlap forming the pull-apart basin of the current Dead Sea. Inset shows the whole length of the DST from the Gulf of Aqaba in the south to the East Anatolian Fault in the north (After Abed, 2000).

By the Pliocene, the Dead Sea rift was occupied by the highly saline water Usdom Lake, similar in salinity to the present day Dead Sea where halite is now precipitated. Rock salt with minor other evaporates was deposited by the lake with a thickness of ~ 4000 m below the Lisan Peninsula (Bender, 1968). To the E and W, the salt beds decrease in thickness and begin to intercalate with fluvial sediments transgressing from the basin shoulders. The huge thickness of salt can be explained by the Dead Sea basin being still connected to the Mediterranean Sea as a lagoon to provide the salt, subsidence to accommodate this thickness, and evaporation to adjust the salinity.

By the end of the Pliocene, the western mountain range became high enough to cut the connection between the Dead Sea-Jordan Valley and the Mediterranean. The former area became depending on precipitation and thus on climate as a source for water throughout the Quaternary. During the last interglacial, the Dead Sea rift was occupied by the fresh-water Samra Lake at ~135-90 ka BP (Waldmann et al., 2007) reflecting wet climatic condition.

After the regression of Lake Samra in the interglacial-glacial transition, the Jordan Valley was filled with the brackish-water Lake Lisan at ~75-14 ka BP (e.g., Waldmann et al., 2007). Lake Lisan receded sharply after the last glacial Maximum and followed by the fresh water Damya Lake at ~14-12 ka BP. The dry climate of the Jordan Valley prevailed during the Younger Drays caused a contraction of Lake Damya to the current hyper-saline DS at ~10 ka BP (Abed and Yaghan, 2000).

1.4 State of the art and research gaps

1.4.1 The Holocene Dead Sea

At the Pleistocene-Holocene boundary, Lake Lisan dropped sharply as indicated by an erosional unconformity on the top of Lisan deposits followed by a massive salt unit (Yechieli et al., 1993). Fine-grained lacustrine sediments were deposited above the unconformity and the salt layers dated to between ~11 and 8 ka BP. This indicates a lake level rise at the beginning of the Holocene marking the early stage of the current Dead Sea water body (Neev and Emery, 1967; Yechieli et al., 1993; Kadan, 1997; Migowski et al., 2004). Two major wet phases at 10-8.6 and at 5.6-3.5 cal ka BP were recorded from a Dead Sea sediment core, interrupted by arid events at 8.6, 8.2, 4.2 and 3.5 cal ka BP

(Migowski et al., 2006). These events are thought to be associated with major interruptions in the Near East cultural evolution (Migowski et al., 2006).

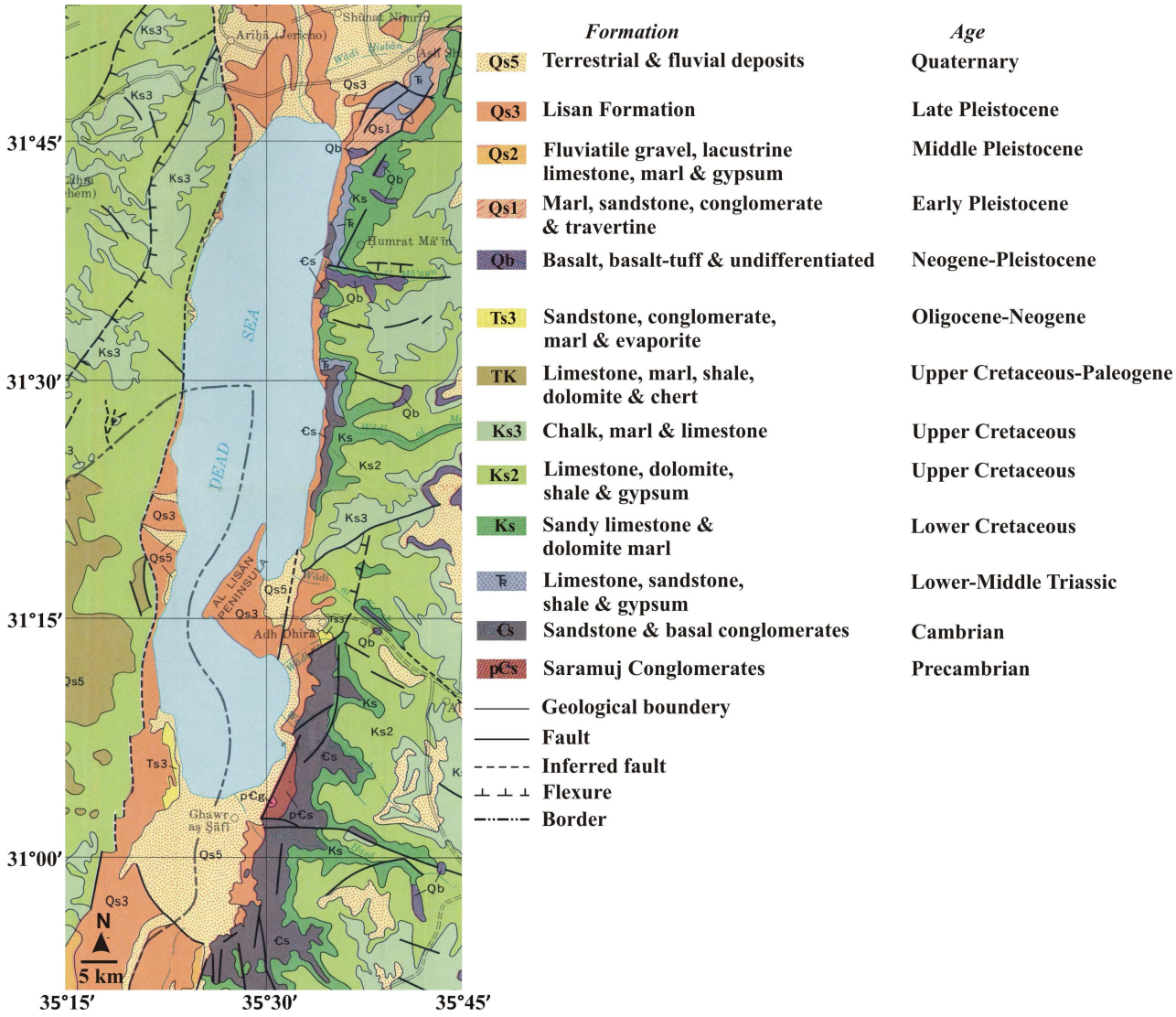

Fig. 1.2: Generalised geological map of the Dead Sea area. Note that strata along the eastern shoulder are much older than those in the western shoulder. Dead Sea area and shorelines as in the early 1960s at -397 m (after Bender, 1975).

Based on the salt cave morphology and radiocarbon dating in Mount Sedom, Frumkin et al. (1991) reconstructed the Dead Sea level curve. They suggested a rapid lake level fall at 7.8 ka BP marked by the earliest salt karst development and the exposure of the top of the diapir. Morphological evidence shows that the cave passages of Mount Sedom were completely filled with Dead Sea water between ~5200 and 3900 years ago, indicating a lake level rise up to -345 m. This wet phase was followed by a lake level drop to - 415 m

at ~3220 to 3703 years ago based on the dating of an unconformity in the Dead Sea deposits (Bookman et al., 2004).

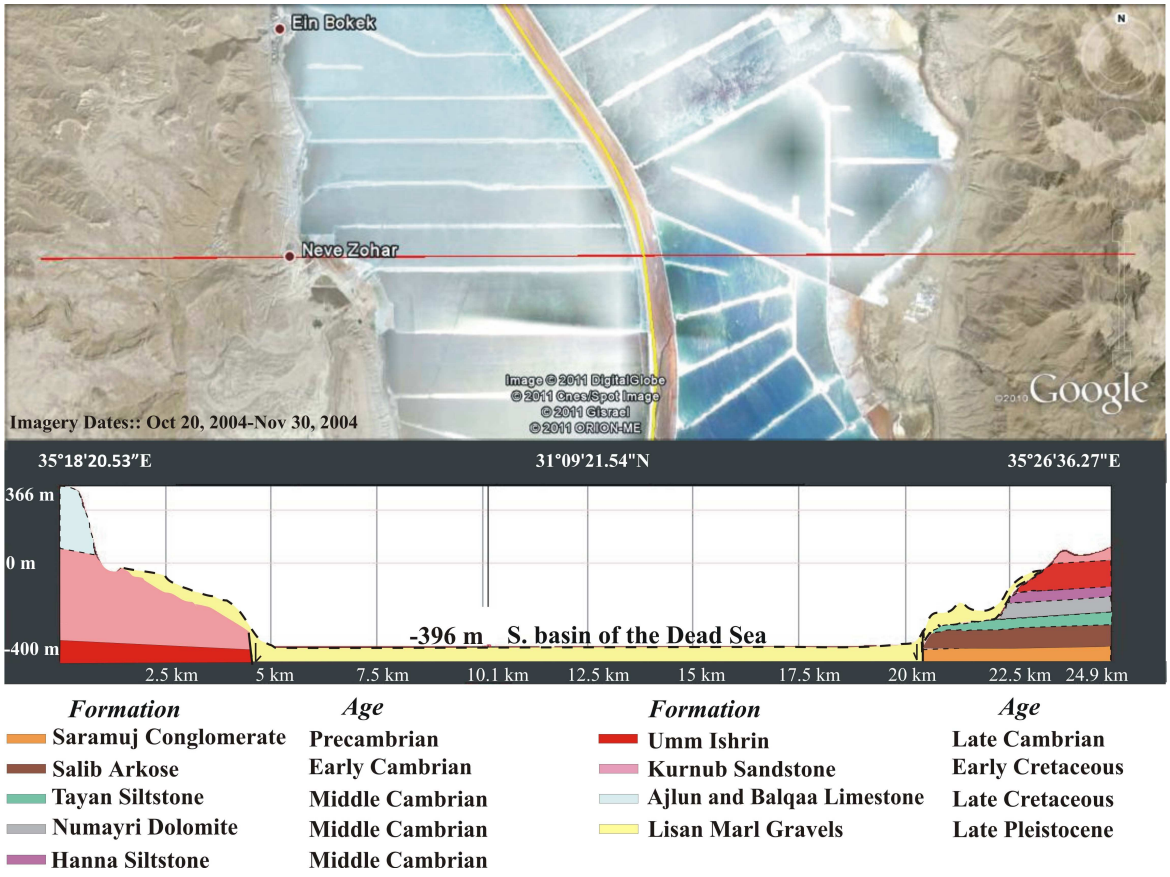

Fig. 1.3: Topographical and geological section of the southern part of the Dead Sea Basin. Topography was derived from Google Earth and geology was drawn based on the Al-Karak Sheet 1:50,000 and on field observations.

During the last 4000 years, the Dead Sea fluctuated within a smaller range around -400 m. The Dead Sea rose four times above -400 m, flooding the southern basin for few decades during the Roman and Byzantine periods (Bookman et al., 2006). Modern measurements of the Dead Sea level started in the middle of the nineteenth century. The first large expedition to the Dead Sea and the Jordan River was conducted by Lynch in 1848 from the US Navy. Lynch arrived at the Dead Sea after sailing down the Jordan River from Lake Tiberias. He was the first to determine the lake level accurately at 401.2 m below sea level and to make a bathymetric map of the Dead Sea based on reliable measurements of the lake water depth (Lynch, 1854). Systematic observations of the lake level changes were also made by Allen (1855) as a part of the first proposal for the Mediterranean-Dead Sea Canal. However, the Dead Sea level was continuously measured only since 1899 (Bookman et al., 2006).

Nowadays, the increasing water demand in the Dead Sea basin -as one of the most arid regions on Earth- puts a big strain on the limited water resources and caused a significant change in the water balance of the lake. As a result, the level of the Dead Sea dropped by more than 30 m in the last 70 years, and it is still dropping with serious environmental impacts.

The steep morphology of the eastern shore of the Dead Sea allowed large bodies of alluvial fan-deltas to develop at the mouth of the main west-draining wadis. The top-sets of these deltas were eroded by wave action forming a unique sequence of shore line terraces that represents annual lake level standstills. In spite of the great importance of these terraces in reconstructing the recent lake level changes, they have not been investigated by any of the previous studies. Moreover, no attempt was made to develop a terrain model of the lake basin that enables calculating changes in water volume and surface area at different altitudes.

1.4.2 Lake Lisan

After the retreat of the interglacial fresh-water Samra Lake, the Dead Sea depression was occupied by the brackish-fresh water Lake Lisan at ~70 to 14 ka BP (e.g., Waldmann et al., 2007). Older ages of the early stage of Lake Lisan of ~100 and ~115 ka BP were reported by Neev and Emery (1967) and Langozky (1963), respectively. Deposits of Lake Lisan occur from Lake Tiberias in the north to > 60 km south of the Dead Sea, indicating a total length of the lake of >200 km. However, there is a lack of studies and much uncertainty exists regarding the exact date of the beginning of Lake Lisan.

The history of Lake Lisan is recorded in its deposits, known as the Lisan Formation. This term was first used by Lartet (1869). However, many others have mentioned these deposits (e.g., Picard, 1943; Quennell, 1956; Bentor and Vorman, 1960; Bender, 1968). Begin et al. (1974) defined two members of the Lisan Formation: the Lower Laminated Member and the Upper White Cliff Member. They also divided the Lisan Formation into three facies: gypsum facies in the west of the Dead Sea, aragonite facies in the south and north of the Dead Sea, and diatomite facies north of Wadi Al-Malih. The diatom distribution gives evidence of a separation of Lake Lisan into northern and southern basins with different water salinities.

Abed and Yaghan (2000) and Abed (2000) found it difficult to divide the Lisan Formation into members because these deposits are not the same in different parts of the lake. On the Lisan Peninsula, these deposits are chemical, consisting of grey aragonite laminae deposited in winter and white gypsum laminae deposited in summer. South of the Khunizera fault, the Lisan Formation consist of chemical laminae with sand. The Lisan Formation can be divided into three members only in the area between the north of the Dead Sea and Marma Feiyad: the Lower Laminated Member (15 m) consisting of interlaminated calcareous silt and aragonite, the Middle Member (9 m) consisting of massive black clay, and the Upper Laminated Unit (~18 m) consisting of interlaminated aragonite and silt (Fig. 1.4). The upper 5-7 m of this unit is a white cliff identical to the White Cliff of Begin et al. (1974). It consists of gypsum and aragonite, indicating a change to dry climatic conditions and a negative water balance within the Lake Lisan basin. Radiocarbon dating of the White Cliff sediments indicates that it accumulated between 33-15 ka BP (Kaufman, 1971) or 35-15 ka BP (Vogel and Waterbolk, 1972). Abed (2000) gave a younger age of 23-22 to 16-15 ka BP, depending on the sedimentation rate assumed. A similar age of about 24 cal ka BP was also derived by Landmann et al. (2002) based on a rough varve count. The two gypsum layers at the top of the sections in Massada Plain and Perazim Valley which may represent the White Cliff yielded an age of 17 cal ka BP (Stein, 2000; Stein et al., 1997; Bartov et al., 2002).

After the dry period leading to the deposition of the White Cliff, Lake Lisan recovered again as indicated by the overlying fresh-water Damya Formation (Abed and Yaghan, 2000), which is equivalent to the Unnamed Unit of Begin et al. (1974) and to the Fatzael Member of Horowitz (1979). It consists of 14 m of clastics (gravel, sands, silts, and clay) and contains fresh water gastropods and fresh-brackish water ostracods (Begin et al., 1974; Horowitz, 1979; Abed, 1985). The period of Damya Lake corresponds to the pluvial and high level periods of 14-11 ka BP (Neev and Emery, 1995), 14.6 and 12.04 ka BP (Landmann et al., 1996) and 15 ka BP (Klinger et al., 2003; Klinger, 1999). The age of the Damya Formation was also estimated by Abed and Yaghan (2000) to ~15-12 ka BP. Epipaleolithic stone tools found within the Fatzael Section indicate an age of 19-10 ka BP (Bar-Yosef et al., 1974).

However, the final stage of Lake Lisan is not well dated because the top of the Lisan Formation has been eroded (Niemi, 1997). Also the paleogeographic relation of the fresh-

water deposits (Damya) overlying the Lisan Formation is not clearly defined. Therefore, further research is required in order to obtain more details on the final stage of Lake Lisan as well as on the timing and amplitude of the lake level highstands and the age of erosional cycles.

The retreat of Lake Lisan left a number of shoreline terraces, mentioned by many travelers and geologists. Blanckenhorn was the first to describe the erosional terraces of Lake Lisan during his visit to the Dead Sea in 1894 (Blanckenhorn, 1912). He recognised the terraces as paleoshorelines and investigated them up to 70 m above the present Dead Sea level. Blanckenhorn correlated these terraces with the glacial period in Europe and concluded that they are not horizontal due to tectonic activity of the Dead Sea basin. Huntington (1911) identified a series of terraces on the margins of the basin and connected them to glacial advance and retreat in Europe. He also concluded that the lake level must have fluctuated in response to climatic changes.

Picard (1943) measured the terraces on the escarpment near Jericho at an altitude of -200 to -210 m and regarded the terraces as recessional. Neev and Emery (1967) found the terraces to be horizontal, unfaulted and undisturbed, ranging in altitude between the recent level of the Dead Sea and -180 m. Thus they concluded that post-terraces vertical movement of considerable magnitude could not have occurred along the main border faults. They also added that subsidence of the central parts of the basin may be due to "rearrangement of the fills" in addition to "the structural effect of the movement along the main north-south strike-slip fault".

Three terrace profiles were studied with the aid of leveling by Bowman (1971). The three profiles have been integrated into one generalised profile consisting of 28 terraces, ranging in altitude between -180 m and -380 m. The terraces were found to be horizontal and undisturbed, indicating that they were not affected by tectonic activity.

The highest shoreline of Lake Lisan is often given at -180 m based on the top elevation of Lisan marls and of Lisan terraces (Neev and Emery, 1967; Begin et al., 1974; Bowman, 1971). A sequence of raised beaches in the form of bars encircling the Lisan Formation in the Hazeva area was observed up to -150 m. This suggests that the highest level of Lake Lisan is probably -150 m instead of -180 m (Bowman and Gross, 1992). A higher stand of

-130 m was suggested by Sheinkman (2002) based on lacustrine deposits found in Zin Valley - southwest of the Dead Sea - dated to 30.4 ± 2 and 34.2 ± 2 ka BP). However, this evidence is still debated since elevation higher than -160 m was not reported elsewhere in the Dead Sea basin (Bookman et al., 2006). Therefore, Bookman et al. (2006) suggested that further studies in the eastern margin of Lake Lisan would shed more light on the exact elevation of the Lake Lisan highest stand.

The palaeoclimatic fluctuations recorded by the Lake Lisan deposits were discussed by Neev and Emery (1967). They deduced a high, constant runoff/evaporation ratio for the period 48-18 ka BP, followed by a dry period (Fig. 1.5). In contrast, Begin et al. (1974) postulated a decrease of the runoff/evaporation ratio between 60 and 18 ka BP, followed by a pluvial period. Begin et al. (1985) constructed a curve of Lake Lisan levels from the elevation and radiocarbon age data of algal stromatolites (Fig. 1.5). This curve is not reliable because the dated stromatolite samples are contaminated with young carbon (Begin, 1985).

Neev and Emery (1995) reconstructed the Lake Lisan level for the last 20 ka. They found two major highstands at -200 m in the periods from 20 to 18 ka and from 14 to 11 ka BP, interrupted (16.5-15.5 ka BP) and followed by a drop to the present level at 7 ka BP. These results correlate well with those of Lake Van/Turkey (Landmann and Kempe, 2002; Kempe et al., 2002). They concluded that Lake Van had a highstand during the LGM at ~20 ka BP followed by a strong drop of the lake level between 20 and 15 ka BP. Between 14.6 and 12.04 ka BP the lake level recovered by ~250 m to fall again during the next 1.4 ka. By 10.6 ka BP, the lake began to rise and reached a relative highstand by about 7.5 ka BP (Fig. 1.6).

By investigating the geochemistry of two profiles of the Lisan Formation at the eastern Dead Sea shore, Landmann et al. (2002) discerned three major and several minor transgressive depositional cycles of Lake Lisan, all terminating with massive gypsum precipitation. From 70-45 cal ka BP, the Lisan Formation was characterised by a high gypsum/aragonite ratio and a low lithogenic content, implying a regression of an initially high water level, caused by reduced water input.

Stein (2001) reconstructed a lake level curve for the interval 55-35 ka BP. He found that Lake Lisan had a relatively low stand (-280 to -290 m) between 55 and 30 ka BP. A minimum lake stand of -330 m was reached at 47 ka BP and lasted for 3-4 ka. The maximum elevation of the lake was achieved at 27-23 ka BP, receding at 17-15 ka BP. A similar conclusion was derived by Bartov et al. (2002): From 55 to 30 cal ka BP, Lake Lisan fluctuated between -280 and -290 m, punctuated at 48-43 cal ka BP by a drop to at least -340 m. About 27 cal ka BP, the lake began to rise sharply, reaching its maximum elevation of about -164 m between 26 and 23 cal ka BP. At ~15 ka BP, the lake started to drop again until it reached -300 m. Bartov et al. (2002) presented a curve of Lake Lisan levels based on stratigraphic and chronologic correlation between Perazim and Massada profiles (Fig. 1.7).

The low resolution of the curve during the period 27-15 ka BP was attributed to the poor preservation of depositional indicators that onlap the escarpment (Bartov et al., 2002). However, the good preservation of shore line terraces overlapping the eastern escarpment of the Dead Sea paves the way to reconstruct the lake levels during this period more precisely.

Prasad et al. (2004) compared Lisan data with the oxygen isotope record from the Greenland ice shield and found a close link between climate in Greenland (North Atlantic) and the Eastern Mediterranean on decadal and centennial time scales in the period 26-17 ka BP.

Horowitz (1979, 1992) and Begin et al. (1974, 1985) related the palaeoclimate of Lake Lisan during the latest Pleistocene to the North European palaeoclimate with a cold and wet (pluvial) climate during the Glacial and a warm and dry (inter pluvial) climate during the Interglacial.

In contrast, Abed and Yaghan (2002) suggested a cold and dry climate for the Jordan Valley during the Last Glacial Maximum (LGM) similar to palaeoclimatic trends of monsoon-affected North Africa, Sahara, Arabia and SE Asia where cold climate associated with low precipitation and the expansion of desert conditions. Consequently, this may indicate that monsoon rain reached the interior southern Levant during the warm, wet periods. Here, we face two different conclusions. Therefore, investigations of the lake

terraces are needed in order to get more information on palaeoclimatic changes and compare them with palaeoclimatic data of other regions. This will help to understand whether the climate of the Lake Lisan basin was similar to that of monsoon-affected North Africa or to that of Europe and the North Atlantic.

Because of the absence of syndepositional faulting, Manspeizer (1985) concluded that the facies of the Lisan Formation reflects climatic rather than tectonic cycles. This conclusion was also reached by Frostick and Reid (1989). Langozky (1963) stated that “along the margins of the whole rift valley there is clear evidence that the Lisan Formation is undisturbed.” Bentor and Vorman (1960) suggested that the slumped layers represent soft sediment deformation features caused by slow transport.

However, El-Isa and Mustafa (1986) concluded that deformation features of the Lisan sediments such as faults, folds, fissures, slumps, etc. resulted from earthquake-induced deformation and mixing of the water-saturated bottom sediments of Lake Lisan.

Kouchy and Smith (1989) recorded a highstand (-100 m) of fresh water Lake Bisan (the Northern Part of Lake Lisan which extended from Lake Tiberias to Marma Feiyad). The southern outlet of this intermediate lake may have been structurally blocked by uplift in the Marma Feiyad area. This may have cut the flow of water to the Dead Sea region, causing a major fall in Lake Level to the south and a separation from the northern basin. However, there was not much research effort invested to find out whether the southern basin of the lake experienced also a highstand of -100 m or not. Therefore, this study should provide evidence on the lake highstands in the southern basin that helps to determine whether the separation was caused by a tectonic uplift of the northern basin or by a climatic-induced fall of the lake level.

Because of the existence of recent small deltas and the absence of Lisan age deltas at Wadi Al-Mujib and the other Wadis along the Dead Sea, Nir (1967) suggested down-faulting (post-Lisan) of the rift valley by several hundred meters. In contrast, our field investigation and analyses of aerial photos show Lisan age deltas in fronts of the main wadis such as Al-Mujib, Ma’een and Al-Shaqiq. Although much of these deltas were eroded by the rejuvenated west-draining wadis, the remaining parts are still exposed south of the main courses, suggesting a left lateral displacement, not a down-faulting.

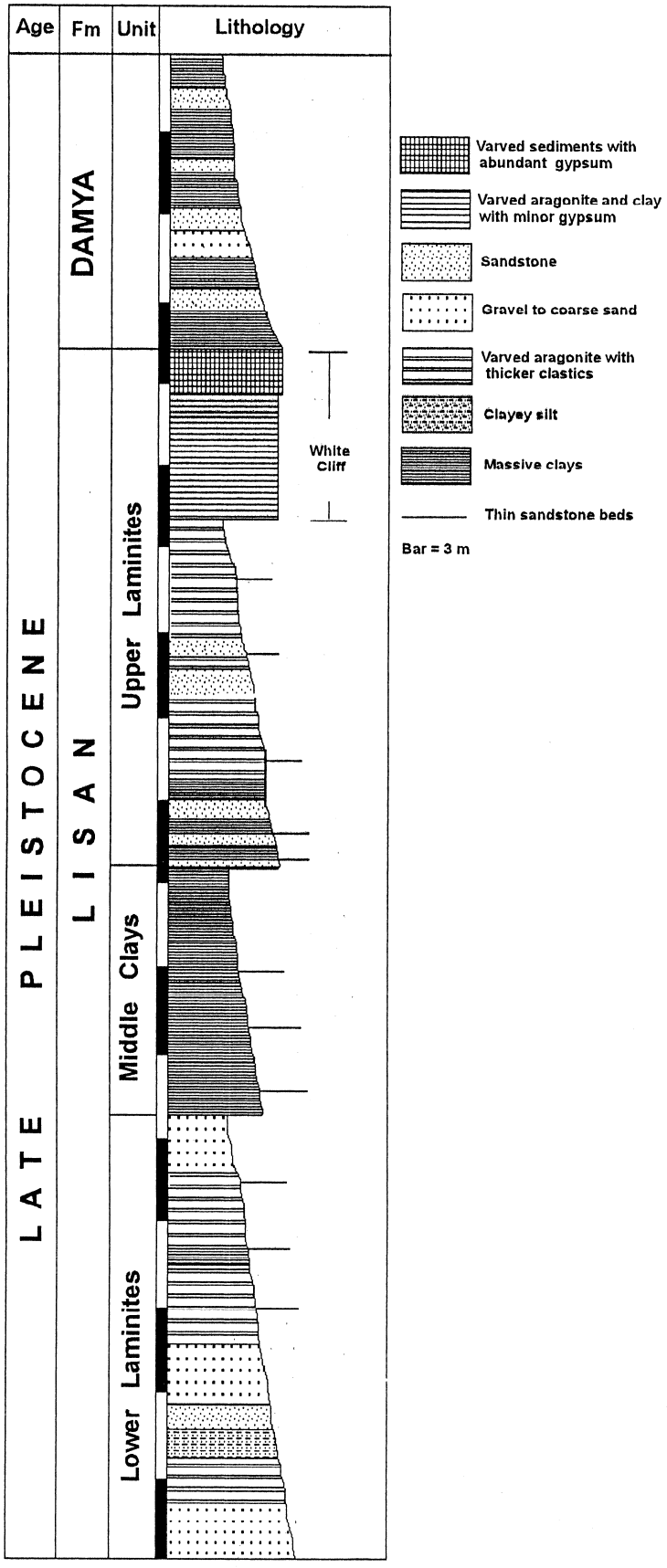

Fig. 1.4: Lithology of the Lisan and Damya Formations north of the Dead Sea at the Al-Karameh Dam site (Abed and Yaghan, 2000).

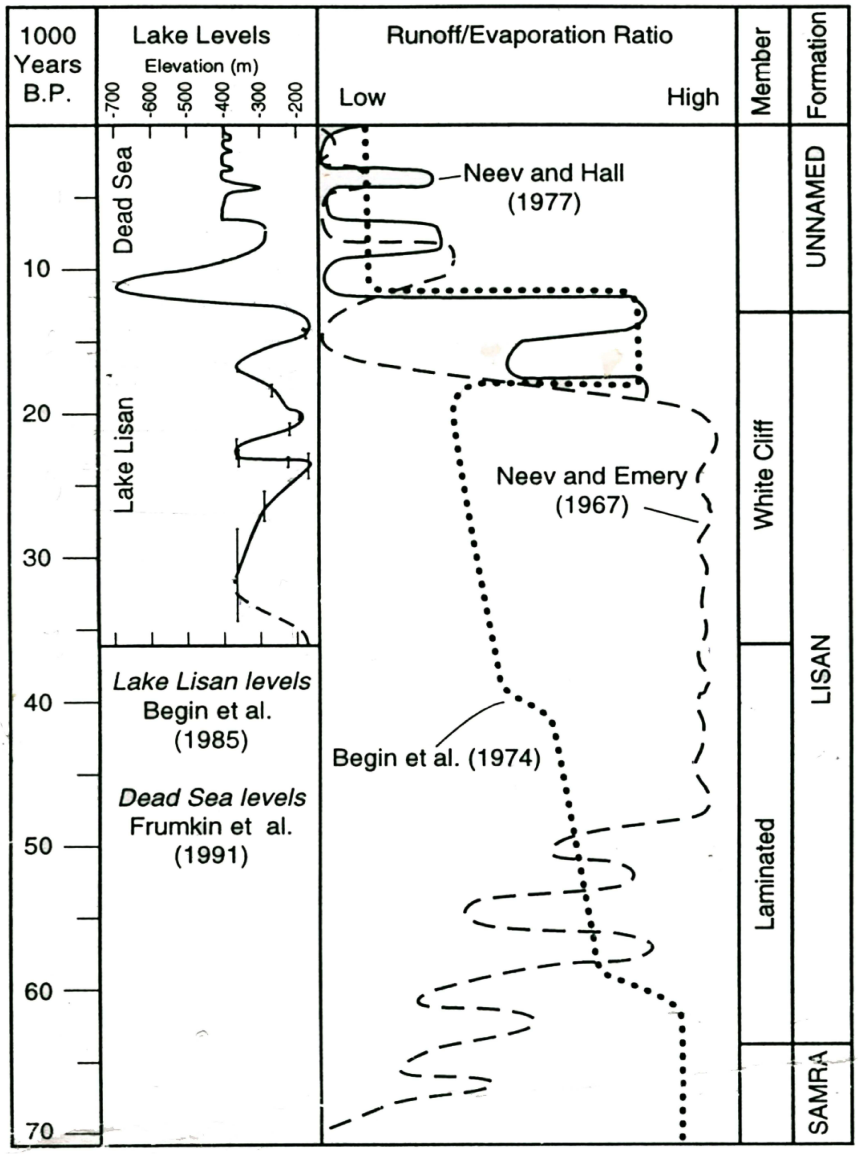

Fig. 1.5: Fluctuation curves of Lake Lisan level (after Niemi, 1997).

Al-Zoubi (2001) concluded that the Lisan salt diapir was formed during the Quaternary due to basin transtension and subsidence. He inferred that the diapir started rising during the early to middle Pleistocene as this section of the basin underwent rapid subsidence and significant extension of the overburden. Neev and Emery (1967) suggested that subsidence of the northern and southern basin of Lake Lisan occurred at the end of the Lisan Formation deposition leaving the Lisan Peninsula as a horst block. This subsidence was controlled both by faulting and by the diapiric rise of salt, and may have been responsible for the rapid recession of the Lake Lisan. Horowitz (1979) followed Neev and Emery (1967) by suggesting that the demise of Lake Lisan about 18 ka BP was caused by

tectonic subsidence. This opinion was also held by Begin et al. (1974), who described the maximum water depth of Lake Lisan as 200 m (between -180 and -380 m). Depending on the present elevation of the Dead Sea floor at -730 m, a subsidence rate of 19-29 mm/a is required for a 350 m drop of the basin floor from 18 to 12 ka BP (Niemi, 1997). However, this assumption seems not to be reasonable, since most researchers estimate the Dead Sea subsidence rate of 0.6-1 mm/a (Zak and Freund, 1966; Freund et al., 1970; Garfunkel et al., 1981; Joffe and Garfunkel, 1987).

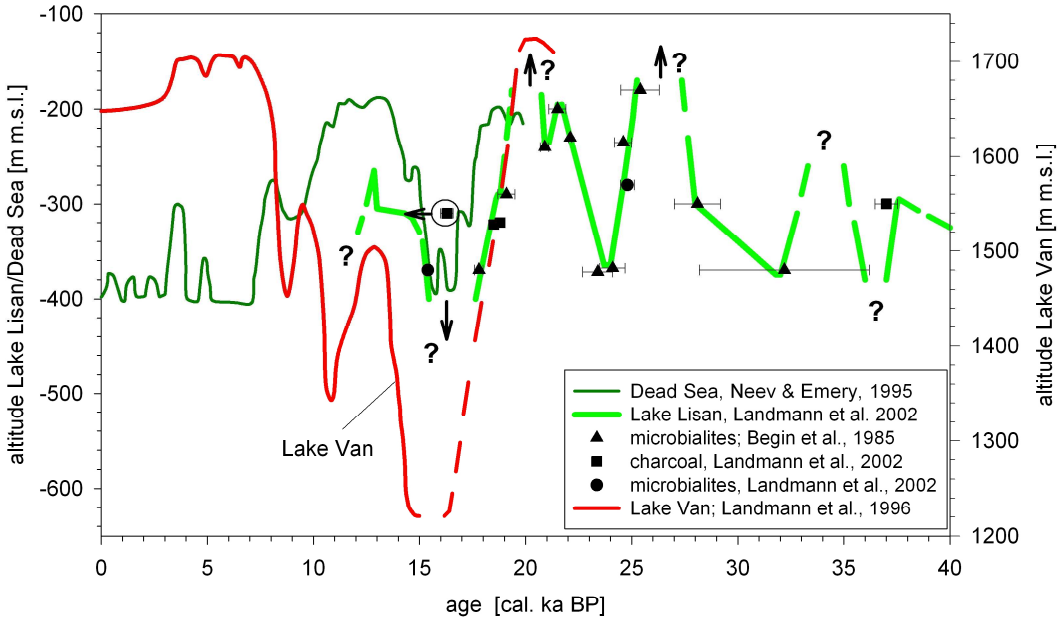

Fig. 1.6: Reconstruction of Lake Lisan/Dead Sea level curve in comparison with Lake Van level curve (Landmann et al., 2002).

The vertical displacement of the normal faults that were active during the Lake Lisan period at the Massada plain yielded an average subsidence rate of < 0.1 mm/a (Stein, 2001). Post Lisan and Holocene displacement recognised on the margin of the Massada plain yielded subsidence rates in the range of 0.3-0.6 mm/a (Bartov and Sagy, 2003). This is lower than the sedimentation rate calculated in the Ze'elim site (3-13 mm/a, Ken-Tor et al., 2001). This result implies that the tectonic subsidence has been compensated by the sediment accumulation at the margins of the Lake (Bookman et al., 2004). Therefore, further research on the morphological characteristics of the shoreline terraces are required

in order to determine the real contribution of the tectonic subsidence on the lake level lowering.

It is noticed that most of the pervious studies of Lake Lisan have been conducted on the western side, while very few studies covered the eastern side. Generally, the previous studies have used depositional environments and sedimentary stratigraphy as tools to reconstruct Lake Lisan levels and palaeoclimatic changes. None of the reviewed studies have used the terraces of Lake Lisan to achieve this purpose. Thus, our study is the first to use such a morphological approach. Since these terraces represent the actual positions of the lake levels, they promise to answer unresolved questions on Lake Lisan history and to fill some of the research gaps left by the previous studies.

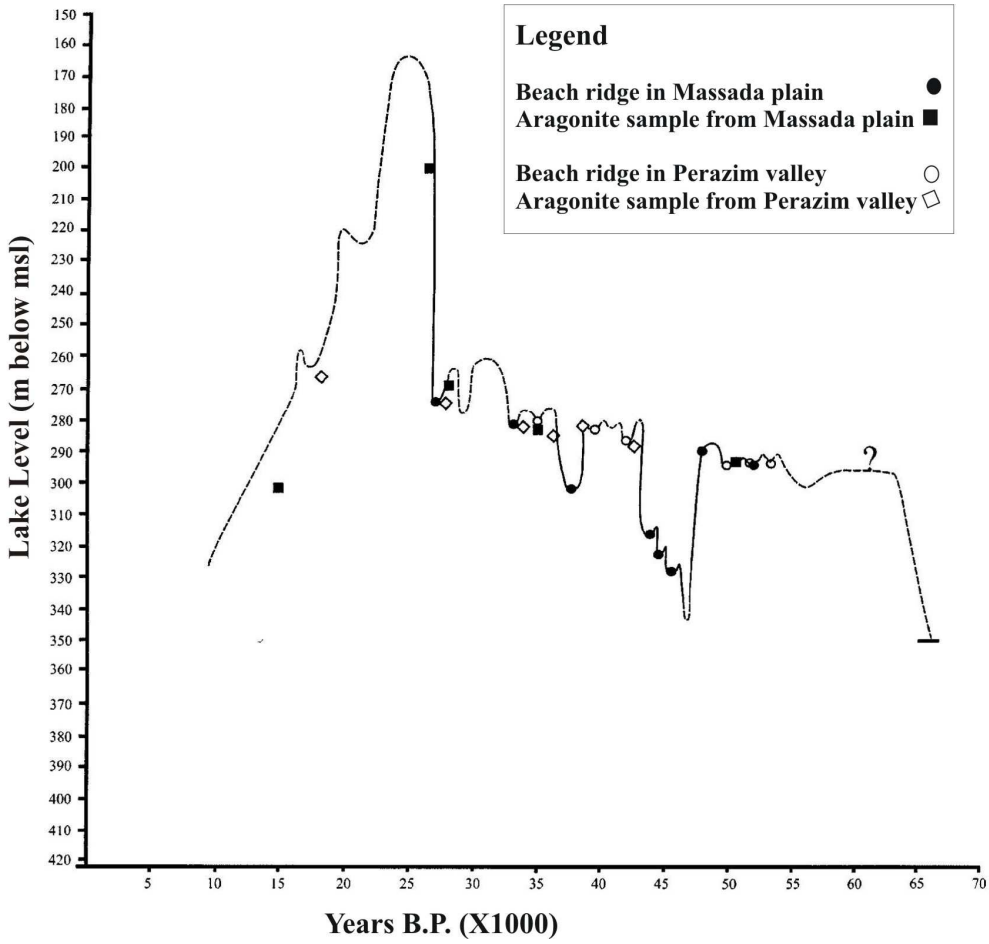

Fig. 1.7: Lake level curve of Lake Lisan between 55-15 cal ka BP (Bartov et al., 2002).

1.5 Scientific results of the thesis

Based on the results of the terrace research and of the Dead Sea Valley terrain model several publications in international journals and books appeared (Chapter 2: Abu Ghazleh et al., 2009; Abu Ghazleh et al., 2010; Chapter 3: Abu Ghazleh and Kempe, 2009; Abu Ghazleh et al., 2011, in press, see publication list). Two further papers are planned to be submitted within the next few months based on Chapter 4. Additionally the shrinking of Dead Sea and its implications has caused wide interest in these studies in the public media.

In this study, well-correlated and dated profiles of the modern shoreline terraces of the Dead Sea are presented for the first time. The timing and amplitude of the lake level changes recorded in these terraces forms an analogue to past level changes of the Dead Sea and even to level changes of other lakes. Furthermore, a terrain model of the Dead Sea Rift Valley was developed based on SRTM data that served as a tool to calculate the volume and area functions versus altitude. The model was further used in macro-engineering implications to calculate the water input requirements of the rapidly shrinking Dead Sea and to determine the capacity of the projected Dead Sea-Red Sea Canal. The terrain model could be also used to evaluate the water balance of the glacial Lake Lisan and as a useful approach for other lake basins.

Unlike the previous reconstructions of Lake Lisan history that were based on sequence stratigraphy, our study reconstructed the lake level changes based on the actual altitudes of the shoreline terraces and on the dating of their deposits. This enabled us to present a new curve of the lake level during the last glacial period, including new fixes on past lake level elevations as well as on the chronology of the regression and transgression cycles.
Thus, the present thesis highlights the potential of a geomorphological approach in reconstructing lake level changes more precisely.

Furthermore, the thesis answered some of the unresolved questions on Lake Lisan history and reduced the research gap of the previous studies as follows:

- The discovery of high level terraces of Lake Lisan at altitudes of -150 to 0 m along the eastern escarpment and the dating of their stromatolites, revealed the time and the elevation of the highest lake stand. This also clarified the previous doubt on the paleoenvironment conditions of the early stage of Lake Lisan as well as on the

transition period from Lake Samra to Lake Lisan. The newly discovered maximal level is 150 m higher than previously reported and occurred at the beginning of the last glacial period (79-76 ka BP).

- The morphological and chronological evidence presented in this study allowed generating a high resolution curve of the lake level for MIS 2 (~32-19 ka BP). It can now be assumed with certainty that the lake stood as high as -160 to -137 m during this period; this is in accordance with the LGM highstand of Lake Van (Turkey).

- Compelling evidence from the altitudes of the terraces and from their U/Th dates allowed correlating the levels of Lake Lisan with global climatic records. Transgressions of Lake Lisan occurred during the warm MIS 5 and 3 while regressions occurred during the cold MIS 4 and 2 as well as during the cold Heinrich events 6, 3 and 2. This demonstrates a strong linkage between the palaeoclimate of the Jordan Valley and monsoon-affected North Africa rather than that of Europe and the North Atlantic.

- Integration of morphological, chronological and sedimentological evidence presented in this study suggests that climate and not tectonics is the cause of lake level lowering.

2. Water input requirements of the rapidly shrinking Dead Sea

Abstract

The deepest point on Earth, the Dead Sea level, has been dropping alarmingly since 1978 by 0.7 m/a on average due to the accelerating water consumption in the Jordan catchment and stood in 2008 at 420 m below sea level. In this study, a terrain model of the surface area and water volume of the Dead Sea was developed from the Shuttle Radar Topography Mission (SRTM) data using ArcGIS. The model shows that the lake shrinks on average by 4 km^2/a in area and by 0.47 km^3/a in volume, amounting to a cumulative loss of 14 km^3 in the last 30 years.

The receding level leaves almost annually erosional terraces, recorded here for the first time by Differential Global Positioning System (DGPS) field surveys. The terrace altitudes were correlated among the different profiles and dated to specific years of the lake level regression, illustrating the tight correlation between the morphology of the terrace sequence and the receding lake level. Our volume-level model described here and previous work on groundwater inflow suggest that the projected Dead Sea-Red Sea channel or the Mediterranean-Dead Sea channel must have a carrying capacity of > 0.9 km^3/a in order to slowly re-fill the lake to its former level and to create a sustainable system of electricity generation and freshwater production by desalinisation. Moreover, such a channel will maintain tourism and potash industry on both sides of the Dead Sea and reduce the natural hazard caused by the recession.

2.1 Introduction

The Dead Sea surface is the lowest terrestrial point on Earth at 420.86 m below sea level as of 20 January 2008 (Arab Potash Company records) and it is shrinking rapidly. The salt concentration of 34% is already close to halite saturation. The Dead Sea occupies the central part of the Jordan Rift Valley and serves as a terminal lake for a catchment area of 40,650 km², with the Jordan River as the main tributary. It used to deliver 1.21 km^3/a (Salameh and El-Naser, 1999) to the Dead Sea, to which water of several wadis draining to the lake from the western and eastern peripheral mountains is added (Fig. 2.1 a).

The interest in the Dead Sea and its fate has been constant throughout history due to its prominent role in religious mythology. The first serious expedition was conducted by Lt. W.F. Lynch of the US Navy in 1848. With a blunderbuss-armed crew of 14 and two patent metal boats, he managed not only to establish the lake's altitude below sea level correctly but also to produce the first accurate map of the Jordan and of the lake and to measure its depth by plumbing (Lynch, 1854). The channel between the eastern Lisan Peninsula and the western Dead Sea bank, named Lynch Strait, was about 5 m deep in 1848 but is now more than 20 m above the current level. Since that time, the lake shrank from > 90 km in length to 52 km today. At the same time, a series of terraces was left along the shores evidencing the drop in water level (Fig. 2.1 b).

This study aims at: (a) developing a terrain model based on the SRTM data of the Dead Sea Rift that allows calculating the area and volume losses of the lake for the various stages of its recession; and (b) investigating the most recent changes in the Dead Sea level and the shore morphology by surveying the modern lacustrine terraces and dating them according to the Dead Sea hydrograph.

2.2 Materials and methods

Accurate level records are kept since 1976 by the Israel Hydrological Survey when the lake stood at -398 m. To calculate the volume and area loss functions of the Dead Sea, a model of the rift valley volume and surface area in meter intervals was developed from SRTM data (3 arc second; CIAT 2004). ArcGIS (3D)-Analyst (ESRI)-"Surface Volume" tool-functionality was used to calculate surface area and water volume of the Dead Sea below a certain altitude. The tool was applied for each meter change of the level from -389 to -415 m (Appendix 4). Since the bathymetric contours of the Dead Sea below -415 m are not available in the SRTM data, the water volume of the current Dead Sea of 147 km^3 (Dead Sea Data Summary. *International Lake Environment Committee Foundation*) was added to our calculated volume in order to determine the total volume of the Dead Sea. The calculated water volume and surface area were plotted against the altitude. Polynomial functions (1, 2) were derived using a least-square method.

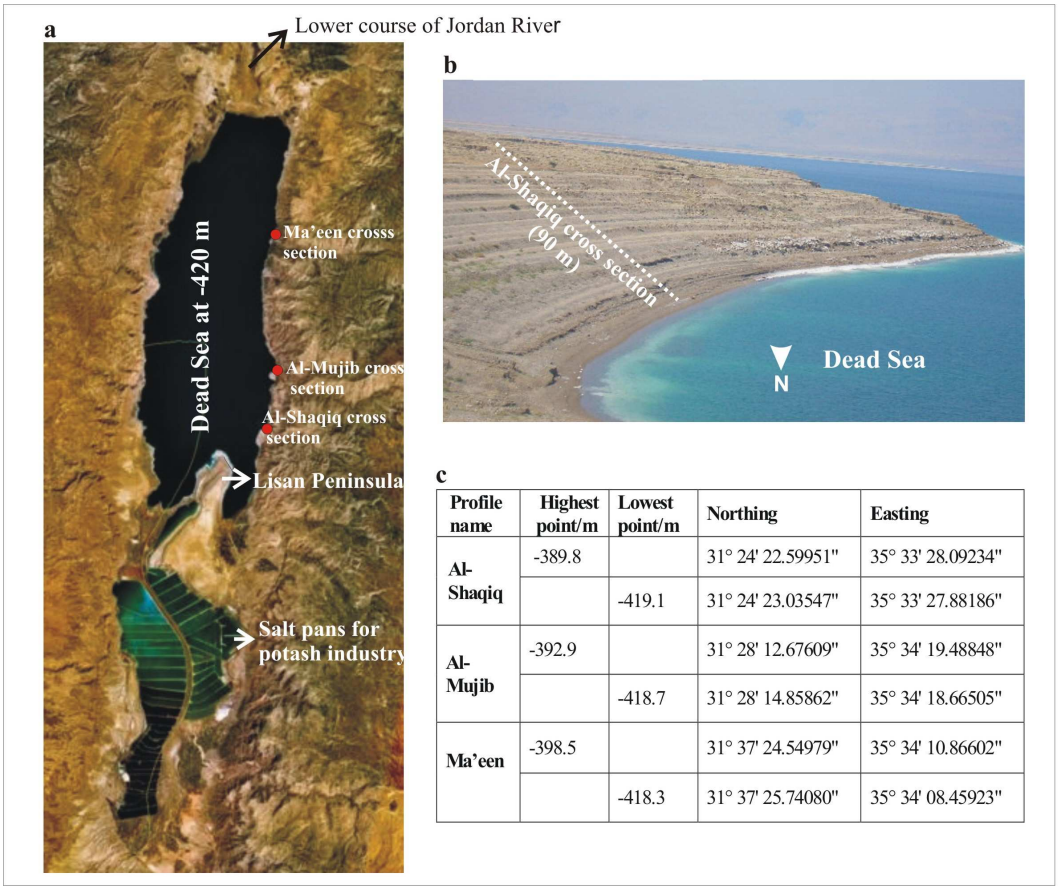

c

Profile name	Highest point/m	Lowest point/m	Northing	Easting
Al-Shaqiq	-389.8		31° 24' 22.59951"	35° 33' 28.09234"
		-419.1	31° 24' 23.03547"	35° 33' 27.88186"
Al-Mujib	-392.9		31° 28' 12.67609"	35° 34' 19.48848"
		-418.7	31° 28' 14.85862"	35° 34' 18.66505"
Ma'een	-398.5		31° 37' 24.54979"	35° 34' 10.86602"
		-418.3	31° 37' 25.74080"	35° 34' 08.45923"

Fig. 2.1 a: Location of the Dead Sea and the measured terrace profiles. The image was taken from w.NASA World Wind. b: Recent Dead Sea terraces north of Wadi Al-Shaqiq fan delta. c: The coordinates of the highest and lowest points of the surveyed profiles.

In order to investigate the terraces formed by the lake level drop, we used aerial photos of 1:25,000 (Royal Jordanian Geographical Centre) to pinpoint the locations of the most continuous and best preserved sequences of terraces.

Then, a field survey of the eastern coast of the Dead Sea was conducted to examine the suitability of the chosen sites for cross-section measurements and to determine the location of the Global Positioning System (GPS) benchmarks available in the area. The benchmark of Ghour Hadithah (31°17′21″.7455 N, 35º32′09″.13807 E and -346.428 m) was chosen for the DGPS base station. Three profiles of the Dead Sea terraces were surveyed with the DGPS rover (Leica SR-20). These are the profiles at (1) Al-Shaqiq in the northern part of the Wadi Al-Shaqiq fan delta, (2) Al-Mujib in the northern part of the Wadi Al-Mujib fan delta, and (3) Ma'een, north of the Wadi Ma'een fan delta (Fig. 2.1 a).

Two GPS altimetry points were measured on each terrace; each was occupied for 15 min for high accuracy. The measured data were then processed using Leica Geo Office (LGO)

software in order to obtain accurate altitude, latitude, and longitude. The coordinates of the measured profiles are presented in Fig. 2.1 c.

In addition, the width and slope of the terraces were measured using tape and inclinometer. The terrace altitudes were correlated among the different profiles and dated to specific years of the lake level regression according to the hydrograph of the Dead Sea as made available by the Hydrological Survey of Israel (personal communication, Eliyahu Wakshal, The Hebrew University of Jerusalem) and previous publications.

The data of the shore terrace levels and their morphology were derived from the three terrace profiles that represent the sample population. The target population consists of all lake terraces. The sites of the profiles were selected to represent the best continuous and best preserved terrace series, as well as the different parts of the lake (north, center, and south). However, it was difficult to select the sites using probability sampling because the terraces vary in their degree of preservation and lateral continuation. The profiles represent a large enough sample of the terraces, i.e., $n = 68$. Since the sample population is large enough and the current lake represents one water body experiencing similar regression rates in its different parts, the obtained conclusions from the measured profiles can be extended to the whole lake basin.

2.3 Results

2.3.1 Surface area and water volume of the Dead Sea

The level of closed lakes - such as the Dead Sea - is a result of the hydrological balance between runoff into the lake plus direct precipitation on the lake surface minus evaporation; therefore, it serves as an indicator of climatic conditions. However, the recent Dead Sea level change (and its associated changes in surface area and volume) is mainly due to (a) transferring 500 Mio m^3/a of water from the upper Jordan River by the Israel National Water Carrier project to the Mediterranean coastal plain; (b) diverting an additional water amount of 75 Mio m^3/a from the Yarmouk River to the same carrier; (c) diverting 110 Mio m^3/a of the Yarmouk River water to the King Abdullah Channel in Jordan and an additional 135 Mio m^3/a from the same resource by Syria; (d) consuming (cumulative from 1976 to 1997) 2.4 km^3 of the surface and ground water inflow to the Dead Sea from the eastern coast and Wadi Araba by Jordan and 3.3 km^3 from the same resource in the western side by Israel; and (e) abstracting 5 km^3 from the Dead Sea water

for the potash industry by both Israel and Jordan (Salameh and El-Naser 1999; Al-Weshah 2000). The level change is therefore mainly due to human water consumption and not a result of climate change.

The terrain model shows that water volume and surface area correlate highly with lake level (volume R^2=0.9993, area R^2=0.9899; Fig. 2.2 a, b) reflecting the bathymetry of the flanks of the former Dead Sea and the morphology of the rift valley, according to Eqs. 1 and 2 developed based on our model.

$$WV = 0.0077x^2 + 6.8905x + 1{,}688.8 \quad (1)$$

$$SA = -0.373092x^3 * 10^{-5} - 0.173775x^2 * 10^{-2} + 10.2099x + 4990.43 \quad (2)$$

Where

WV: Water volume (km^3)
SA: Surface area (km^2)
x: altitude below sea level (m)

According to our GIS data analysis, the Dead Sea has lost 9.7 km^3 (0.2 km^3/a) from its volume and 365 km^2 (7.9 km^2/a) from its area during the period between 1932 and 1978. Since 1978, the volume decreased dramatically from ~157.7 to ~147 km^3 with an average of 0.47 km^3/a (Fig. 2.2 a, b). Meanwhile, the surface area shrank from 729.4 to 636.7 km^2 with 4 km^2/a on average. The recession of the lake level caused additional groundwater inflows of about 0.5 km^3/a (Salameh and El-Naser, 2000). This, plus our calculated volume loss, suggests that surface water inflow has to increase by more than 150% or by ~0.9 km^3/a, in order to stop the continuous drop of the Dead Sea. However, this is unlikely to happen due to the current intensive consumption of water resources in the Dead Sea basin that is still increasing, e.g., by recent migrations to Jordan from Iraq and Lebanon.

2.3.2 Shoreline terraces and level changes

The wadis draining to the Dead Sea experienced rapid erosion due to the lowering of the base level during the Holocene. Consequently, Gilbert-type fan deltas (consisting of horizontally bedded bottomsets that deposited radially in front of the river mouth, basinward-dipping foreset beds that prograde from the river mouth and horizontal topset beds which result from the river downcutting and advance of the channel deposits; Richard and Davis, 1985) were formed in front of the mouths of the main wadis such as

Al-Mujib, Al-Shaqiq, and Ma'een (Fig. 2.3 a). These unconsolidated delta bodies are now emerging from the receding lake. Wave action has cut a unique set of shoreline terraces into these deltaic, lacustrine-alluvial foreset deposits composed of gravel and sand (Figs. 2.1 b, 2.3 a). Each terrace consists of a sub-flat foreshore (tread) and a steep backshore cliff (riser). Widths and slopes of the treads show normal distribution with averages of 1.68±0.8 m and 4.5°±1.2°, means and standard deviations, respectively. Although the widths of the risers show also normal distribution with an average of 1.91±1.2 m, the slopes of the risers show non-normal distribution with an average of 24.4°±6.6°.

a

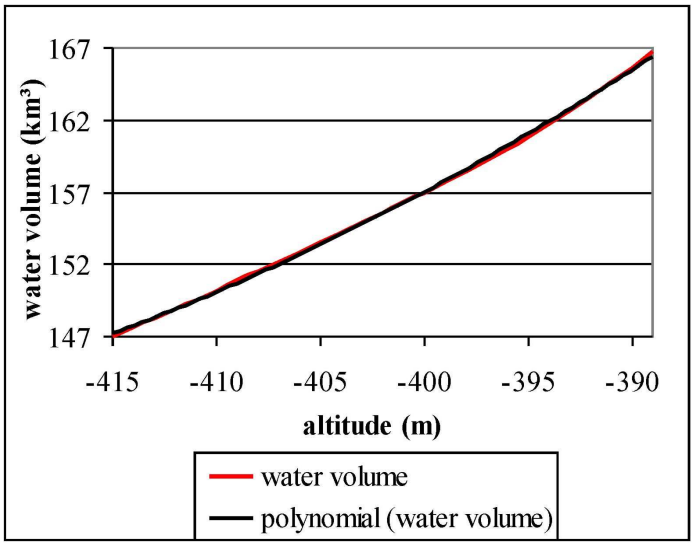

b

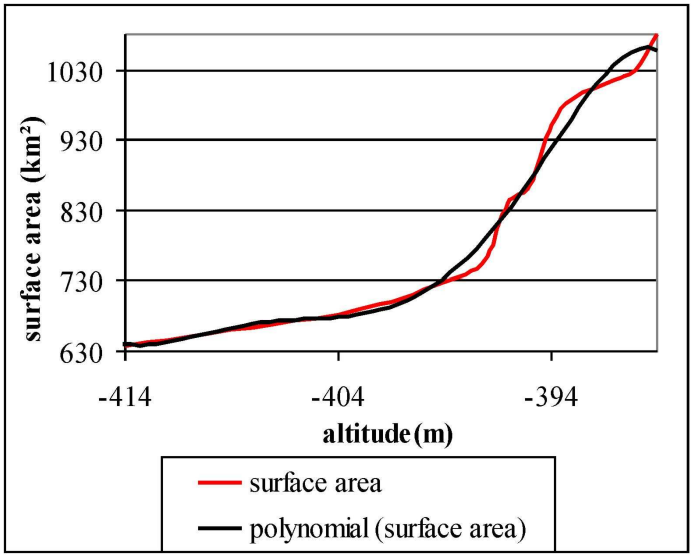

Fig. 2.2 a: Volume-altitude relation of the Dead Sea. b: Surface area-altitude relation of the Dead Sea.

These terraces are not long-living since the wadis have already started to cut into the topsets of the delta bodies, creating new streambeds with migrating mouths (Fig. 2.3 a).As it turned out, the best preserved terrace profiles all are along the northern corners of the deltas. This is possibly because the wadis tend to discharge their water near the apex of the delta and because winter storms have a northwesterly direction so that the waves are more intensive on the northern shores of the deltas, compared to their southern banks. It is interesting to note that the delta bodies do not show any morphological traces of recent movements of the eastern boundary transform fault of the Dead Sea pull-apart structure that should run through the landward section of the deltas (Fig. 2.3 a).

In Fig. 2.3 b, the three terrace profiles are compared and their terraces correlated. These terraces were formed during the last 77 years as a result of a lake level drop of 30 m with an average of 0.4 m/a. Recorded levels (Klein, 1986; Hassan and Klein, 2002; Hydrological Survey of Israel) suggest that the highest terrace at -389 m formed in 1932 (and previous years). The recorded level curve allows correlating most of the terraces to specific years. The lowest here documented terrace at -419 m formed in winter 2006-2007 (Fig. 2.3 b). Levels stagnate in winter when more water input occurs and recede most steeply in summer during times of high evaporation. Some years show a more pronounced recession than others but many of the terraces represent one winter season only.

The comparison between the Dead Sea hydrograph and total annual precipitation (Fig. 2.4) shows that changes in rainfall do not contribute significantly to lake level changes. For instance, the Dead Sea continued its rapid lowering in 1997 in spite of the high precipitation amount of 849 mm compared to 571 in 1996. Only exceptional high rainfall such as in 1991 and 1992 (915 and 1,038 mm, respectively) was able to cause a noticeable rise in the lake level of 2 m. This wet event destroyed any pronounced terraces in this period by the lake level rise (Fig. 2.3 b).

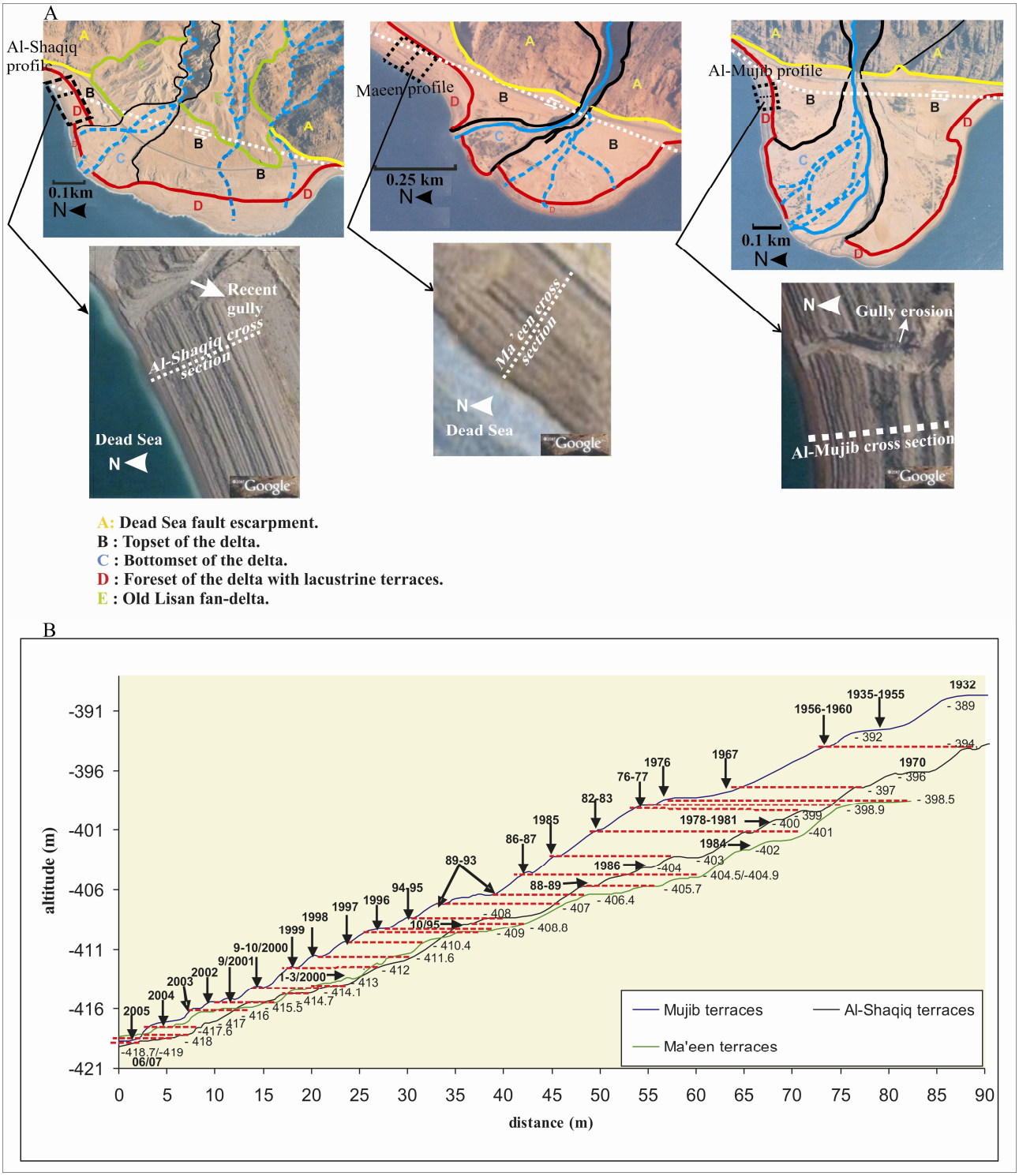

Fig. 2.3 a: Gilbert fan deltas and sequences of lacustrine terraces north of Wadi Al-Shaqiq (*upper left*), north of Wadi Ma'een (*upper middle*), and north of Wadi Al-Mujib (*upper right*). Note roads crossing the deltas on the landward sections at positions near to the presumed trace of the Dead Sea eastern boundary transform fault. The *lower images* in this figure were taken from Google Earth. The date of these photos is 16 January 2007 http://earth.google.com. b: Three profiles of Dead Sea terraces surveyed by DGPS, correlated among each other and dated according to the recorded Dead Sea levels.

The average of lake level recession increased in rate throughout time: From 1932 to 1977, the Dead Sea level dropped relatively slowly from -389 to -399 m with an average of 0.2 m/a. In this relatively long period, only seven larger terraces can be recognised in the different profiles. This could be due to the prolonged times of stable water level that allowed the waves to abrade wide terraces. The intensive water consumption in the Dead Sea basin in the last 29 years caused an accelerated drop from -399 m in 1978 to -419 m in 2007 with an average of 0.7 m/a. In this short period, 25 terraces formed, but with smaller dimensions. This is interpreted as a result of the fast recession and of the short period of constant water level that has not allowed the waves to form wide terraces.

Moreover, the low-level terraces are less affected by rill erosion and gravitational mass movements due to the short time of their exposure and due to their wetness (caused by sea spray) compared to the high-level ones. This explains the good correlation between the low-level terraces and the poor correlation between the high-level ones. Furthermore, it implies a relation between the age of the terraces and their degree of preservation.

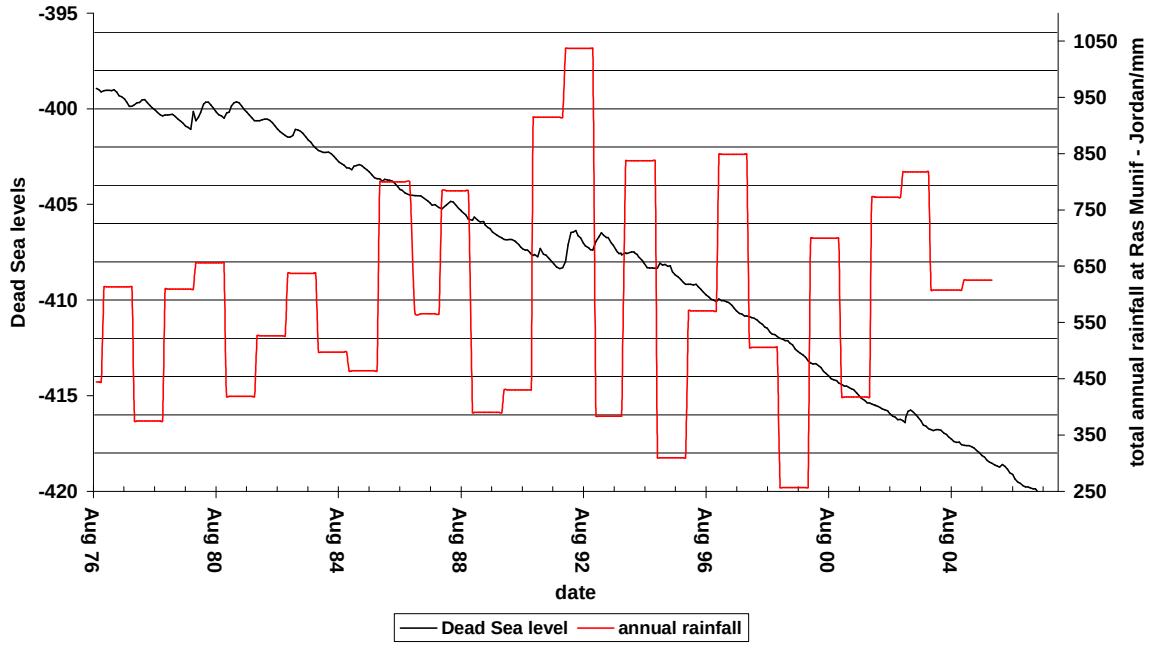

Fig. 2.4: Dead Sea hydrograph (Hydrological Survey of Israel) and total annual rainfall in Ras Munif/Jordan (Jordan Metrological Department).

2.4 Discussion

The hydrological balance of the Dead Sea significantly changed since the beginning of the twentieth century mainly due to (a) the consumption of water from the Jordan River and other tributaries for irrigation, and (b) the use of the Dead Sea water for potash industry. Our terrain model of the Dead Sea shows that water volume and surface area correlate highly with lake level throughout the observation period, reflecting the basin morphology of the Dead Sea Rift Valley. These equations allow calculating volume and area losses from lake level curves: During the last 30 years, water consumption caused an accelerated decrease in the water level, volume, and surface area amounting to 0.7 m, 0.47 km³, and 4 km² per year, respectively. Based on the assumption that the basic morphology of the lake's basin will not drastically change within the next decades, the polynomials can also be used to predict near-future volume and area losses. Thus, in 2020, the lake will have dropped presumably to -427.8 m and will have lost 5.6 km^3 and 48 km^2 of its current volume and area, respectively.

The rapid drop of the Dead Sea level is accompanied by the formation of new shoreline terraces as well as it causes rapid erosion of the topsets of the emerging deltas. Wide terraces reflect a slow drop rate and a longer time of water level stability, while narrow terraces represent a fast drop rate and shorter times of water level stability.

The declining water level has caused and will continue to cause severe detrimental effects both to its function as a resource and to the natural state of its shores. These effects include:

- Higher pumping costs for the factories using the former southern sections of the Dead Sea to extract potash, salt, and magnesium.
- An accelerated outflow of fresh water from surrounding aquifers, thus causing a loss of this important resource.
- The receding shoreline makes it difficult (and in some places even dangerous) for tourists and hotel guests to access the water of the Dead Sea for medical bathes.
- The freshwater outflow has enhanced the dissolution of buried salt deposits creating a treacherous landscape of sinkholes and mud along the entire shore of the

Dead Sea (Closson et al., 2005; Yechieli et al., 2002, 2004) that caused severe damage to roads, salt pans, and other civil engineering structures.

- The rapid emergence of delta bodies and the thereby caused decrease in buoyancy could cause sudden (or earthquake-triggered) slips (mass waste movement and landslides, such as what happened in the north of the Dead Sea in 2000) of sections of the deltas with the prospect to trigger small tsunamis within the lake.
- The rapid downcutting of the west-draining wadis due to the lake level lowering threatens the bases of the bridges built at the mouths of these wadis.
- The lake could soon become halite-saturated, causing incrustation along its entire perimeter (today only spray water forms intermittent salt deposits).

Given the mounting stress on the water resources in the Dead Sea basin and the environmental hazard caused by its lowering, two projects were suggested to maintain the Dead Sea and stop its lowering: the Red Sea-Dead Sea Channel (RSDSC) and the Mediterranean-Dead Sea Channel (MDSC). Two alignments were suggested for the MDSC: in the north from the Mediterranean coast through Bet She'an to the Jordan River and in the south from the Gaza strip to Masada at the Dead Sea (The Harza JRV Group, 1996). Although the northern route of the MDSC is the shortest and the cheapest one, the RSDSC would be under the control of all riparian countries, and its benefits could therefore be distributed fairly. Such projects cannot only stop the level decrease, but can also exploit the net altitude difference of 400 m to produce energy and hence freshwater by desalinisation. It also introduces new salt to the lake, ensuring the long-term sustainability of the salt extraction.

However, one of the long-term negative impacts of the channel might be the continuous infiltration of seawater into underground aquifers. Since this would diminish energy output, the channel should be planned with an impermeable bed to begin with. Possible ruptures of the RSDSC bed during earthquakes along the Dead Sea Fault would not be such a risk since the channel would be segmented by pumping and turbine stations, thus sections of it could temporarily be emptied and repaired. Based on the water volume loss calculated by our model and the ground water inflow to the Dead Sea, we suggest that the RSDS or MDSC should have a capacity of more than 0.9 km^3/a in order to slowly fill the lake back to levels as of 30 years ago and to ensure its long-term sustainability.

If the diversion of Jordan water to the Mediterranean coast would be stopped (replacing the water need by desalinisation of seawater), then the recession of the Dead Sea could be considerably slowed, buying time to consider the long-term alternatives.

Acknowledgements

The field work for this research was made possible by grants from the Deutsche Akademische Austauschdienst (DAAD) and the Deutsche Forschungsgemeinschaft (DFG-Ke-287/28-1). We thank Prof. E. Wagshal, Jerusalem, for providing the Dead Sea hydrograph; Prof. I. Sass, Darmstadt, for the DGPS equipment; Prof. A. Al-Malabeh, Al-Zerqa', and Dr. M. Nawasrah, Amman, for fieldwork support; and Dr. M. Abo Kazleh for assistance in the field work and GPS postprocessing. We also thank the Natural Resource Authority, Amman, for allowing us to use their GPS base station and field house at Ghour Al-Hadithah.

3. Geomorphology of Lake Lisan terraces along the eastern coast of the Dead Sea, Jordan

Abstract

Lake Lisan, the lake that filled the Jordan graben during the Last Glacial, left behind a well developed sequence of erosional and depositional shore terraces in the south east of the current Dead Sea. These terraces record a series of stillstands that were caused by small transgressions within an overall trend of falling lake levels. The terraces were observed in places where they had not been identified previously. The morphology of the terraces was investigated in six cross-sections using differential GPS altimetry. The levels of the terraces range between -370 and -148 m a.s.l. The high stand of Lake Lisan at -148 m correlates well with the high level of -150 m reported by Bowman and Gross (1992)

The lake terraces are horizontal, elongated and tectonically undisturbed, and have a sub-horizontal foreshore (tread) with an average slope of 8.2° and steep backshore cliff (riser) with an average slope of 17.7°. The six cross-sections show a good altitudinal correlation between their terraces. Moreover, the terraces appear in undisturbed continuity on the aerial photos. These morphological characteristics demonstrate that the retreat of the lake was a result of substantial climatic changes, not of tectonic subsidence.

Autochthonous stromatolites were found on most of the terraces, reflecting a shallow water environment and emphasizing that these terraces are recessional. Well developed desert varnish and Tafoni observed on blocks sitting on the terrace surfaces imply a long period of exposure and a low rate of post lacustrine erosion. The formation of Lisan terraces is constrained mainly by coastal slope, water depth and underlying lithology. The morphological analysis of these terraces allows identification of two kinds of pseudo-terraces, which were formed as a result of tread or riser destruction.

U/Th and OSL dating allowed the dating of three events within the lake level curve more precisely. The high level of -148 m occurred at 30.5 ± 0.22 ka BP, coinciding with the Heinrich Event 3 and Dansgaard-Oeschger stadial 5, the coldest period in the North Greenland Isotope (NGRIP). The next lower terrace at -154 m was formed at 22.9 ka BP ± 0.29 and corresponds to the stadial 2C, the final phase of the Last High Glacial.

The correlation between the Lisan high stands and climatic stadials suggests that Northern-Hemispheric cold periods led to periods with a more positive water balance in the Near East. At ~ 10 ± 0.8 ka BP Lake Lisan experienced a sharp drop to -200 m followed by a transgression between 9.5 to 7 ka BP.

3.1 Introduction

Lake Lisan was one of a series of lakes that filled the Dead Sea depression between 63-15 ka BP (e.g., Kaufman, 1971; Kaufman et al., 1992; Schramm, 1997; Schramm et al., 2000). It extended for 300 km from Lake Tiberias in the north to about 60 km south of the present Dead Sea (Begin et al., 1985) (Fig. 3.1). The lake left characteristic deep-water deposits consisting of series of mostly laminated aragonite and gypsum strata known as the Lisan Formation (e.g., Landmann et al., 2002).

Lake Lisan experienced a transgression and reached a level of -160 m (i.e., below sea level) at about 27 cal ka BP (Bartov et al., 2002; Matmon et al., 2003). Then it started to drop and reached -300 m at about 15 cal ka BP (Bartov et al., 2002). This drop is recognised by a sequence of deposits and paleoshoreline terraces that provide an integrated proxy with which to determine the lake level changes and to evaluate hydrological changes, tectonic activities and palaeoclimatic conditions during and after the Last Glacial. High Glacial lake levels are also reported from other Near East lakes, such as Lake Van, Eastern Anatolia (Kempe et al., 2002).

3.2 Previous studies

Previous authors mentioning Lake Lisan terraces were Huntington (1911), Butzer (1957), and Bender (1968). Blankenhorn (1912) measured the altitude of the terraces up to 70 m above the Dead Sea level, and concluded that they were not horizontal due to tectonic activity. In contrast, Neev and Emery (1967) found that the terraces were horizontal and undisturbed. Picard (1943) found the highest terraces near Jericho at an altitude of -200 to -210 m and regarded the terraces as recessional. The most recent and detailed study on the Lisan terraces was done by Bowman (1971) on the western coast of the Dead Sea. He investigated the terraces with the aid of a level in three cross-profiles.

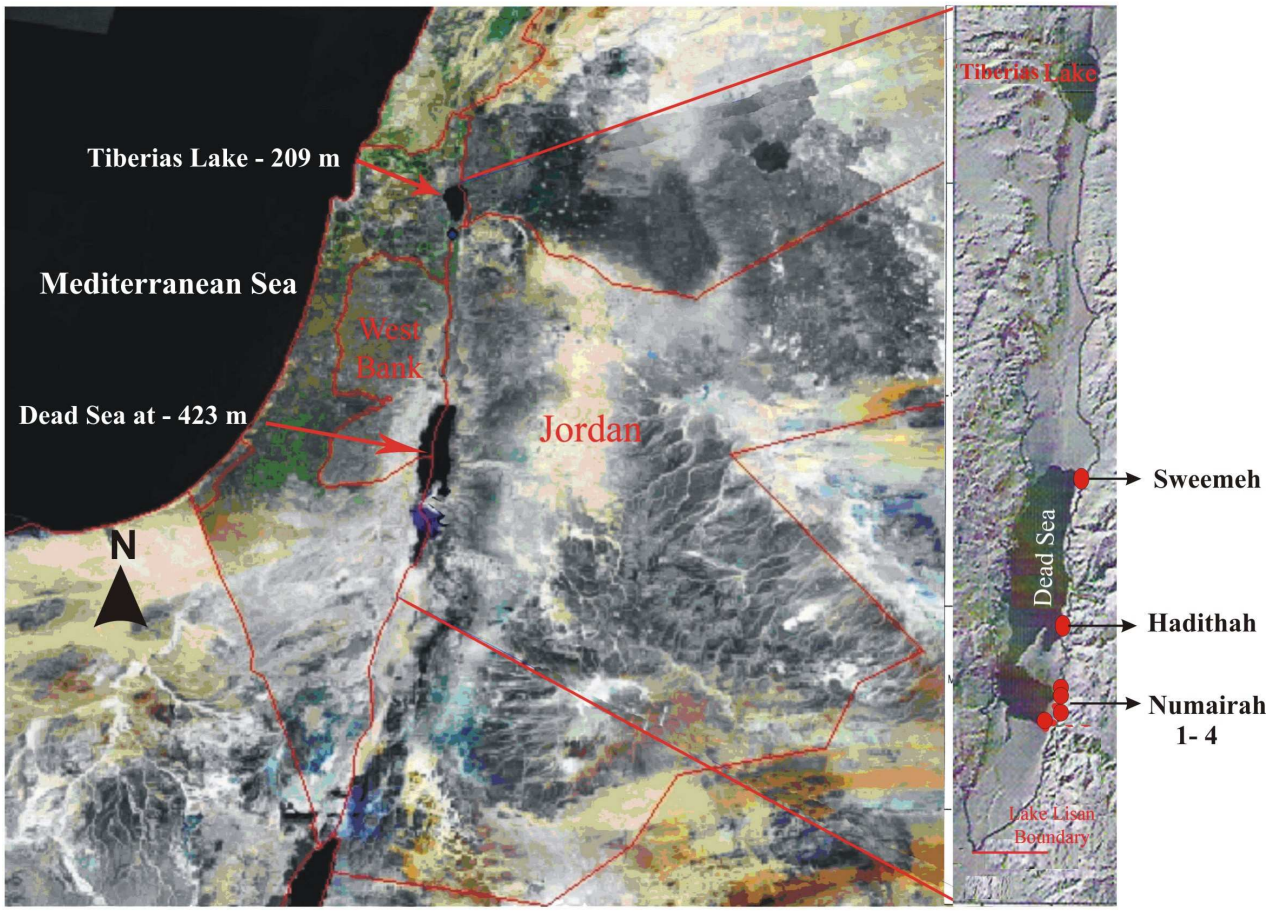

Fig. 3.1: Location of the Dead Sea (left) (ESRI, 2006), Lake Lisan and the cross-sections (right) measured along the eastern side of Jordan graben (Lisan boundary from Begin et al., 1985; shaded topography from Hall, 1993).

The three profiles have been integrated into one generalised profile consisting of 28 individual terraces, ranging in altitude between -380 and -180 m. The terraces were found to be horizontal and undisturbed, indicating that they were not affected by tectonic activity. Bowman divided each terrace into tread and riser that exhibit a definite geometrical relationship to each other (Fig. 3.2). A sequence of high beach bars was found by Bowman and Gross (1992) along the south-western boundary of Lake Lisan. They range in altitude between -180 and -150 m and suggest the highest stand of Lake Lisan at -150 m instead of -180 m. It should be noted that very few studies have dealt with Lake Lisan terraces. Moreover, the previous studies were carried out only on the western side of the Lake Lisan, while no study thus far has been conducted on the terraces in the eastern part and no attempt has been made to date them.

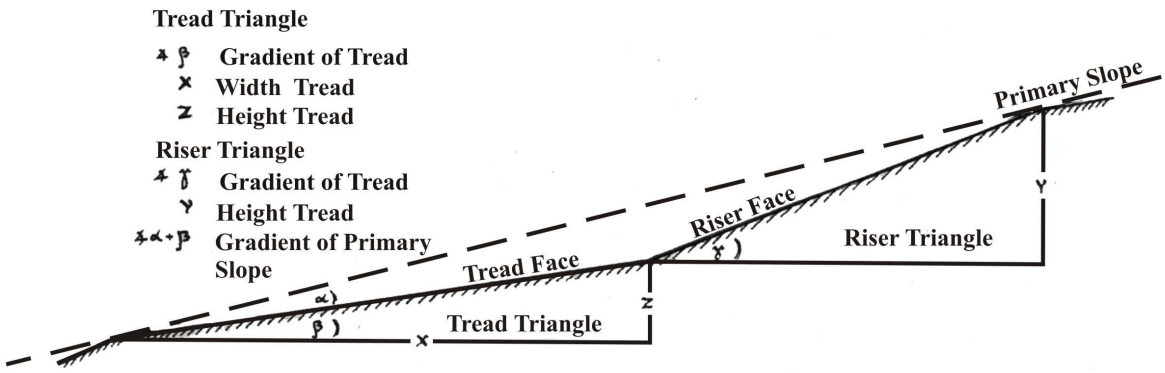

Fig. 3.2: The geometry of terraces after Bowman (1971).

3.3 Aims

This study aims to investigate the geometrical, morphological and sedimentological characteristics of Lake Lisan terraces along the eastern side of the Jordan Graben in order to: (a) obtain additional water level data; (b) reconstruct the lake level changes; (c) determine the main geomorphologic processes that formed these terraces and contributed to their development or destruction during and after the lake lowering; and therefore (d) obtain indicators of the climatic conditions and possible tectonic activities influencing the terraces during the Late Pleistocene.

3.4 Geological and regional setting

The left-lateral Dead Sea Transform Fault (DSTF) separates the northward-moving Arabian plate from the stationary Sinai-Palestine subplate, a northern extension of the African plate. It can be followed from the northern end of the Red Sea to southern Turkey for over 1100 km. The Jordan Valley is the morphological consequence of a series of pull-apart basins along the DSTF. One of the pull-apart basins is the current Dead Sea. To the east of DSTF, basement rocks, covered by Cambrian dolomite, silt- and sandstones have been uplifted. Branches of the DSTF cut through the Cambrian formations, off-setting them by hundreds of meters. Two of these faults, striking NE-SW (Powell, 1988), form Al-Tayan Valley, along which the members of the Burj-Formation reoccur several times at different altitudes (Fig. 3.3). The oldest bedrock in the study area is the Salib Arkose from the early Cambrian, which consists of coarse-grained arkosic sandstone (Fig. 3.4). This formation crops out as steep cliffs along the coast of the Dead Sea, particularly north of Wadi Numairah.

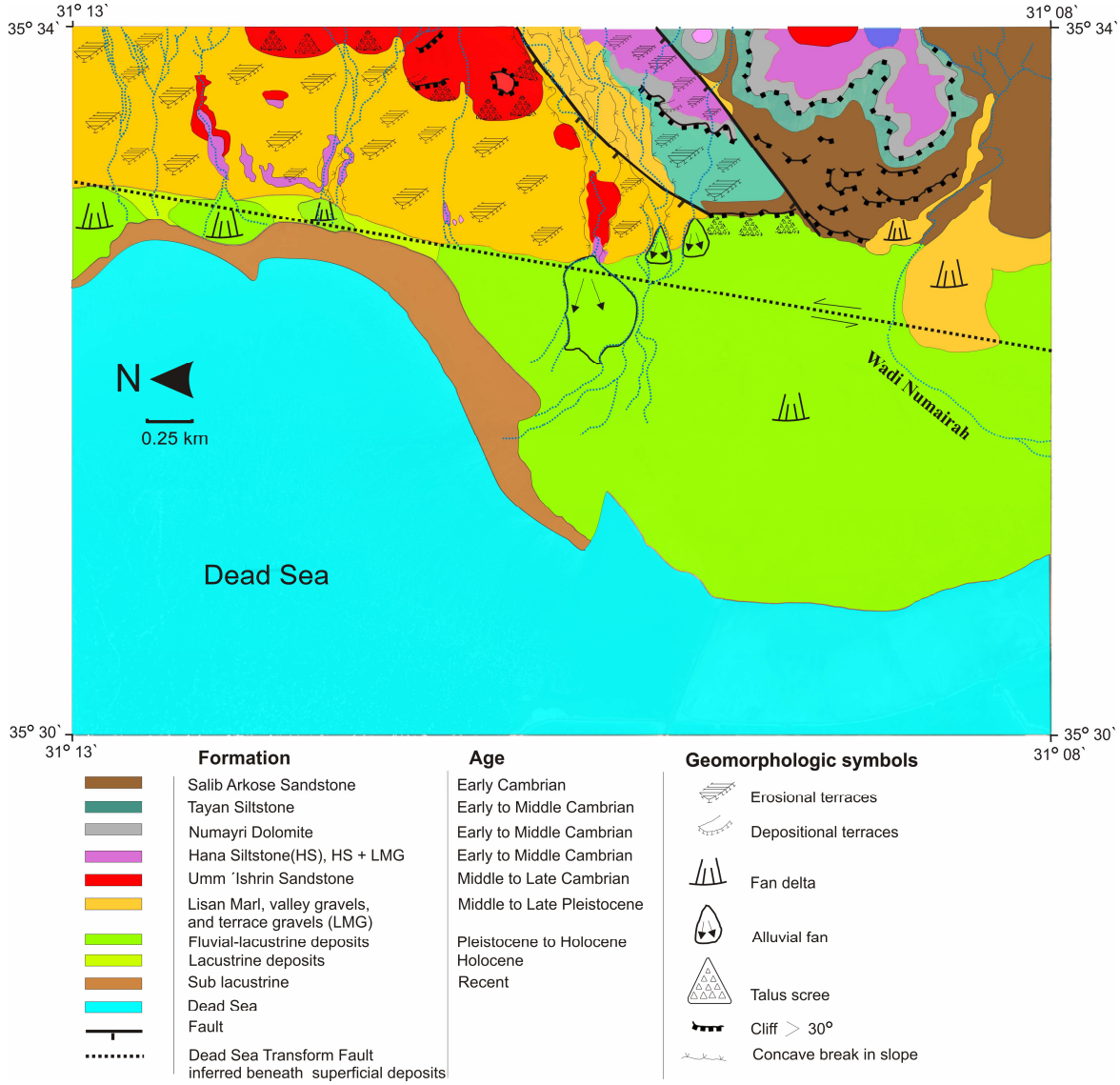

Fig. 3.3: Geological and geomorphological map of the study area according to Al-Karak sheet 1987, aerial photos 1: 25,000 and own observations.

The overlying Burj Dolomite-Shale Formation from the middle Cambrian consists of three members: at the base, the Tayan Siltstone is exposed along Wadi Al-Tayan; in the middle, the Numayri Dolomite crops out between Wadi Numairah and Wadi Al-Tayan forming prominent, brownish-weathering cliffs; and on the top, the Hannah Siltstone is exposed south of Wadi Al-Tayan and north of Wadi Numairah (Powell, 1988). In the same area, small exposures of the Tayan and Hannah members are present along wadis eroded through the overlying sediments. The Hannah member is overlain by the red-brown, coarse-grained sandstone of the Umm Ishrin Formation (Figs. 3.3, 3.4). It crops out prominently north of Wadi Al-Tayan along the Dead Sea escarpment forming steep cliffs.

Tayan and Hannah Siltstones are relatively soft and can therefore be eroded quickly during short lake level stillstands (Fig. 3.3). The Dead Sea depression was occupied by two major lakes during the Pleistocene, the Samra fresh-water lake in the Last Interglacial (140-75 ka BP) and the brackish Lisan Lake in the Last Glacial (70-14 ka BP) (e.g., Waldmann et al., 2007).

The study area is located along the south-eastern coast of the Dead Sea, north of Wadi Numairah, one of the main wadis draining to the former southern basin of the Dead Sea (Fig. 3.3). The area varies in altitude from -420 m on the current shore of the Dead Sea (Abu Ghazleh et al., 2009) to -148 m along the eastern escarpment of the Dead Sea Rift, an elevation difference of 272 m within about 2 km. The low relief area, adjacent to the Dead Sea, features alluvial fans and fan-deltas that were deposited during the existence of the lake and by the wadis flowing from the eastern mountains to the Dead Sea depression.

The rugged west-facing escarpment running parallel to the Dead Sea rift was dissected by the head-ward erosion of the major wadis (Powell, 1988). Geomorphological and geophysical evidences indicate that the (DSTF) lies close to the eastern shoreline of the southern Dead Sea (Powell, 1988). However, the DSTF in the study area is not exposed at the surface because it is covered with young lacustrine and alluvial deposits (Fig. 3.4).

3.5 Geomorphological processes forming Lake Lisan terraces

Lake Lisan terraces were formed when the lake level was stable or fluctuated only within narrow limits. These standstills occur when (a) the rate of lake level fall declines due to wetter climatic conditions; or when (b) the rate of the lake level rise decreases due to drier climatic conditions. In both cases, near-stability of the coastal position is achieved (Wilgus et al., 1988). During these periods of stability, the waves are able to cut a platform. In areas of low sediment supply, standstills are marked by a sequence of wave-cut terraces; but near major rivers and other areas of high sedimentation, standsstill could be represented by seaward thinning sediment wedges (Carter and Carter, 1986; Carter et al., 1986). If a stillstand is followed by a regression, the terrace will be preserved; but if it is followed by a transgression, the terrace will be deformed and buried under lacustrine deposits.

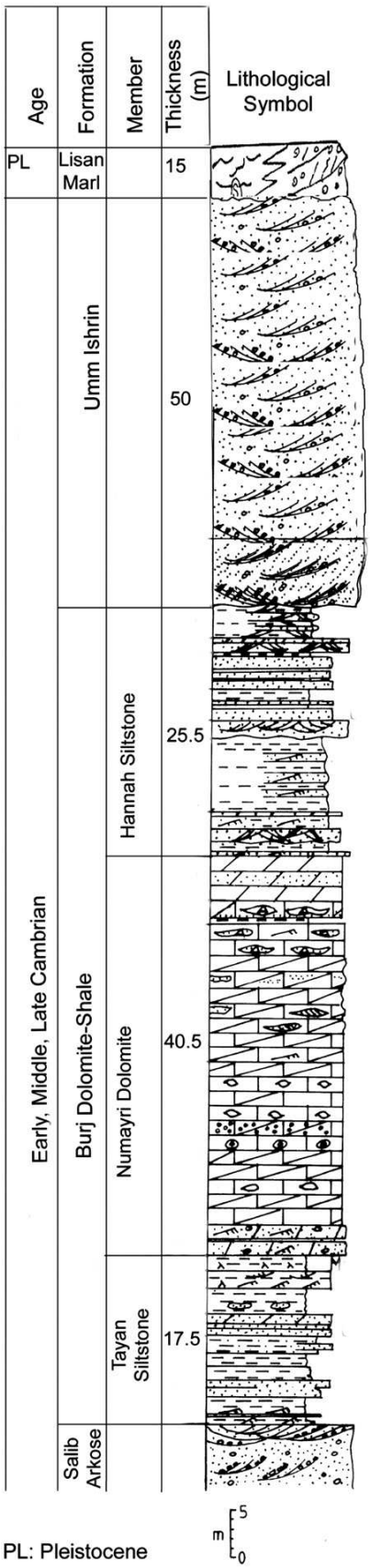

Fig. 3.4: Geological section of the Ghour Numairah area (modified after Powell, 1988).

Consequently, the geomorphological record of this stillstand will be lost. Local progradation can occur on sandy coastlines and deltaic sectors during phases of stillstand that interrupt the transgression. In contrast, aggradational conditions arise on the coastal plain during phases of stillstands that interrupt the regression (Bird, 1985). Therefore, it seems that the Lake Lisan terraces preserved today formed during phases of stillstands that interrupted either regression or transgression cycles. This indicates that the Lake Lisan basin has experienced abrupt, short-term and highly frequent climatic changes during the late Pleistocene, probably associated with Dansgaard-Oeschger events.

Apart from terraces that formed on the soft siltstones of the Tayan and Hannah Formation or on Lisan marl, terraces may have cut into gravels delivered by wadis preceding the lake level rise, or moved down by slope wash, rock fall, mass wasting movements and creep processes. Lake shore waves then rounded these materials further and redistributed them upward, downward and along shore.

Therefore, several processes acted to form the terraces as follows (Fig. 3.5). (1) During periods of stable water level, the waves eroded and abraded the pre-existing slopes to form a wave-cut platform or abrasion terrace (tread) (Fig. 3.5 a); (2) meanwhile, the waves move the sediments across the surface of the abrasion terrace, depositing them down- and up-profile (Fig. 3.5 a); (3) when the lake level drops, the waves start to erode the lower part of the tread cutting a steep cliff or riser (Fig. 3.5 b); (4) once the lake level stops lowering, a new tread begins to form at the base of the riser, constituting a wave-cut terrace (Fig. 3.5 b); (5) the eroded material from the wave-cut terrace moves down-profile, forming a wave-built terrace (Fig. 3.5 b); (6) when the lake level drops for the second time, the wave-built terrace will be re-eroded creating a second wave-cut terrace (Fig. 3.5 c); and (7) consequently, a series of wave-cut terraces will be formed one below each other (Fig. 3.5 d).

3.6 Methods

We used black and white aerial photos of the scales 1:10,000 and 1:25,000 taken in the 1960s, that are kept at the library of the Bundesanstalt für Geowissenschaften und Rohstoffe (BRG) at Hanover, to examine the eastern side of the Dead Sea for the best preserved terraces and the best locations for making cross-sections. Then a field survey was conducted along the eastern side of the Jordan Graben beginning from Al-Baqoorah

in the north to Wadi Dahel in the south, in order to (a) look for Lake Lisan terraces north of the Dead Sea (an area that was not covered by the aerial photos), and (b) locate the available bench marks and the positions of the terrace profiles in the field. This field survey resulted in the selection of six locations with prominent terraces and location of two benchmarks suitable for our purposes (Table 3.1).

The terraces were then surveyed using a Leica SR20 differential GPS instrument. Each GPS measuring point was occupied for 15 min for highest altitude precision; repeated occupation of the same station yielded an elevation precision of ± 1 cm. The GPS coordinate system used was the World Geodetic System 1984 (WGS 84) and the altitude system was Ellipsoidal. Leica Geo Office (LGO) software was used for post-processing of the GPS data and converting Ellipsoidal altitude into meters below sea level. From the data the altitudes of the terraces were calculated. The surveyed cross-sections are: Sweemeh (S) along the northern coast of the Dead Sea, Hadithah (H) north of Wadi Ibin-Hamad, and Numairah 1-4 (N1-4) north of Wadi Numairah (Figs. 3.1; 3.6 a, b).

Table 3.1: Coordinates and altitudes of the benchmarks.

Benchmark name	Northing	Easting	Altitude
Ghour Hadithah	31° 17′ 21.7455″	35° 32′ 09.13807″	-346.428 m
Al Ramah	31° 50′ 42.97797″	35° 41′ 47.6393″	49.8 m

The locations of the cross-sections S, H and N1 were chosen because of the long continuity of the terraces and the good degree of their preservation, while the locations of N2, N3 and N4 were chosen not only due to the good degree of preservation, but also because of the possible existence of high-level terraces. The slope and width of all terraces were measured with inclinometer and tape, the deposits of the terraces were described and stromatolite samples were collected for thin sections investigation and X-ray analysis. Two samples of the terrace stromatolites were submitted for U/Th dating and one sand sample was dated by OSL. Moreover, a geological and geomorphological map of the study area was drawn based on the aerial photos, field investigation and the Al-Karak geological map produced by Powell (1988).

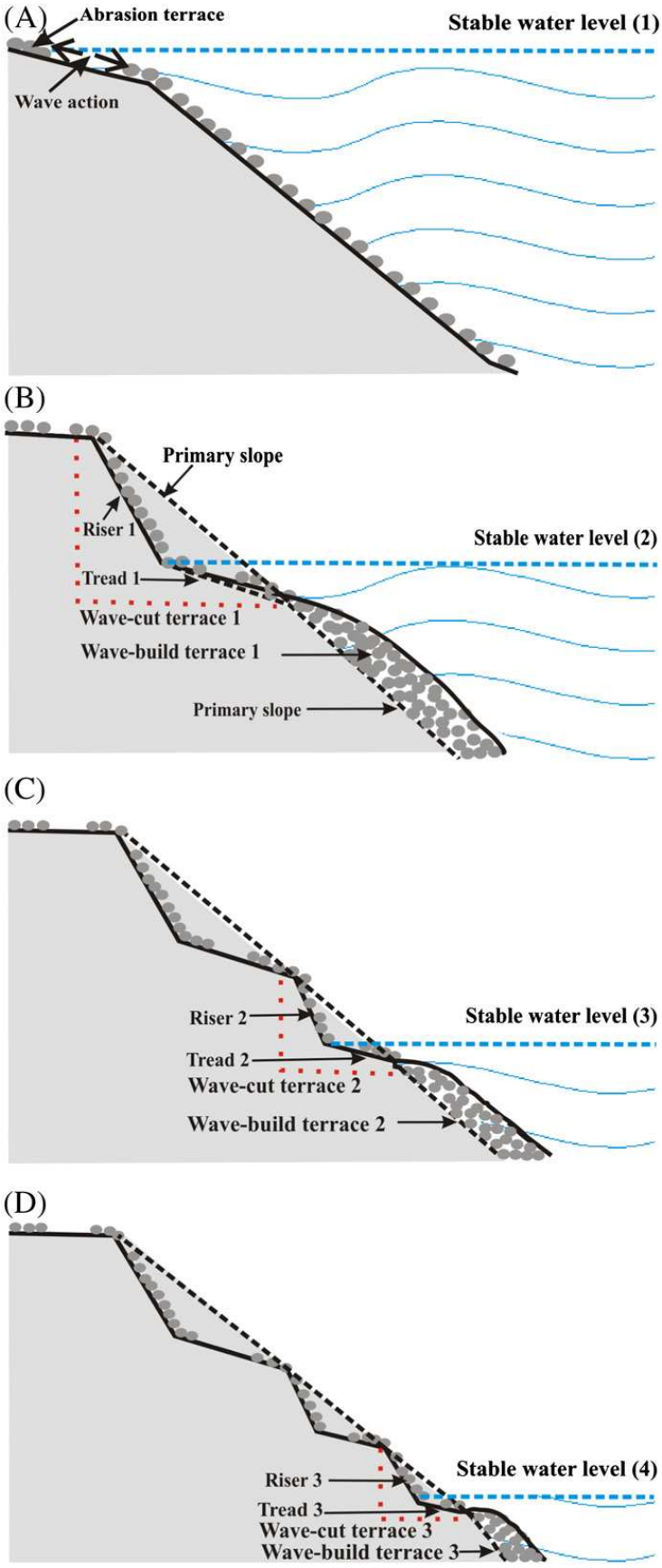

Fig. 3.5: Stages of terraces formation, for discussion see text.

3.7 Results and discussions

3.7.1 Regional distribution of terraces

Lake Lisan terraces were not found north of the Dead Sea. This may be either due to (a) the gently-sloping morphology of the Jordan Valley that does not allow terraces to be cut; or/and (b) the relatively wet conditions in the north that caused the erosion of these terraces in the Post-Glacial. In contrast, prominent terraces were found in some areas along the south-eastern shore of the Dead Sea. This circumstance is mainly due to (a) the steeply sloping morphology in this area that allows the terraces to be formed, and (b) the dry conditions that preserved these terraces from erosion.

3.7.2 Morphological characteristics

In general, the shoreline terraces were found to be horizontal, elongated and undisturbed (Fig. 3.6 a). The sub-flat foreshore or tread dips gently toward the lake with slopes ranging between 2 and 10.5°, while the backshore cliff or riser dips steeply toward the lake with slopes ranging from 11 to 27° (Fig. 3.7).

3.7.2.1 Altitudes of terraces

In Sweemeh, 25 terraces were recognised ranging in level from -370 to -238 m, 24 in Numairah 1 ranging from -317 to -180 m, 13 in Numairah 2 ranging from -340 to -148 m, 19 in Numairah 3 ranging from -316 to -164 m, 11 in Numairah 4 ranging from -178 to -148 m, and 13 terraces in Hadithah ranging from -308 to -195 m (Fig. 3.8).

These morphologically well-preserved shoreline terraces represent a regression of 222 m in lake level during the Late Pleistocene, i.e. from its high stand at -148 m to a low level at -370 m. The re-occurrence of the high terraces in Numairah 2, Numairah 4 (> -180 to -148 m), and Numairah 3 (> -180 to -164 m), suggests, without doubt, that Lake Lisan reached its high level at -148 m, which correlates with the high stand found by Bowman and Gross (1992) at -150 m along the western side of the Dead Sea.

a

b

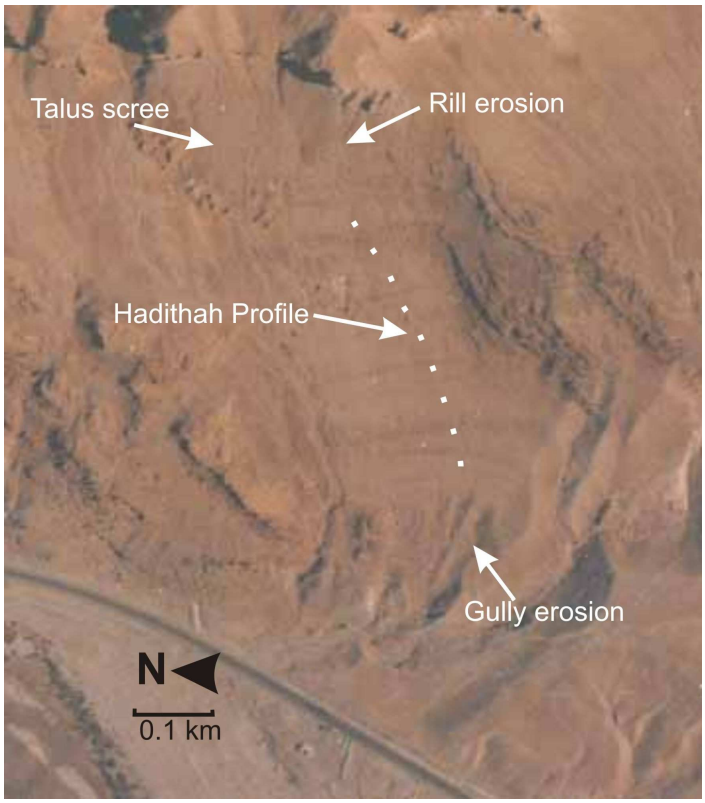

Fig. 3.6 a: Aerial photo showing sequences of Lake Lisan terraces in the eastern coast of the Dead Sea and the locations of the cross-sections. Notice that the lower to middle terraces were completely bulldozed, so that the profiling was carried out only on the well-preserved upper terraces. b: Aerial photo to the east of the Dead Sea showing the terraces of the Hadithah profile. On the top, talus scree buried the terraces while on the lower part gully erosion destroyed the low-level terraces.

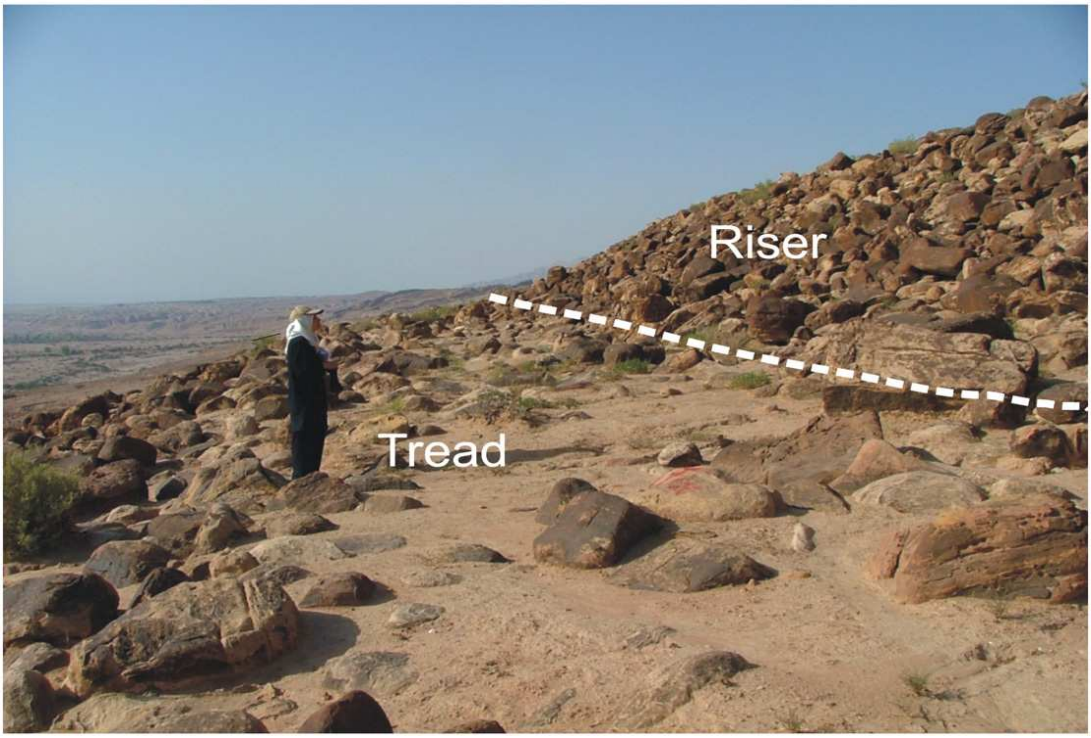

Fig. 3.7: The two parts of a terrace at about -202 m: tread and riser.

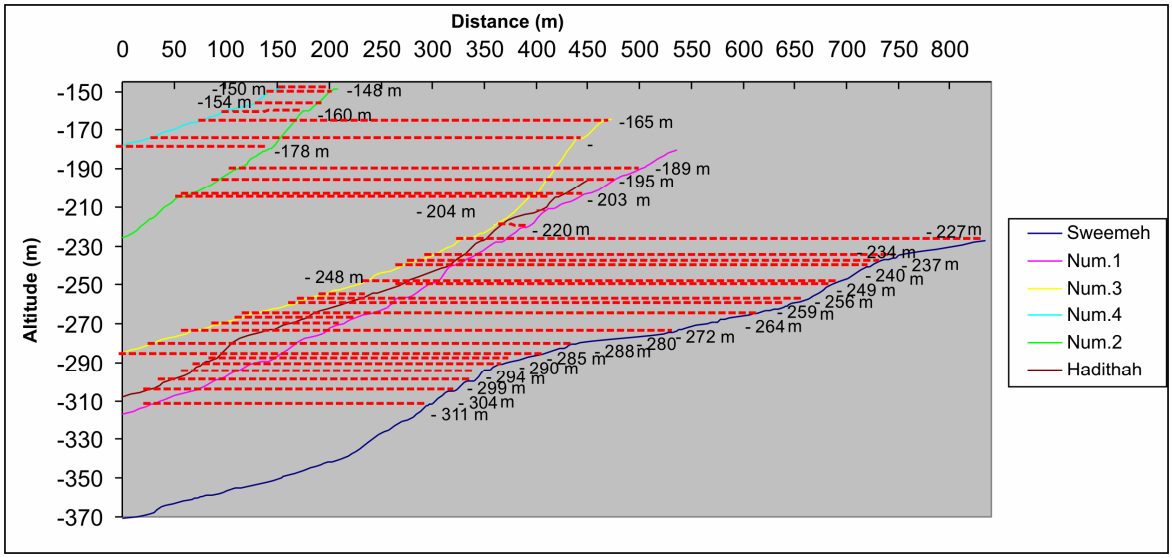

Fig. 3.8: The correlation between the terraces in the six cross-sections.

The most continuous and best preserved sequence of high terraces was found in Numairah 1 (Fig. 3.6 a). The two highest terraces at -160 to -159 m and -150 to -148 m found in Numairah 2 are still preserved because they are (a) cemented by a hard, laminated, and calcareous stromatolitic crust that increases their resistance to erosion, and (b) situated out of the reach of gully wash, and below a hill with only a short slope, so that the colluvial material accumulated on the terraces is insufficient to bury them. However, the middle and southern parts of these terraces that face directly into rain storms have been eroded or buried by talus scree.

In Numairah 3, the terraces are missing between -202 and -174 m over a distance of 40 m. This is due to (a) bedrock exposure of hard Cambrian Burj Dolomite Shale that is very resistant against wave erosion. This correlates with the suggestion of Sunamura (1992) that the development of shore platforms depends on the relation between the assailing force of waves (Fw) and the resisting force of rock (Fr). If Fw > Fr, the erosion will occur; conversely, if Fw < Fr no erosion will occur; a similar conclusion was made by Stephenson and Kirk (2000); and (b) a very steep slope of more than 35°; causing the water to be very deep in front of the cliff, an environment that does not allow the cutting of terraces, because 'the wave does not break against a sea wall but simply is reflected back in the deep water' (McCullagh, 1985). Stephenson and Kirk (2000) also pointed out that the depth of water controlling wave breaking causes larger storm waves to break further from shore, preventing direct attack at the cliff base. Similarly, Bowman (1971) concluded that a steep slope (≥ 30°) causes the reflection of a considerable proportion of the wave energy, and the missing breakers or secondary breakers do not allow a terrace to be formed.

Many caves of different sizes were observed in the dolomite cliff, possibly indicating that subaerial weathering is more effective than wave erosion. However, on the top of the dolomite cliff there is a sub-flat at -174 m that is cemented by massive and hard stromatolite crusts, protecting it from erosion. The highest terrace in this profile at -164 m constitutes an abrasion terrace, which is also overgrown by solid, dark grey, calcareous, laminated stromatolite crusts.

The high terraces (> -180 m) are not present in the cross sections Numairah 1 and Hadithah because they may (a) have not formed due to the exposures of hard and steep

Cambrian sandstone or Paleocene chert-limestone, (b) have been buried under the talus scree associated with the steep slope (Fig. 3.9), and/or (c) have been eroded by rain and surface runoff.

The correlation between the cross-sections (Fig. 3.8) shows that there are many terraces of the same altitude in most of the profiles. The terraces of the same altitude can also be traced on the aerial photos for considerable horizontal distances without any indication of vertical displacement or uplifting (Fig. 3.6 a). This indicates that these terraces were not significantly affected tectonically and thus represent the original levels of Lake Lisan. Moreover, the re-occurrence of the high terraces (> -180 to -148 m) in more than one site, and their appearance as part of a continuous system of terraces, in addition to the similarity in morphological characteristics between the higher and lower terraces, indicate that these high terraces were derived from Lake Lisan and not from the older Samra Lake.

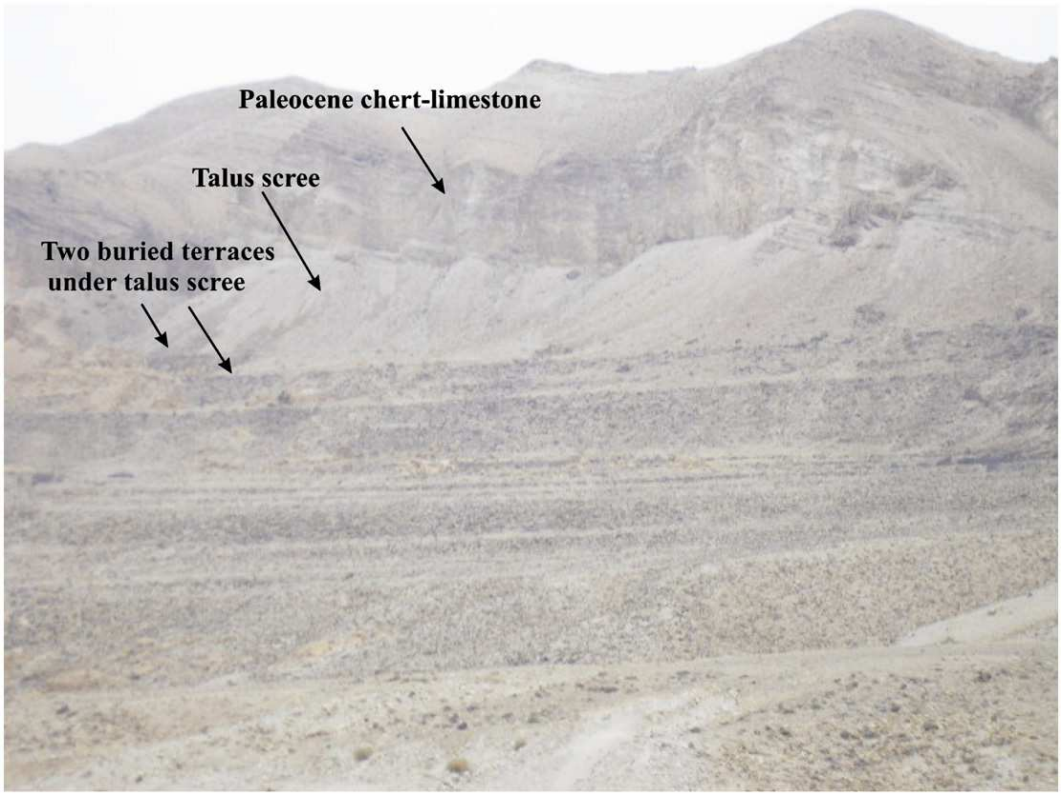

Fig. 3.9: View to the east showing the well preserved terraces of the Hadithah profile. The highest two terraces were partly buried by talus scree. Higher up, the terraces were not formed due to the steep slope and the exposure of hard rocks.

Geomorphological processes such as rill and gully erosion play a key role in the destruction or/and development of the terraces. In some places, such as the lower part of the Hadithah profile, they have destroyed the terraces completely (Fig. 3.6 b). In other places, they eroded the treads and caused the two risers above and below to merge into one extended riser. This was noticed specifically in Numairah 1 and Numairah 2 (Fig. 3.10).

3.7.2.2 Width of terraces

The average width of the tread ranges from 5.8 m in Numairah 2 to 22.4 m in Sweemeh with an overall average of 13.3 m (σ = 6.8 m), while the width average of the riser ranges from 7.1 m in Numairah 4 to 12.6 m in Numairah 1 with an overall average of 9.8 m (σ 1.9 m) (Table 2). Thus, the width of the tread varies much more than that of the riser.

Based on tread and riser width averages, the terraces can be divided into two groups: (a) terraces with very wide treads and relatively narrow risers such as those in Sweemeh, Numairah 3, Numairah 4 and Hadithah; and (b) terraces with wide risers and relatively narrow treads such as those in Numairah 1 and 2 (Table 3.2; Fig. 3.6 a). The first group was formed primarily in gently-sloping areas, where 'the lake water is too shallow and the wave breaks before arriving at beach, so that the pressure of the waves is greatly reduced, and the potential erosion is negligible' (McCullagh, 1985). Consequently a wide tread will be formed and no riser will be cut. This agrees with Fleming (1965), who concluded that slope gradients of up to 15° cause the energy to be expended on abrasive action. Moreover, the minor fluctuations of the lake in such gently sloping areas do not allow risers to be cut, since 'the duration of sea level remains constant, the maximum possible width of a wave-cut platform (tread) is attained' (McCullagh, 1985). Even if a riser was formed, it could be rapidly and easily destroyed by wave action or gravity mass movements due to its small dimension. Accordingly, both the treads above and below the eroded riser will be merged into one extended tread, adjoining the upper riser of a new extended terrace.

The second group was formed in primarily steeply-sloping areas, where the lake water is deep and the waves break against the beach, releasing their energy. Therefore, a wide riser will be formed and a relatively narrow tread will be abraded. This corresponds with the conclusion of Allan and Kirk (2000) that in deep and steeply-floored lakes such as Lake

Waikaremoana (New Zealand), high frequency waves are little modified by the bed so that wave breaking occurs close to the shore, producing narrow surf zones, and consequently narrow treads, with minimal loss of energy during shoaling. In this case, the tread could be later eroded or destroyed by wave undercutting and creep process, or by rill and gully erosion due to its small width (Fig. 3.10).

Table 3.2: Averages and standard deviations of the terrace widths and gradients.

Cross-sections	Tread width	Riser width	Tread slope	Riser slope
Sweemeh	22.4 ± 7.08	10.1 ± 0.12	7.6 ± 0.6	16.7 ± 1.53
Num.1 (up to -180)	10.2 ± 5.12	12.6 ± 2.38	8.4 ± 0.2	18.1 ± 0.13
Num.2 (up to -148)	5.8 ± 9.52	10.4 ± 0.18	8.4 ± 0.2	21.7 ± 3.47
Num.3 (up to -164)	14.3 ± 1.02	8.7 ± 1.52	7.3 ± 0.9	16.2 ± 2.03
Num.4 (up to -148)	13.6 ± 1.72	7.1 ± 3.12	7.7 ± 0.5	16 ± 0.5
Hadithah (up to -195)	25.6 ± 10.28	12.4 ± 2.18	9.8 ± 1.6	20.7 ± 2.47
Mean	15.32	10.22	8.2	18.23
Standard deviation	6.79	1.94	0.82	2

As a result, the risers below and above the eroded tread would be merged in one extended riser, which then joins together with the lower tread to form a new extended terrace (Fig. 3.12 a, b). Both types of extended terraces do not represent the original dimensions of the lake terraces and are considered to be “pseudo-terraces”. Bowman (1971) described one type of pseudo-terrace that formed due to the reflection of wave energy on the steep coast, and consequently no platform would be formed. However, he did not pay attention to other geomorphological factors (e.g., rill and gully erosion, gravity waste movements and wave undercutting) that lead also to such pseudo-terraces (Fig. 3.11).

Therefore, it appears that the width of the terraces is determined mainly by coastal lithology and wave energy that is controlled by water depth, coastal gradient and wind speed. However, the geomorphological processes also play an important role in changing the terraces' width.

Our conclusions correlate well with some models of shore platform evolution presented by Trenhaile (2001a) and Trenhaile and Layzell (1981). They concluded that wave erosion is most important in developing shore platforms. However, the subaerial processes such as weathering play an important role in influencing the gradient, width, and other features of platform morphology, and in determining rates of platform development.

Trenhaile (2001a) argued that even severe weathering which reduced the strength of the rocks by 75% plays only a secondary role in platform development. Equilibrium platform width is more than 40% larger under severe weathering than without weathering. However, weathering could be of more fundamental influence on the development of narrow shore platforms in resistant rocks with weaker wave environment. The role of the weak waves is only limited to removing the weathered debris (Trenhaile, 2000; 2002). mentioned other factors that influence the platform width, suggesting that shore platform width increased with tidal range and decreased with rock resistance, roughness of the platform surface, amount and persistence of the cliff-foot debris, and wave period.

3.7.2.3 Gradients of terraces

The average slope of the treads ranges between 7.3° in Numairah 2 and 9.8° in Hadithah, with an overall slope average of 8.2° and a standard deviation of ± 0.8° (Table 3.2) suggesting that there is no significant difference between the average slope of the treads in the different profiles, and that the slope of the treads was not altered significantly. However, the measured slope of the tread seems to be slightly higher than the original due to: (a) local factors such as the gravels and cobbles covering the treads and affecting their slope, and/or (b) rill erosion, which increases the tread gradient notably. It is also noticed that the average gradient of the treads in the gently-sloping areas is slightly lower than that in the steeply-sloping areas. Moreover, it was noticed that there is a reversed relation between the tread width and slope. This agrees with Allan et al. (2002) who found that the gently-sloping platforms of Lake Waikaremoana are the widest.

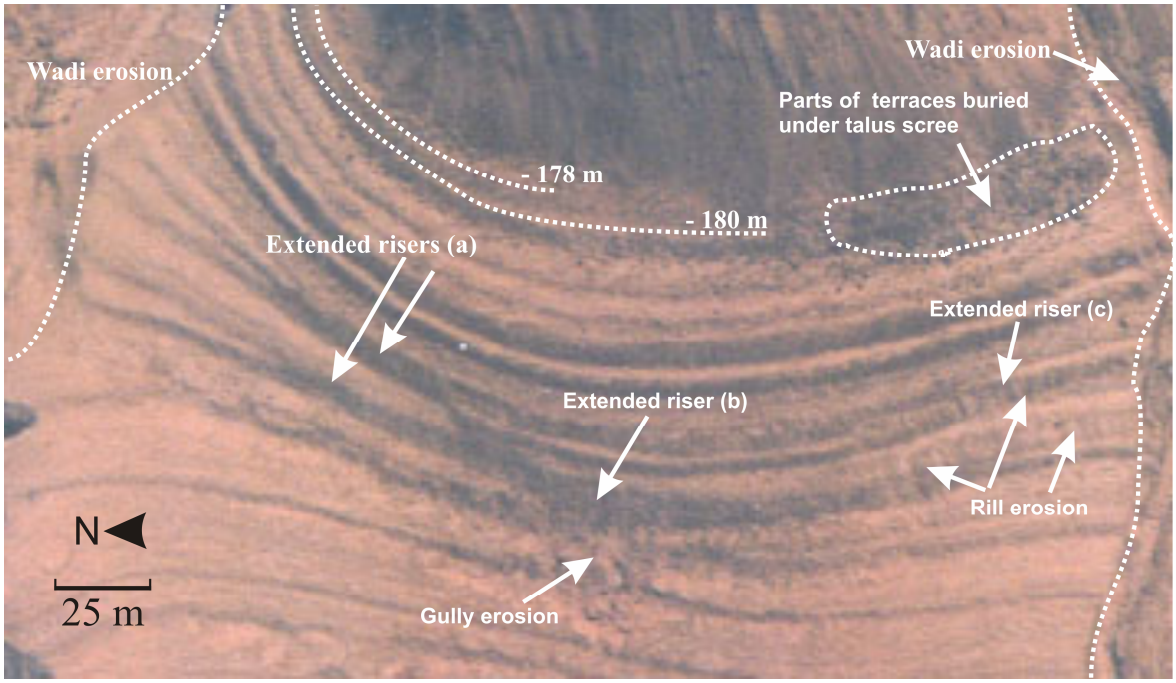

Fig. 3.10: Aerial photo showing some pseudo terraces in Numairah 1. Each consists of extended riser and tread: (a) extended risers as a result of tread destruction by wave undercutting or creep processes; (b) four risers were merged in one extended riser as a result of treads destruction by gully erosion; and (c) extended risers as a result of treads destruction by rill erosion. Notice also the buried southern parts of the two highest terraces at -180 and -178 m.

The average slope of the risers ranges between 16.2° in Numairah 3 and 21.7° in Numairah 2 with an overall slope average of 17.7° and a standard deviation of ± 2°. Thus, the standard deviation of the riser gradient is larger than that of the tread. In general, the gradient of the risers formed in the primarily steeply-sloping areas (Numairah 1, Numairah 2 and Hadithah) is higher than that of the risers formed in the primarily gently-sloping areas (Sweemeh, N. 3 and N. 4) (Table 3.2). This could be due to the difference in the primary gradient between these profiles.

3.7.3 Sedimentology

Based on our field observations, the Lake Lisan terraces consist of four kinds of deposits:
(1) A surface cover of alluvial and colluvial deposits, consisting of well rounded gravels, cobbles and boulders. They show a mixed lithology, indicating that they are derived from different sources and resulted from wadi and slope transport, and lateral wave- and current induced transport. The distribution and characteristics of these deposits on the treads are different to those on the riser; a thin veneer of rounded beach gravels and pebbles covers the tread, while a thick layer of rounded gravels, cobbles and boulders covers the riser. The size of the blocks on the riser is much bigger than that on the tread and the deposits

covering the riser are also much thicker (Figs. 3.7, 3.11 a). This was observed in the field and can be recognised on aerial photos. However, some treads are covered completely with a thick layer of large rock blocks, very similar to that of the riser. This could be due to (a) rill erosion and creep processes that moved the surface deposits from the riser to the tread, (b) an undercutting of the riser by the waves that allowed the materials to fall down from the riser to the tread surface, and/or (c) a sharp and rapid drop in lake level that enabled the waves to bring large blocks down without allowing the time to sort the material. Likewise, the distribution and the sorting degree of the surface deposits of the treads vary from one terrace to the other. Some terraces are characterised by well-sorted deposits covering the entire tread equally, others are covered with poorly-sorted deposits inconsistently, the rest is covered with colluvium lakeward and shoreward, while the center tread consists of fine material.

It is noticed that there is a relation between the slope of the terraces and the sorting degree of the surface deposits. In the gently-sloping terraces such as those in Sweemeh, Hadithah and Numairah 3, the deposits are well sorted, while in the steeply-sloping terraces such as those in Numairah 1 and 2, they are poorly sorted. This could be due to a gradual drop of the lake level in the gently-sloping areas, which allows the lake water to remain over the terraces for a longer time and therefore sort the surface deposits better. This is consistent with the conclusion of Seiders et al. (1970), who reported that the rapid retreat of sea level allowed the surface deposits of the terraces to remain, while the slow retreat allowed removal and sorting of the terrace deposits by wave-reworking and surface runoff.

The existence of a thick layer of fine deposits covering a layer of colluvium in some terraces may indicate a temporal transgression of the lake. In general, the thickness of the surface deposits increases on the high-level terraces because they are near to the sources of material from steeper upslope areas. This contributes to the preservation of these terraces from erosion. In contrast, the degree of roundness increases downward, because the lower terraces obtain material that has been transported for a longer distance and that lack recent deposition from rock fall.

a

b

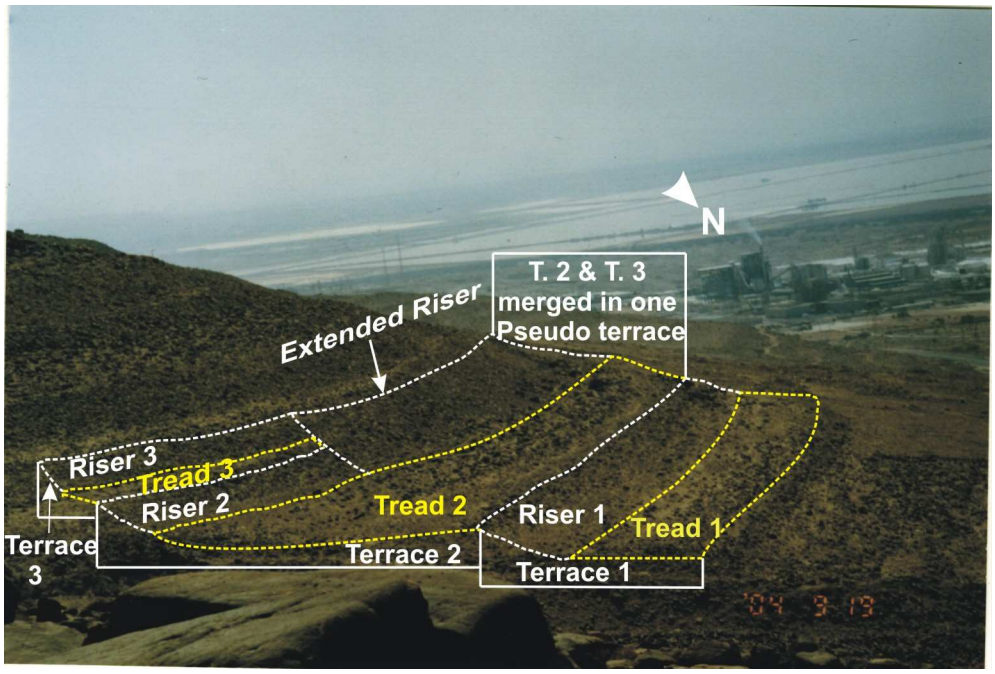

Fig. 3.11 a: A sequence of the terraces north of Wadi Numairah, southeast of the Dead Sea. b: The formation of an extended riser as a result of tread destruction.

It is observed that the high-level terraces, especially those located near to dolomite cliffs (Numairah 3 and 4) are mostly covered with angular fragments. This indicates that most of these deposits have accumulated after the lake lowering as a result of physical weathering and gravity mass movements.

In some terraces that were secondarily cut by Wadis, shore-line deposits of well-rounded colluvium occurred twice alternating with layers of fine sediments, suggesting two cycles of lake regression and transgression. The alternation between coarse shore deposits and fine lacustrine deposits exposed on both sides of the south canyon of Wadi Al-Tayan reflects several cycles of lake regression and transgression. Furthermore, in situ lake beach deposits cemented by fine materials have been seen in the course of the same wadi, indicating that the wadi was formed before the lake transgression and filled by material from its own tributary area during the lake transgression.

(2) Calcareous stromatolites are preserved on most of the terraces between -370 to -148 m (Fig. 3.12). Stromatolites are layered, mostly calcareous organic build-ups or bioherms that form in highly $CaCO_3$-supersaturated water by permineralisation of algal, mostly cyanobacterial mats (e.g., Kempe and Kazmierczak, 2007). Some of these stromatolites form large, laminated, massive, head-like blocks; others are finely laminated crusts cementing and overgrowing beach gravels and stabilising piles of rocks in the forms of small islands and cones.

X-ray diffraction measurements on 20 samples indicate that the stromatolites consist of varying proportions of aragonite and calcite. Thin section investigation shows that the stromatolites are similar in shape and structure on the low and high terraces (Figs. 3.13, 3.14). This emphasizes that all terraces were derived from the same lake.

Dissolution by rain and/or dew has partly dissolved the stromatolitic limestone so that they have pointed micro-karren-like surfaces. In places cavities and small caves (possibly additionally enlarged by animals) have formed. Stromatolite blocks buried under a layer of colluvial and alluvial deposits in Numairah 1 and in situ stromatolite blocks observed on the banks of some branches of Wadi Al-Tayan indicate that (a) Lake Lisan has experienced some transgression cycles in the late Pleistocene, and (b) Wadi Al-Tayan was incised before the rise of the lake.

(3) Below and in between the colluvium cover and the stromatolites, there are fine deposits of sand, silt and clay, which were derived from the bedrock by weathering and slope wash process, before they were re-deposited by the lake water (Fig. 3.15).

(4)The lower-most layer consists of lacustrine deposits of aragonite and gypsum that were deposited in a deep water environment pre-dating the lake terraces. They were observed particularly in the low-level terraces (Fig. 3.16) and in a few high-level ones up to -197 m, where the modern wadis cut the terraces and exposed these deposits. However, these deposits were observed on the surface of some terraces of lower to middle elevation which could indicate a transgression of the lake at the boundary between the late Pleistocene and early Holocene.

Fig. 3.12: Stromatolite block with a wavy lamination in Numairah 1 at -317 m.

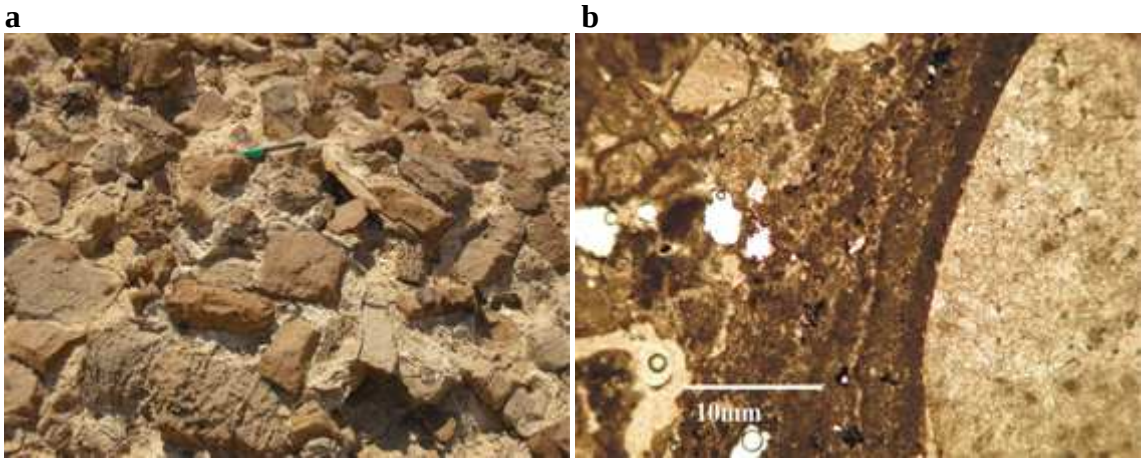

Fig. 3.13 a: Stromatolitic crusts cementing locally bedrock derived Cambrian dolomite stones and blocks in Numairah 3 at an altitude of -204 m. b: Thin section in plain light showing the contact between a dolomite (right) and the stromatolite. As the water depth decreased, more allochtonous grains were incorporated into the growing algal mat (left).

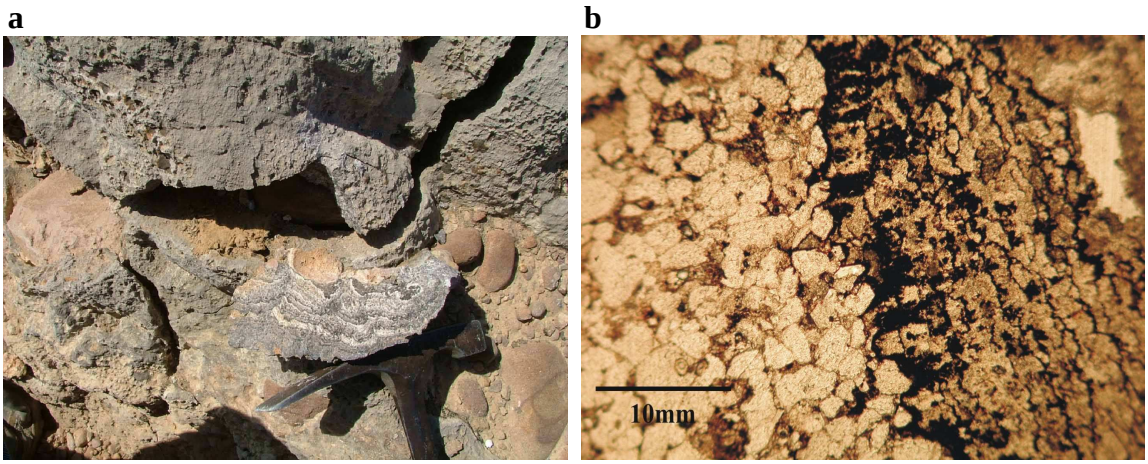

Fig. 3.14 a: Lake Lisan microlaminated stromatolite cementing and overgrowing Cambrian sandstone blocks in Numairah 2 at an altitude of -159 m. b: Thin section in plain light showing the contact between sandstone (left) and the stromatolite (right) with the typical laminated structure of stromatolites build by cyanobacteria.

3.7.4 Post-Lisan weathering

Dark and massive desert varnish was observed on the surface blocks sitting on the terraces, which implies a long period of exposure and a low rate of erosion. The degree of desert varnish development on the terraces is remarkably different. On the high-level terraces the desert varnish is darker and more massive than that on the low-level ones. This emphasizes that the high terraces are older than the lower ones and that the entire series is recessional. This can be also recognised on the aerial photos where a color change from dark to light is noticed from the higher to the lower terraces. Moreover, the degree of

desert varnish development on the same terrace is not always the same, which reflects different deposition ages of the surface colluvium. Stromatolite crusts overgrowing varnished cobbles and gravel indicate that they were deposited before the last transgression. However, desert varnish was not observed on the dolomite colluvium blocks covering the terraces in Numairah 3, 4 and Hadithah because the dolomite has a surface that is too soluble for the varnish to be preserved (Cooke and Varren, 1973).

Most of the large sandstone blocks are heavily affected by Tafoni and pit weathering. Some of the blocks are completely tafonised from below, so that only tent-like remnants of the blocks remain (Fig. 3.16 b). Most of the Tafoni-cavities face west, southwest and northwest, in the direction of the longest shadow duration. These cavernous forms seem to be caused by a combination of physical and chemical weathering in the micro-fractures and weak textures of the rocks. Salt weathering caused by lake water and spray in micro-fracturing rocks along the shore zone could also lead to such forms (Huinink et al., 2004).

However, the degree of development of the Tafoni varies according to altitude. Most affected is sandstone, while dolomite is less prone to tafonisation, reflecting differences in weathering resistance. Moreover, the size of these cavities increases on the high level terraces corresponding to their relative age. Physical weathering of the blocks covering the terraces is more active and dominant than the chemical weathering due to arid climatic conditions prevailing in the study area.

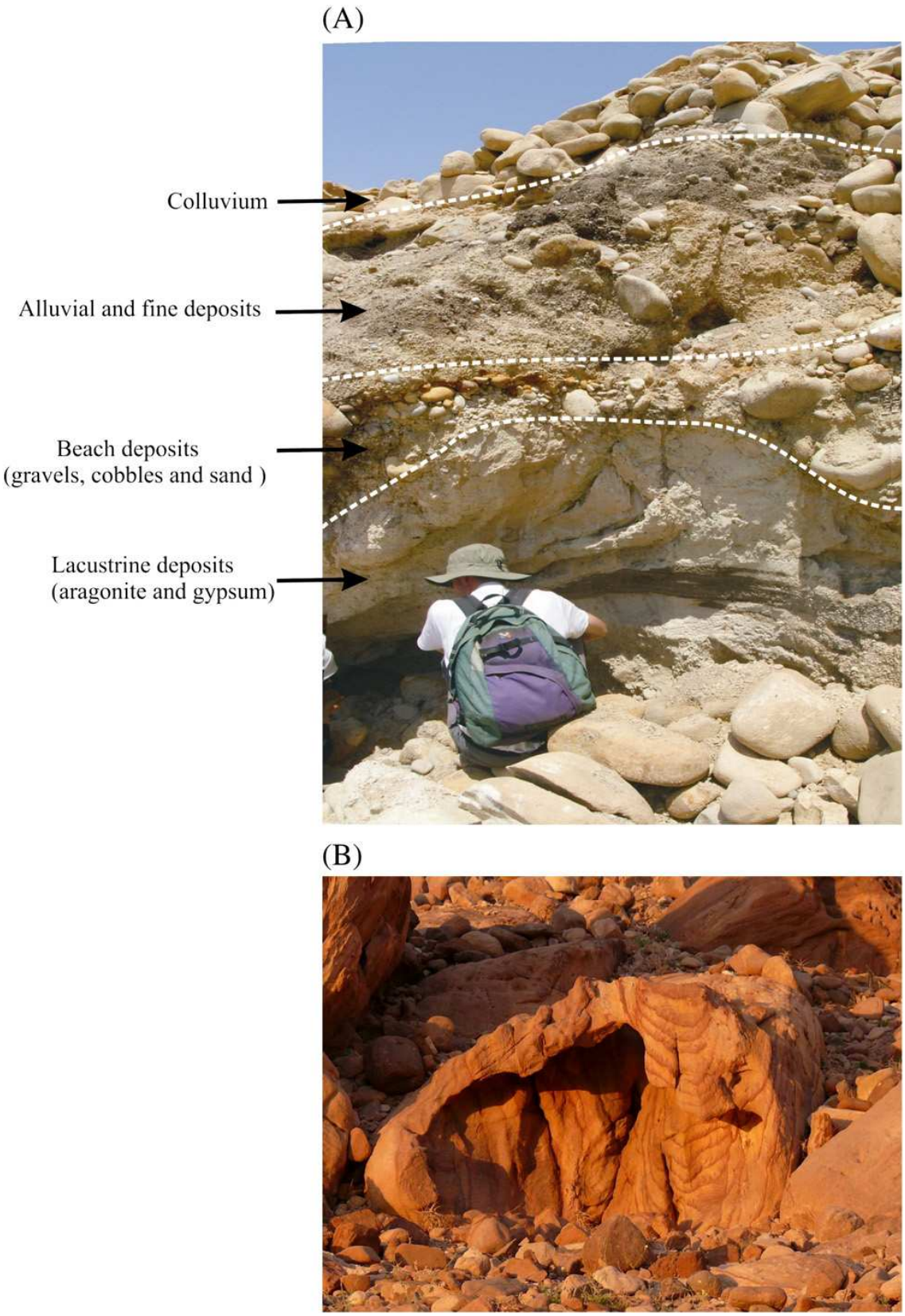

Fig. 3.15 a: Colluvium, fine and lacustrine deposits of the terraces at -340 m.
b: Tent-like Tafoni at a terrace of -300 m in Numairah 3.

3.7.5 Palaeoclimatology

In order to date the terraces surveyed in this study, we submitted several stromatolite samples for U/Th dating. The highest terraces at -148 and -154 m were dated to 30.55 ± 0.22 and 22.9 ± 0.29 ka BP, respectively (Table 3.3 a). These terraces represent prolonged high stands of Lake Lisan that must have been caused by climatic conditions with a more positive water balance than today.

After these high-level stages, Lake Lisan dropped sharply to lower than -200 m at around 20 ka BP as reported by Landmann and Kempe (2002), Landmann et al. (2002) and Bartov et al. (2002). The dates reported by this study correlate with the relative age of the terraces. Moreover, they correlate well with ages of the highest beach ridges (up to -150 m) found by Bowman and Gross (1992) in the south-west of the Dead Sea and dated by Matmon et al. (2003) to 20-36 ka BP. The dates of this study are also consistent with the age estimates of the Lake Lisan high stand derived from dating of the Lisan Formation to 27-23 cal ka BP (Begin et al., 1985, Kaufman et al., 1992; Bartov et al., 2002).

The age of the -148 m terrace correlates well with that of the lower part of the Upper Lisan Member dated by Bartov et al. (2002) to ~ 31 cal ka BP. This member consists of interlaminated calcareous silt and aragonite (e.g., Abed, 2000) and is thought to be associated with the lake high stand. The second highest terrace of -154 m correlates with the period of the upper part of the Upper Lisan Member, dated to 25-23 cal ka BP (Bartov et al., 2002). Moreover, it coincides with the fast rise of Lake Kinneret between 23 and 22 ka BP reported by Hazan et al. (2005). They concluded that Lake Lisan in the south and Lake Kinneret in the north converged only during the high stand of about -170 m between 24.6 and 24 ka BP (Hazan et al., 2005). However, our dates suggest that both lakes were merged for a longer period.

Superimposing our terrace ages on the North Greenland Isotope (NGRIP) record (Svensson et al., 2008) of the Last Glacial (Fig. 3.16) shows that the high-level terraces at -148 to -154 m were formed during the Dansgaard-Oeschger stadials 5 and 2c, respectively.

Martrat et al. (2004) recorded abrupt changes of the Western Mediterranean sea surface temperature, consistent with the warm interstadials and the gradual cold stadials of the

NGRIP during the Last Glacial. It appears that the cold stadials caused minor transgressions of Lake Lisan superimposed on an overall trend of falling lake levels. Consequently, standstills occurred after theses transgressions allowing the formation of pronounced terraces and the growth of stromatolites.

Moreover, our ages of the high level terraces are consistent with the timing of the Heinrich cold event 3 (29-31 ka BP) and the Last Glacial Maximum (~ 23-19 cal ka BP), respectively. This suggests that cold periods in the northern latitudes are correlated with wet conditions and high levels of Lake Lisan, while warm periods are correlated with dry conditions and low levels.

Table 3.3 a: The U/Th ages of the terrace stromatolites.

S. n.	Description	Altitude (m)	U (corr.) ‰	Error Abso.	238U (µg/g)	Error abso.	232Th (ng/g)	Error abso.	230Th (pg/g)	Error abso.	Age (corr.) (ka)	Error Abso.
34	Laminated grey stromatolite	-148	448	2.7	5.687	0.006	85.25	0.39	33.55	0.19	30.55	0.22
30	Laminated grey stromatolite	-154	413.5	4.7	4.909	0.005	62.78	0.46	21.88	0.24	22.90	0.29

Table 3.3 b: OSL dating results of the sand sample, U-, Th- and K-concentrations based on low-level γ-spectrometry. Equivalent dose estimate (De) was calculated using SAR protocol of Murray and Wintle (2000), measuring small aliquots to check for insufficient bleaching (Fuchs and Wagner, 2003).

Sample Description	Altitude (m)	Mineral	Grain size (µm)	Aliquots No.	Th (ppm)	U (ppm)	K %	De (Gy)	Total Dose Rate (Gy/ka)	OSL Age (ka)	Age Error (ka)
Sand within Lisan Formation	-200	Quartz	90-200	25	7.4 ±0.7	3.5 ± 0.2	0.4 ± 0.1	19.4 ± 0.7	1.9 ± 0.1	10.4	± 0.8
Lisan Sand lagoon	-117	Quartz	-	-	-	-	-	-	-	40	-

Other lacustrine climatic records from western United State and eastern Africa agree also with our terrace dates. Wilkins and Currey (1997), Allen (1991) and Phillips et al. (1992) have reported that Lake King (West Texas and South-Central New Mexico), Lake Estancia and Lake San Augustin basins have experienced four rapid transgressions with high stands at about 22, 19, 17 and 16 ka BP. Similarly, wet climatic conditions were

identified from the East African lakes at 28 ±3, 23, 20 ± 1, 15.8 ± 2.5, 13.8 ± 2.8, 10.4 ± 0.6 and possibly at 8.6 ± 0.5 ka BP (Shanahan, 2000; Kingston et al., 2007).

Another sample of sand was dated using OSL. It was taken from a layer situated at -200 m in the Wadi Dahel fan-delta, south east of the Dead Sea. The sand layer appears to be of aeolian origin. Beach gravels and braided stream deposits were observed below the sand layer indicating a shallow water environment. The sand layer was dated to 10 ± 0.8 ka BP (Table 3.3 b), documenting a regression phase of Lake Lisan (Fig. 3.17). This regression must have been caused by arid conditions that allowed strong wind erosion at the end of the Younger Dryas (~ 11-10 ka BP). These dry conditions were associated with a decline in oxygen-isotope values of North Greenland, implying a distinct rise in the temperature.

Below the fluvial deposits a layer of laminated marl was noticed, suggesting a lake level high stand and wet climatic conditions prior to the Younger Dryas, probably associated with the Bølling-Allerød warm interval (~ 15-13 ka BP). This is also supported by the conclusion of Landmann and Kempe (2002) that both of Lake Lisan and Lake Van returned to a positive water balance at about 15 ka.

The existence of deep water deposits of marly silt and white laminated marl above the sand layer up to -195 m (Fig. 3.17) suggests a transgression of Lake Lisan due to wetter conditions after 10 ka BP. Because a water depth of at least 30 m is required to protect the laminated deposit from the destruction by wave action (e.g., Landmann et al., 1996), the transgressive deposit of the mostly laminated marl suggests a much higher level of the early Holocene Lake Lisan of at about -165 m. This level is much higher than that reported from the previous studies.

This conclusion correlates well with other lacustrine, terrestrial and marine climate records. For example, Lake Van began to rise by 10.6 cal ka BP until it reached its Holocene highstand at 7.5 cal ka BP (Landmann and Kempe, 2002 and Kempe et al., 2002).

Stein et al. (1997) found that the transition between the Pleistocene and Holocene was accompanied by the desiccation of Lake Lisan and its contraction to the present Dead Sea. After that, the Jordan Valley was occupied by the freshwater Damya Lake (Abed and

Yaghan, 2000). The high level deposit of the Damya Formation was found by us near to Al-Karamah City, Jordan, and was measured to -180 m using DGPS. This high level of the northern part of the lake corresponds well with that of the southern part, which is obtained from the Wadi Dahel profile.

Based on the climate studies of the Levant and eastern Mediterranean, Robinson et al. (2006) suggested that the early Holocene (~ 9.5-7 cal ka BP) appears to have been the wettest period during the last 25 ka. The paleosol record suggests wet conditions prior to 12.5 cal ka BP and from 10 to 7.5 cal ka BP with a rainfall average of 350 to 800 mm/a (Gvirtzman and Wieder, 2001). Perennial meandering stream deposits of Wadi Fenan from the early Holocene (9.5-8 cal ka BP) indicate that the climate was wetter at this time (Hunt et al., 2004; McLaren et al., 2004). The high abundances of Oak and Pistacia in the Ghab and Hula pollen record in the early Holocene (10.2-6.7 cal ka BP) suggest mild winters with a mean annual precipitation of 300-500 mm (Rossignol-Strick, 1995; 1999).

Based on palynological and palaeobotanical evidence, Hunt et al. (2004) reported that before 8 cal ka BP, Wadi Fenan, south east of the Dead Sea, was on the margin of a Mediterranean forest zone. Bar-Matthews et al. (2003) concluded that the Soreq Cave speleothem oxygen-isotope record was more negative prior to the Younger Dryas and during the early Holocene, consistent with warmer and wetter conditions. They also estimated that rainfall ranged from 550 to 700 mm/a during the early Holocene (8-7.5 ka BP).

The speleothem ^{13}C record from the Jerusalem West Cave shows a negative excursion during the early Holocene, compared to heavier values in the late Pleistocene or in the late Holocene, suggesting more C_3 vegetation and higher rainfall (Frumkin et al., 2000). Emeis et al. (1998; 2000; 2003) suggested that the Eastern Mediterranean was characterised by rising temperatures and lower salinities in the early Holocene due to increased freshwater input.

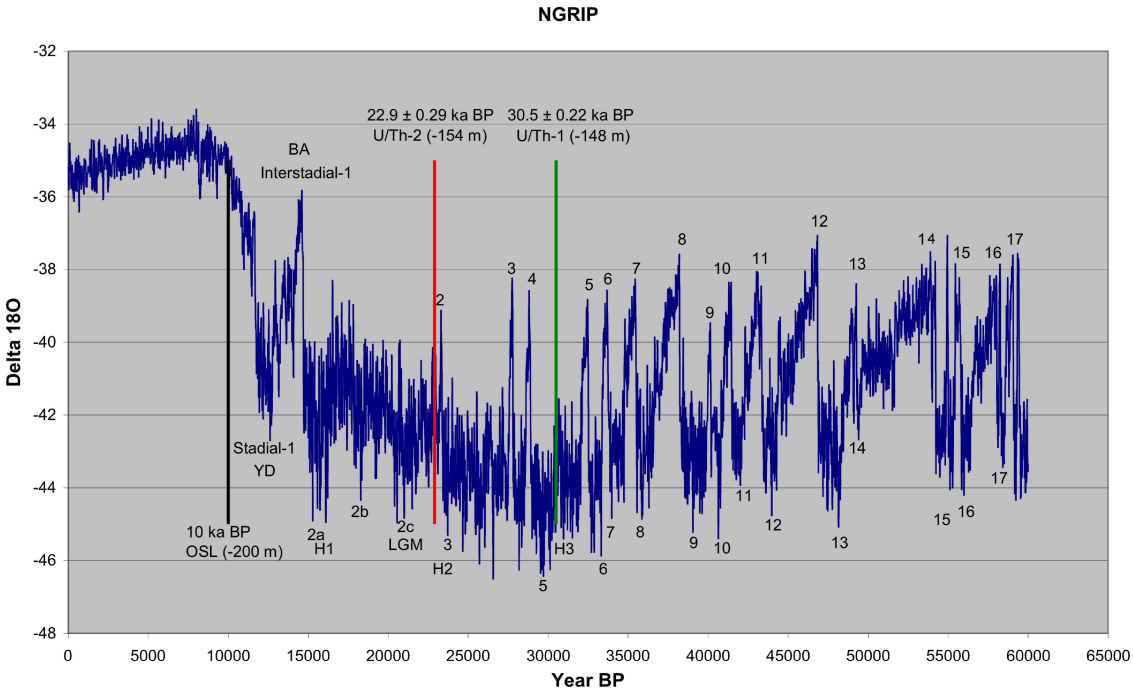

Fig. 3.16: Stadials (lower numbers) and interstadials (upper numbers) and Heinrich events of the NGRIP during the Last Glacial (NGRIP dating group, 2008) in addition to the U/Th and OSL dates of this study.

Based on the U/Th and OSL dates of this study and on the previous discussion, the following scenario for the climatic conditions of the Lake Lisan basin during the last 30 ka can be suggested: Lake Lisan experienced high stands up to -148 m between 30.5 ± 0.22 and 22.9 ± 0.29 ka BP due to wet and cold climatic conditions during stadials 5 and 2C, maintaining high levels for ~ 8 ka. Then it dropped to lower than -200 m around 20-18 ka BP (Landmann and Kempe, 2002; Bartov et al., 2002). After 16 ka BP Lake Lisan rose again probably due to warm and wet conditions in the Bølling-Allerød interval. Subsequently, the lake dropped to about -200 m by 10 ± 0.8 ka BP as indicated by the sand layer in the Dahel profile. Although Lake Lisan has been falling during this period, it maintained a relatively high stand in lake level. In the early Holocene (9.5-7 ka BP) Lake Lisan recovered again to more than -195 m due to wet conditions, as indicated by the deep water deposits overlying the sand layer in the Dahel profile.

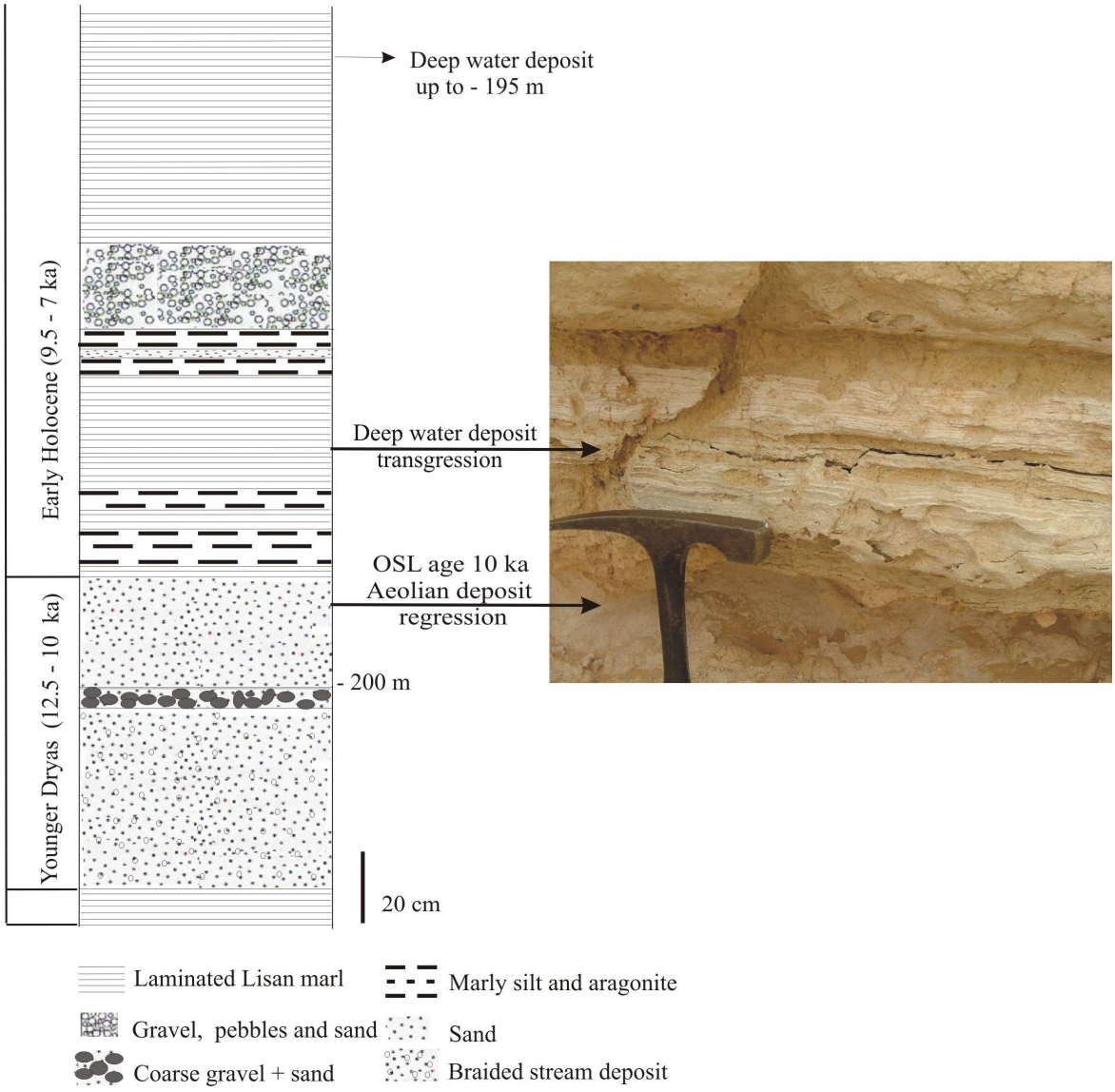

Fig. 3.17: Geological profile of Lake Lisan deposits along the northern bank of Wadi Dahel, south east of the Dead Sea. Notice the dated sand layer below the deep water deposits.

3.8 Conclusions

The terraces of Lake Lisan, situated at altitudes between -148 and -370 m, provide a detailed historical record of its Glacial to Post-Glacial recession and, therefore, of the palaeoclimate of the Near East. The morphological characteristics of the lake terraces and the geomorphological processes influencing them are critical to understanding both development and destruction of the terraces.

The altimetry, morphological and sedimentological investigations and dating of the terraces allow the following conclusions to be drawn:

1. Field observations emphasize that Lake Lisan has experienced a number of transgressions that caused formation of distinct terraces. This is shown by (a) the occurrence of stromatolite and lacustrine deposits in the courses of the wadis draining to the Dead Sea, (b) the existence of stromatolite and beach colluvium deposits under a thick layer of fine lacustrine deposits, (c) the presence of stromatolite crust overgrowing varnished rock blocks, (d) the occurrence of deep water deposits (aragonite and gypsum) on the surface of some terraces and (e) the alternating of lacustrine fine deposits with alluvial coarse deposits along the wadis.

2. Apparent horizontality of the terraces both between the measured profiles and on aerial pictures in general and the reoccurrence of specific elevations in several of the profiles indicate the lack of morphologically important tectonic activity in the last 30 ka.

3. The age of the high altitude terraces (-148 and -154 m) corresponds well with that of the highest terraces on the western side of the Dead Sea up to -150 m. Considering that our measurements were made by high precision GPS altimetry, compared to leveling in the older studies, the difference is well within the measuring error, again suggesting the absence of morphologically significant tectonic activity along the DSTF in the last 30 ka.

4. The slope of the coast, the water depth and the lithology of the underlying rocks play a significant role in determining where Lake Lisan waves could create terraces. The Cambrian siltstones of the Tayan and Hannah Formations were the best suited to create terraces during short intervals of lake level stagnation. This explains the existence of well defined terraces along the southeastern coast of the present Dead Sea and the lack of them throughout much of the rest of the eastern Dead Sea coast.

5. Constructional terraces are preserved also on the Umm Ishrin sandstone at elevations of -148 and -158 m, because they are stabilised by stromatolitic crusts during prolonged still stands.

6. The occurrence of cemented lacustrine deposits in the courses of the wadis draining to the Dead Sea indicates that these wadis were formed before the rise of Lake Lisan, consecutively filled with lake and alluvial fan deposits during the lake transgression and re-incised after Lake Lisan regression.

7. Well-developed desert varnish and Tafoni, preferentially on Umm Ishrin sandstone blocks covering the terraces, imply a long period of exposure and an overall low rate of erosion.

8. The ubiquitous calcareous stromatolites on the investigated terraces show that the terraces are indeed lacustrine in origin. Experience from other lakes show that stromatolites form near shore within the photic zone, most likely in water less than 50 m deep (Kempe and Kazmierczak, 1990). Their presence also implies that the lake chemistry must have been alkaline and highly supersaturated (between 8 and 10 times) with respect to calcium carbonate, indicating that the lake chemistry was similar throughout the high stand. High wave activity prevented the deposition of fine-grained gypsum and aragonite mud; it was apparently re-suspended and deposited in deeper water forming the contemporaneous Lisan Formation.

9. Lake Lisan has experienced prolonged high stands (at -148 to -154 m) at around 30.5 ± 0.22 and 22.9 ± 0.29 ka BP due to higher freshwater input and/or less evaporation. Then, the lake began dropping until it reached -200 m or lower at ~ 20-18 ka BP. Lake Lisan rose again at around 15-13 ka BP, as indicated by the deep water deposits of the Dahel profile, probably associated with the wet conditions during the Bølling-Allerød. By 10 ± 0.8 ka BP the lake dropped sharply to -200 m, followed by a transgression between 9.5-7 ka BP.

10. The U/Th dates show that the stromatolites of the high level terraces grew during the Dansgaard-Oeschger stadials 5 and 2c, i.e., during stable cold periods of the High Glacial. However, the formation of the terraces pre-dates those of the stromatolites growing on them. Terrace formation could therefore have been caused by the transgression at the beginning of the respective cold phases, initiating climatic cooling and therefore lake level rise.

11. The comparison with the Greenland Ice Core record shows that the highest terrace is representative of the coldest period of the Last Glacial (stadial 5 which shows lowest isotope values) and that the second highest terrace is representative of the final phase of the Last Glacial.

12. This agreement of high-level terraces with the stadials of the Last Glacial suggests that the high latitude cold periods are correlated with a positive water balance and high lake levels in the Near East, while warm periods are correlated with a negative water balance and low lake levels. It also illustrates that Lake Lisan reacted abruptly to short-term climatic changes during the Last Glacial.

In spite of their great geomorphological and palaeoclimatological importance, the Lake Lisan terraces have already been damaged by bulldozing over much of their area (for "agricultural" purposes). Their unique landscape should be protected as a natural reserve; otherwise we will lose one of the most important records of Lake Lisan fluctuations induced by climatic changes in the Late Pleistocene and early Holocene in the Near East.

Acknowledgement

We would like to thank Abdulkader Abed from the University of Jordan for his guidance, help in the fieldwork, and useful discussions; Hans-Peter Harres (Darmstadt), Ahamad Al-Malabeh (Zarka), Horst-Volker Henschel (Darmstadt), and Mohammad Nawasrah (Amman) for their support in the field and helpful discussions; Markus Fuchs (Bayreuth) for OSL dating, Augusto Mangini for U/Th dating, Ingo Sass (Darmstadt) for providing GPS equipment; Yahia Al-Farhan (Amman) for his useful comments; Mohammad Abo Kazleh (Amman) for his assistance in the field, GPS measurements and data processing; BGR Hannover for providing aerial photos for Lake Lisan; and NRA Jordan for providing a car and accommodation for two weeks. This work was supported by grants from the DFG and DAAD, Germany.

4. Geomorphological and sedimentological evidence for a high stand of Lake Lisan of up to 150 m higher than previously reported

Abstract

Along the eastern escarpment of the Dead Sea rift, Middle Cambrian, unconsolidated siltstones outcrop repeatedly in Wadi Al-Tayan due to branches of the Dead Sea Transform Fault. On these siltstones terraces have been preserved at altitudes of -150 m to 0 m, ca. 150 m higher than the previously reported high-stand of glacial Lake Lisan. The altitudes of the terraces were determined with DGPS and remains of calcareous stromatolitic crusts were U/Th dated and analysed for their stable isotope, mineral composition (XRD) and Mg/Ca ratios. Together with the results presented in Chapter 3, the history of Lake Lisan can now be reconstructed much more precisely:

According to the new data the lake stood at -56 m at ~80 ka BP and at -66 m at 76 ka BP, reflecting an extraordinary humid climate during MIS 5a in the southern Levant. In two profiles, terraces up to 0 m occur suggesting that the lake stood even up to this level prior to 80 ka BP. After this high stand period the lake level dropped dramatically until it reached -350 m at ~63.6 ka BP, implying a cold and dry climate of the Jordan valley during H6 and MIS 4. Following a low level period between ~63 and 57 ka BP, the lake recovered again, reaching a high stand of >-137 m just before 32 ka BP. This suggests a once again more humid climate and a high water input to Lake Lisan during MIS 3.

By the beginning of MIS 2, the lake receded from its high stand of -137 m at 32 ka BP to -148 m at ~30 ka BP associated with H3. The lake level continued to drop to -152 m at ~27 ka BP and to -154 m at ~23 ka BP. Then, the lake level dropped sharply to -200 m at ~22.5 ka BP, consistent with the dry cold climate of H2. During the LGM, Lake Lisan recovered again to a high stand of -160 m at ~ 19 ka BP, implying a return to a positive water balance. The correspondence of Lake Lisan regressions to the cold MIS 4 and 2, as well to Heinrich events 6, 5, 4, 3 and 2 implies a cold, dry climate of the Levant during these periods. On the other hand, the lake high stands during MIS 5a and the sharp transgression of the lake during MIS 3 suggest a warm, wet climate of the Jordan valley during these periods, most likely caused by an invasion of the Monsoon from the south.

4.1 Introduction

The Jordan rift valley is a tectonically active zone that began to form during late Tertiary (e. g., Powell, 1988). Plio-Pleistocene marine-brackish fossils found in the rock salt of Mount Sedom, south west of the Dead Sea, suggest that the graben was connected with the open sea until early to middle Pleistocene (Neev and Emery, 1967). After the disconnection, the depression was occupied by several water bodies. The Samra fresh-water lake in the Last Interglacial (140-75 ka BP), the brackish Lake Lisan in the Last Glacial (70-14 ka BP) (e.g., Waldmann et al., 2007), the Damya lake at the boundary between the Pleistocene and Holocene (Abed and Yaghan, 2000) and the hyper-saline Dead Sea during the Holocene.

The ages of Lake Lisan and Samra were determined based on the U/Th dating of primary aragonite found in the lake deposits. U-series ages of the upper part of the Samra Formation near Mt. Sedom range from > 200 to 80 ka BP (Kaufman, 1971; Kaufman et al., 1992). Based on the deposition rate of Lisan sediments, Neev and Emery (1967) suggested 70-100 ka BP for the beginning of Lake Lisan period. The oldest age for the early stage of Lake Lisan was reported by Langozky (1963). He related aragonite-rich beds, found on the top of the Hamarmar (Samra) to the Lisan Formation and dated them to 115 ka BP.

During its high stand, Lake Lisan had N-S extension of > 200 km from Lake Tiberias to > 30 km south of the present Dead Sea. The basin of Lake Lisan can be divided into two sub basins: (a) a narrow 7-km-wide northern basin from Lake Tiberias to Marma Feiyad; and (b) a 15-km-wide southern basin from Marma Feiyad to ~30 km south of Sedom Mountain (Begin et al., 1974) (Fig. 4.1).

The lake fluctuated between -370 and -180 m (Neev and Emery, 1967; Begin et al., 1974; Bowman, 1971) leaving behind lacustrine deposits and sequences of shoreline terraces. Recent studies of these terraces and of the associated stromatolites proved however that the lake reached a much higher level of -150 to -148 m (Bowman and Gross, 1992; Abu Ghazleh and Kempe, 2009). Lacustrine deposits of Lake Lisan were found up to -130 m in Zin Valley -south east of the Dead Sea- and dated between 30.4 ± 2 and 34.2 ± 2 ka BP (Sheinkman, 2002).

Although Lake Lisan history was reconstructed by several studies (e.g., Bartov et al., 2002, Machlus et al., 2000), most of these reconstructions were performed using sedimentological and stratigraphical analyses of the lake deposits and dating of aragonite laminae. Given that the aragonite was deposited on the lake bottom, it does not attest to the level of Lake Lisan (Begin et al., 1974; 1984; Katz et al., 1977). However, very few studies were carried out using the shallow water deposits of stromatolites or the shore line terraces. ^{14}C dates were obtained from Lisan stromatolites by Neev and Emery (1967), Begin et al. (1985) and Landmann et al. (2002). Their results are not entirely reliable because stromatolites are possibly contaminated by young carbonate.

Lisker et al. (2009) reconstructed the Lake Lisan levels using U/Th dating of stromatolites growing in caves along the western coast of the Dead Sea. They reported a high level of -188 m at ~30.6 ka, up to 80 m higher than the previously constructed level at that time. Our study is the first on the eastern shore that uses the lake terraces and stromatolites overgrowing them to reconstruct the lake level changes during the Pleistocene. Since these terraces represent the actual altitude of the water level, they provide an efficient tool to evaluate the lake level changes and associated hydrologic and palaeoclimatic conditions.

4.2 Materials and methods

We examined the aerial photos with scales of 1:10,000 and 1:25,000 of the eastern coast of the Dead Sea (Bundesanstalt für Geowissenschaften und Rohstoffe, Hannover), in order to identify the areas where high-level terraces are well preserved. During the field surveys, we first looked for available geodetic bench marks and selected the one available in Ghour Hadithah as our base station. Then we choose six cross-sections with prominent high-level terraces. The terraces were then surveyed using a differential GPS instrument (Leica SR20). Each GPS measuring point was occupied for 15 min for highest altitude precision; repeated occupation of the same station yielded an elevation precision of < 1 cm. Leica Geo Office (LGO) software was used for post-processing of the GPS data and converting ellipsoidal altitude into meters below sea level.

The surveyed cross-sections are: Numairah 2 (N2), Numairah 4 (N4), north of Wadi Numairah, and Al-Tayan (1-4) (T1-4) south of Wadi Al-Tayan (Fig. 4.2). The slope and width of all terraces were measured with inclinometer and tape.

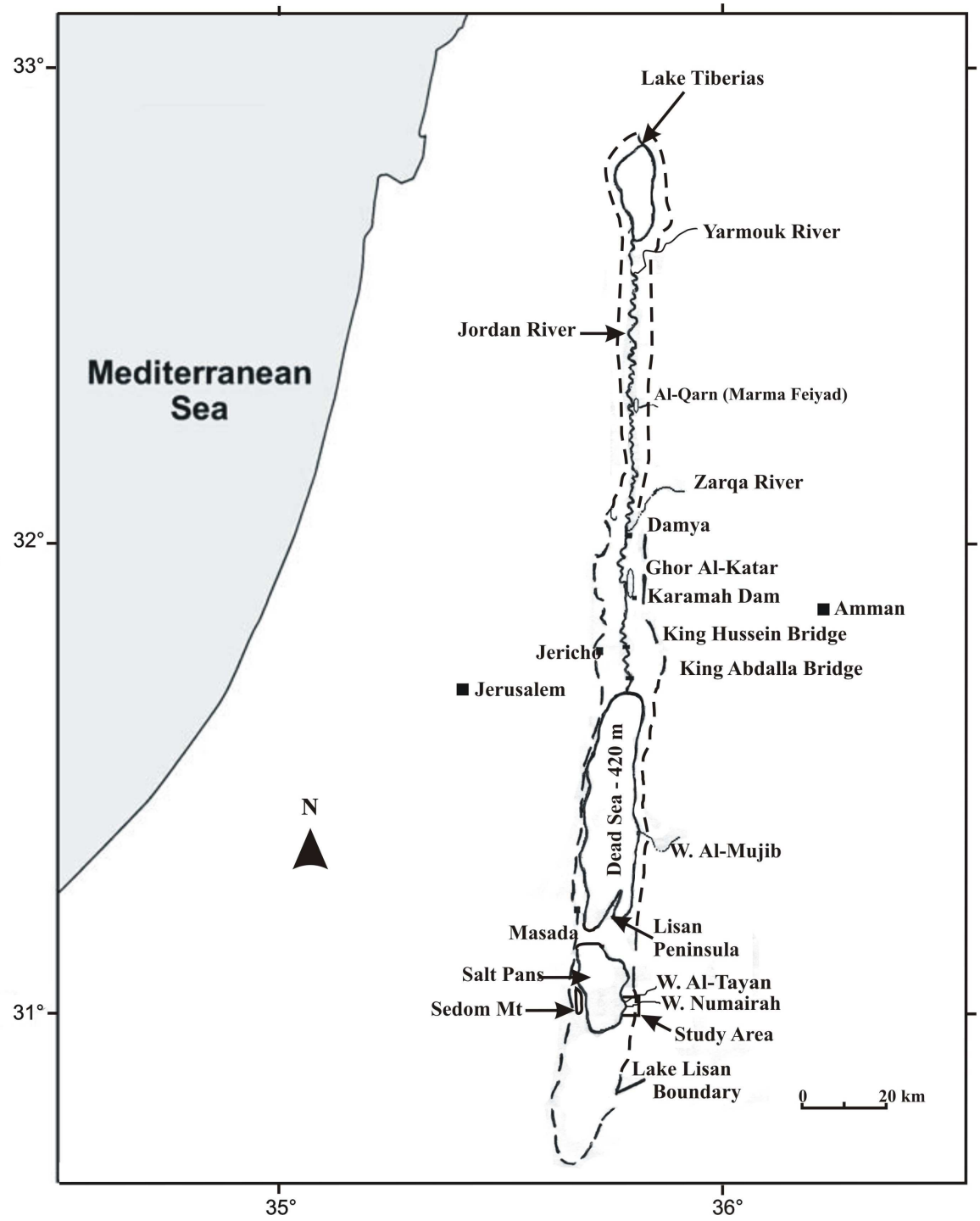

Fig. 4.1: Extent of Lake Lisan during the Last Glacial and location of the study area along the south-eastern coast of the Dead Sea.

The terrace deposits were described. Stromatolites of the terraces were sampled for U/Th dating, thin sections investigation, X-ray diffraction and isotope analysis. To determine Mg and Ca composition of the stromatolites, subsamples were first dissolved in 2-n HCl and filtered into volumetric-flasks.

A buffer solution (Lanthanium/Cesium) was added to the samples that were filled up to 250 ml. Then the samples were measured using Atomic Absorption Spectrophotometry (AAS). From the measurements, the Mg/Ca ratios were calculated and then plotted against altitude.

U/Th dating of Lisan stromatolites was carried out at the laboratories of Heidelberg Academy of Science/Augsto Mangini and GEOMAR-Kiel/ Anton Eisenhauer, Germany. Since the lacustrine carbonates are generally associated with detrital sediments containing significant amount of thorium, ^{230}Th dating isochron techniques has been applied using Multi Collector Inductive Coupled Plasma Mass Spectrometry (IC-PMS). Details of this technique were described in Bourdon et al. (2003). Another two sand samples were dated by OSL (Markus Fuchs, Bayreuth, Germany). In addition, a geological and geomorphological map of the study area was drawn based on aerial photos, field investigation and the Al-Karak geological map produced by Powell (1988).

4.3 Geological setting

The Jordan Graben is a series of pull-apart basins that formed due to strike-slip movement along the Dead Sea Transform Fault (DSTF) (for overview see Quennell, 1958; Bender, 1974; Abed, 2000; Powell, 1988). The DSTF started to develop in the Oligocene to Miocene times separating the northward-moving Arabian plate from the stationary Sinai-Palestine subplate, a northern extension of the African plate, with a sinistral displacement of about 110 km. The Dead Sea rift was connected to the Mediterranean Sea until early to middle Pleistocene. Then it became disconnected probably due to tectonic uplift (Powell, 1988). Although the main Dead Sea fault is obscured under the superficial cover of Lisan deposits and alluvial fans, two branches of the DSTF cutting through Cambrian Formations were recognised. They strike NE-SW (Powell, 1988), forming the Al-Tayan Valley (Fig. 4.2).

There the members of the Burj Formation reoccur several times at different elevations (Fig. 4.3). The oldest exposed bedrock in the study area is the Salib Arkosic Sandstone from the early Cambrian. It crops out as steep rugged cliffs along the eastern coast of the Dead Sea north of Wadi Numairah. The overlying Burj Dolomite-Shale from the middle Cambrian is exposed between Wadi Al-Tayan and Wadi Numairah. It consists of three members: the lower Tayan Siltstone is 20 m thick and consists of red to green finely-

laminated siltstone and cross-laminated sandstone; the middle Numayri Dolomite is about 40 m thick, consisting of grey, cross-laminated sandy dolomite passing up to brown-grey dolomite limestone with prominent steep cliffs; the upper Hana Siltstone is 30 m thick and very similar to the Tayan Siltstone but with a higher proportion of thin-bedded sandstone. The Burj Dolomite-Shale is overlain by the red-brown, coarse-grained sandstone of the Umm Ishrin Formation. It crops out north of Wadi Al-Tayan also with a distinct steep morphology (Fig. 4.2).

The Cretaceous Kurnub Sandstone rests unconformably on the Umm Ishrin Sandstone forming a prominent peneplain. It consists of greywhite, medium- to coarse-grained quartz sandstone with a thickness of 165-240 m. The youngest deposit in the study area is the Lisan Marl Formation from the late Pleistocene (Powell, 1988). It overlies the older rocks unconformably and can be divided into three facies: (a) thin-laminated marl with gypsum laminae, deposited in the deeper part of Lake Lisan; (b) cross-bedded sand and gravels deposited as lacustrine fans, and (c) cross-bedded beach rock (Powell, 1988) cemented by thick laminated stromatolite crusts in the shallow water of the lake.

4.4 Regional and geomorphological setting

The study area extends from Wadi Numairah south east of the Dead Sea to about one kilometer north of Wadi Al-Tayan. Both wadis are draining to the southern basin of the Dead Sea that has been dried out since 1980. The basin is currently occupied by salt pans used for potash industry.

The initial incision of the west-draining wadis including Wadi Numairah and Wadi Al-Tayan seems to have occurred prior to the filling period of Lake Lisan. This is indicated by the presence of Lisan Marl and cemented gravels in the deep canyons of these wadis (Abu Ghazleh and Kempe, 2009; Powell, 1988). The lowering of the lake level by more than 250 m during the late Pleistocene resulted in renewed incision of these wadis. Consequently, vast amount of sediments was removed from the wadi courses and re-deposited into their mouths forming sub-lacustrine fan deltas. In the case of Wadi Al-Tayan, the late Pleistocene fan delta was exposed along its mouth due to the lake regression (Fig. 4.3). During phases of standstills interrupting this regression, sequences of wave-cut terraces were formed in the southern part of the fan-delta ranging between -160 to -130 m (T.1, T.2).

These terraces were preserved due to low sediment supply in this part of the delta. However, in the northern part, aggradational conditions prevailed forming a flood plain with a low slope (Fig. 4.3) and no terraces were exposed due to high sediment supply.

The lowering of the base level of Lake Lisan after the LGM caused a rejuvenating of Wadi Al-Tayan and deep incision of the lower course in the Pleistocene fan delta. Thus, a new fan delta of glacial age was formed in front of the old one. The lowering of the Dead Sea to its present day level induced a rapid incision of Wadi Al Tayan in its glacial fan delta. As a result, a series of alluvial fan deltas of different ages was formed.

The base level lowering since the Pleistocene caused also a rapid head-ward erosion of the west-draining wadis. Both Wadi Numairah and Wadi Al-Tayan were able to reach the Oligocene peneplain of the Kurnub sandstone and erode it, leaving behind some ridges and isolated remnants with sub flat surfaces (Fig. 4.3). The eroded materials were transported along the escarpment face as elongated debris flows postdating the steep-sided wadi incision into the Umm Ishrin Formation (Powell, 1988). The weathered materials of the the Umm Ishrin and Kurnub sandstones moved down under the force of gravity and accumulated on the base of the steep slopes forming a continuous chain of talus scree bodies.

Most of Lake Lisan terraces identified in the field were created on the Tayan and Hanneh Siltstones or on the Lisan Formation (Figs. 4.2; 4.3). The siltstones and the Lisan Formation are relatively soft and thus can be eroded easily by wave action, recording short periods of standstills with constant lake levels.

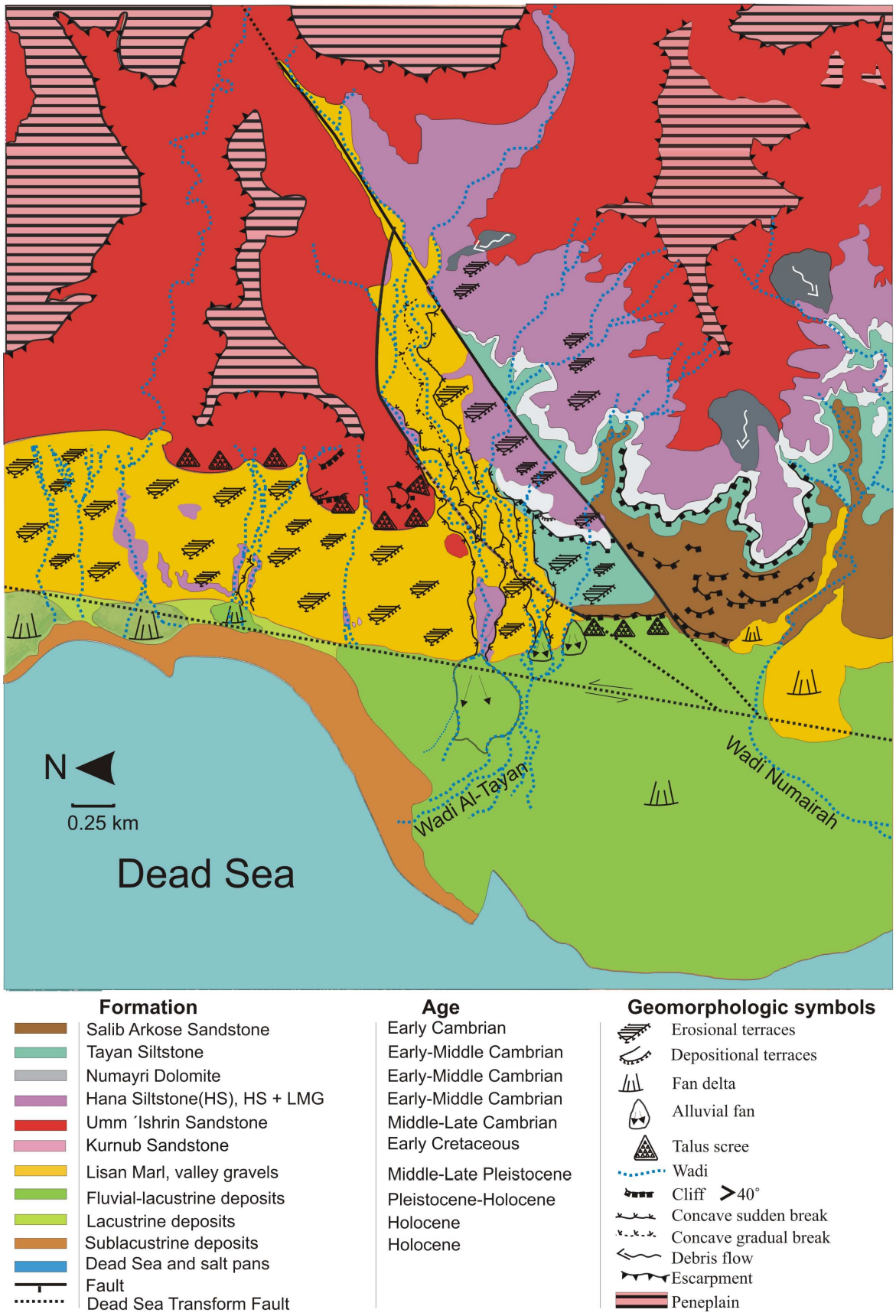

Fig. 4.2: Detailed geological and geomorphological map of the study area based on the field work, aerial photos 1: 25,000 and on the Al-Karak sheet (1987).

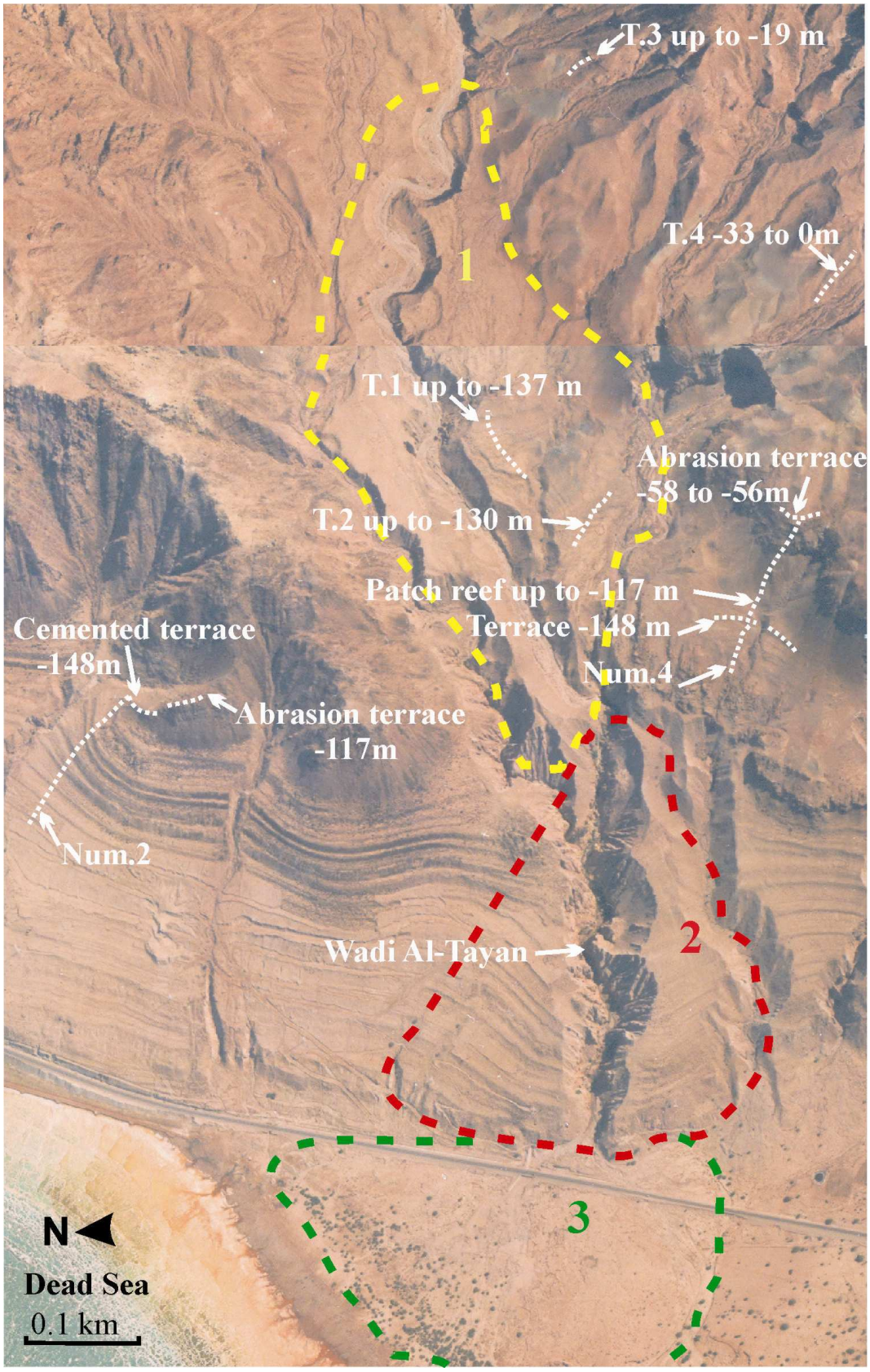

Fig. 4.3: Aerial photo showing sequences of high level terraces of Lake Lisan and the locations of the terrace profiles along the eastern coast of the Dead Sea. Note the sequence of alluvial fan deltas of Wadi Al-Tayan corresponding to, pre-LGM (1), the LGM (2) and the post-LGM (Holocene) (3).

4.5 Result and discussion

4.5.1 Shore line terraces and stromatolites

The highest shore line of Lake Lisan is often cited as -180 m based on the uppermost elevation of Lisan marls and of Lisan terraces (Neev and Emery, 1967; Begin et al., 1974; Bowman, 1971). In Wadi Al-Hasa, the maximum elevation of Lisan marls was found at -160 m. This high elevation was attributed to post-Lisan tectonic uplift (Clark, 1988). Later studies of the Lisan terraces revealed higher water stands. Bowman and Gross (1992) found a sequence of raised beaches encircling the Lisan Formation in the Hazeva area up to -150 m dated by Matmon et al. (2003) to 20-36 ka BP. Abu Ghazleh and Kempe (2009) documented high level terraces of Lake Lisan in the southeastern coast of the Dead Sea at -154 and -148 m dated to 22.9 and 30.5 ka BP, respectively. These high-level terraces correlate well with those found by Bowman and Gross (1992).

Sequences of shoreline terraces, much higher than -148 m, were identified by us during our field expedition 2007 in the south eastern coast of the Dead Sea between the lower course of Wadi Numairah and that of Wadi Al-Tayan (Figs. 4.2, 4.3). In the Al-Tayan 1 profile (T1), a sequence of lake terraces was recognised between -161 and -137 m (Figs. 4.2, 4.4, 4.5 a).

Calcareous stromatolite crusts overgrowing beach gravels and stabilising piles of rocks were observed on all of these terraces. The stromatolite crusts are thick, massive and hard, with a dark-grey or white-grey finely-laminated structure (Fig. 4.5 b, c), indicating that they are mostly calcareous organic build-ups. Stromatolites form in highly $CaCO_3$-supersaturated water by permineralisation mostly of cyanobacterial mats (e.g., Kempe and Kazmierczak, 2007). Although the terrace stromatolites were dissoluted partially by rain water, they maintained their original texture. In addition to the grey laminated stromatolites, red, thin and micro-laminated crusts were observed on some of these terraces. They form distinctive horizons, either overlaying the grey stromatolites (Fig. 4.5 d) or directly overgrowing rock blocks of the terraces. The red crust was mostly noticed on the highest terraces up to -137 m, but in general it is not as common as the dark- grey one. In the T2 profile, four shoreline terraces were identified between -161 and -131 m (Figs. 4.2, 4.4). Ubiquitous calcareous stromatolite crusts overgrow these terraces (Fig. 4.6 a, b). Red crust was also observed on some terraces, especially on the highest ones.

In the Numairah 2 profile (N2), the terraces range from -228 to -117 m (Figs. 4.2, 4.4). Two distinctive accumulation shoreline terraces were observed at -159 to -148 m (Fig. 4.7 a) that are cemented by a thick laminated stromatolite crust aiding in their resistance against erosion. The cementation indicates a long time of standstill and a water chemistry favoring stromatolite growth. On top of this profile, a flat abrasion terrace was formed at -117 m (Fig. 4.7 b). Stromatolites are missing on this terrace, either they could not be formed due to strong wave activity or they were corroded by rain on such an exposed surface. Behind the abrasion terrace and toward the east, two lagoon-like flat surfaces were identified at levels of -119 and -118 m (Fig. 4.7 c). The benches are covered with fine sediments and rounded gravels. Red, thin stromatolite crust was also observed on some of the rock blocks. Thin section investigation of the red crust shows a laminated structure similar to that of the grey one (Fig. 4.11 c).

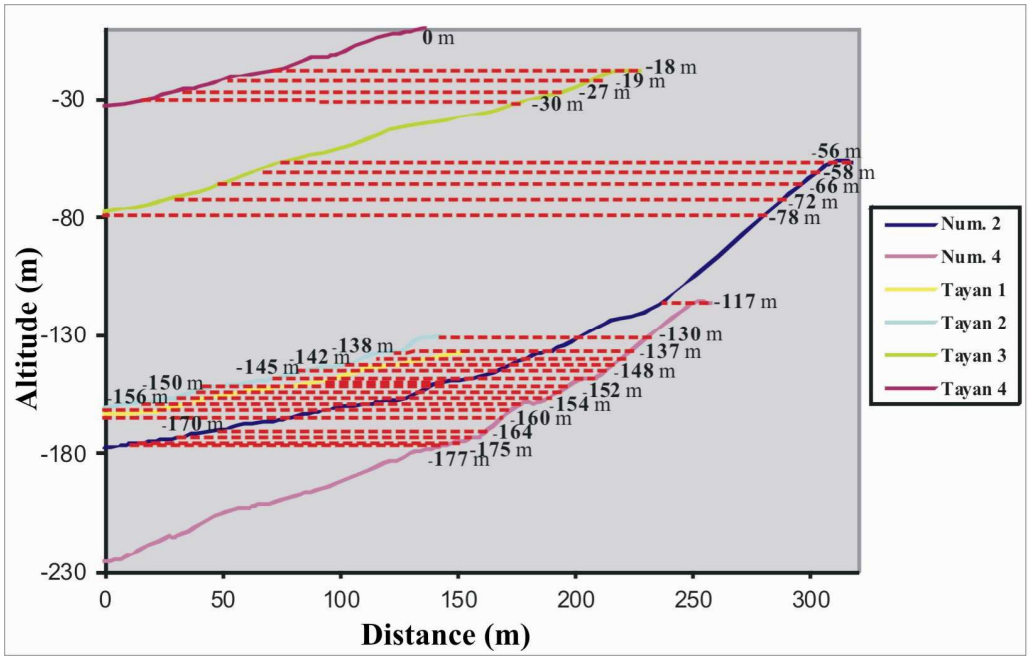

Fig. 4.4: The correlation between the high level terraces of Lake Lisan in the six cross-sections.

In the N4 profile, the terraces range in level between -178 and -56 m (Figs. 4.2, 4.4). Stromatolites grew also on most of these terraces. On the -148 m terrace, a patch reef was formed, consisting of gravels, pebbles and cobbles that have been cemented by calcareous laminated stromatolitic crust up to -117 m (Fig. 4.8 a, b). The steep dolomite cliff above the patch reef did not allow terraces to be cut. However, grey laminated stromatolite crusts occur frequently on the dolomite cliff between -117 and -58 m (Fig. 4.8). The top of the dolomite cliff was cut by abrasion forming a terrace at -56 m (Fig. 4.8 d).

a

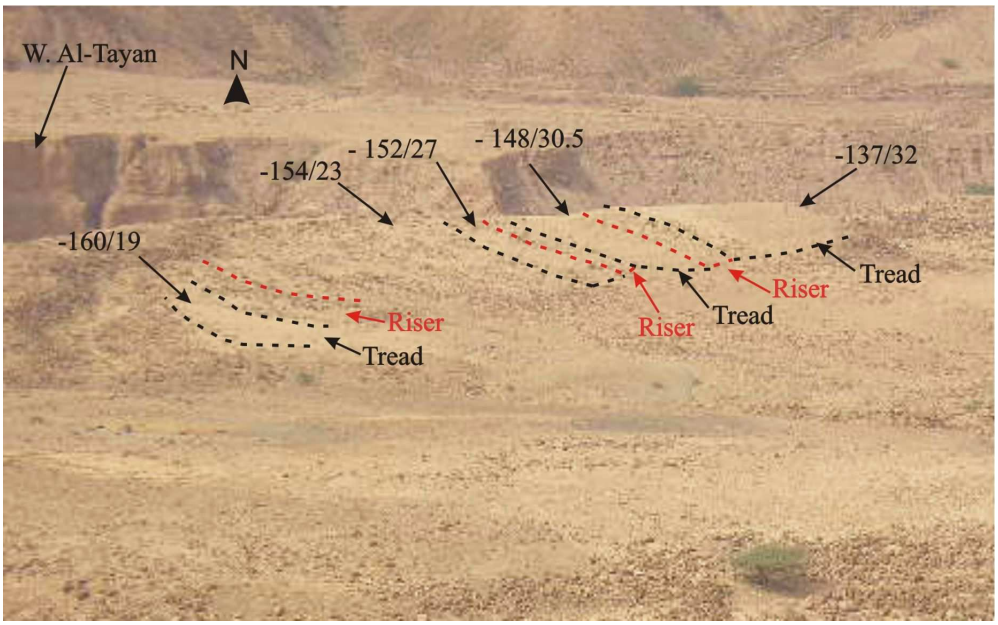

b

Fig. 4.5 a: Sequence of high Lake Lisan terraces in T1 ranging between -160 to -137 m, the left numbers refer to the altitude and the right ones to the age in ka BP. b: Grey laminated stromatolite crusts cement and overgrow the surface deposits of the -137 m terrace in T. 1.

c

d

Fig. 4.5 c: Mixture of grey and red microlaminated stromatolites overgrow and cement sand stone blocks on the -137 m terrace. d: Grey, laminated stromatolite overgrown by red stromatolite crust from the -137 m terrace.

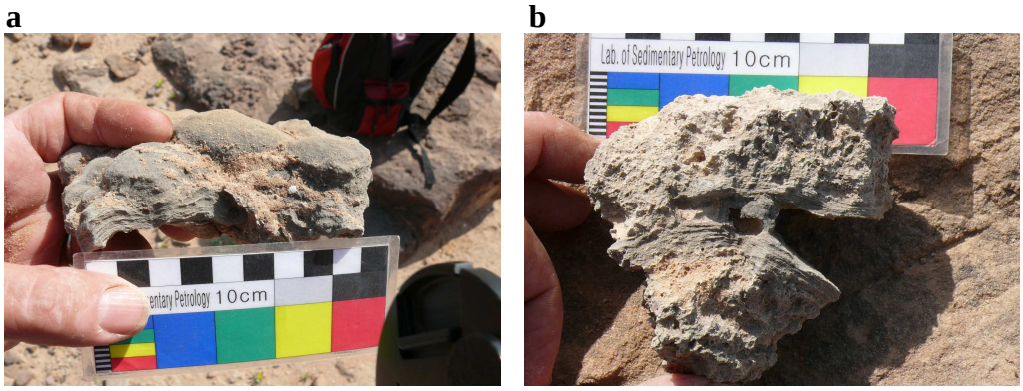

Fig. 4.6 a, b: Lake Lisan microlaminated stromatolites overgrowing Cambrian sandstone Blocks in T. 2 at an altitude of ~ -154 m.

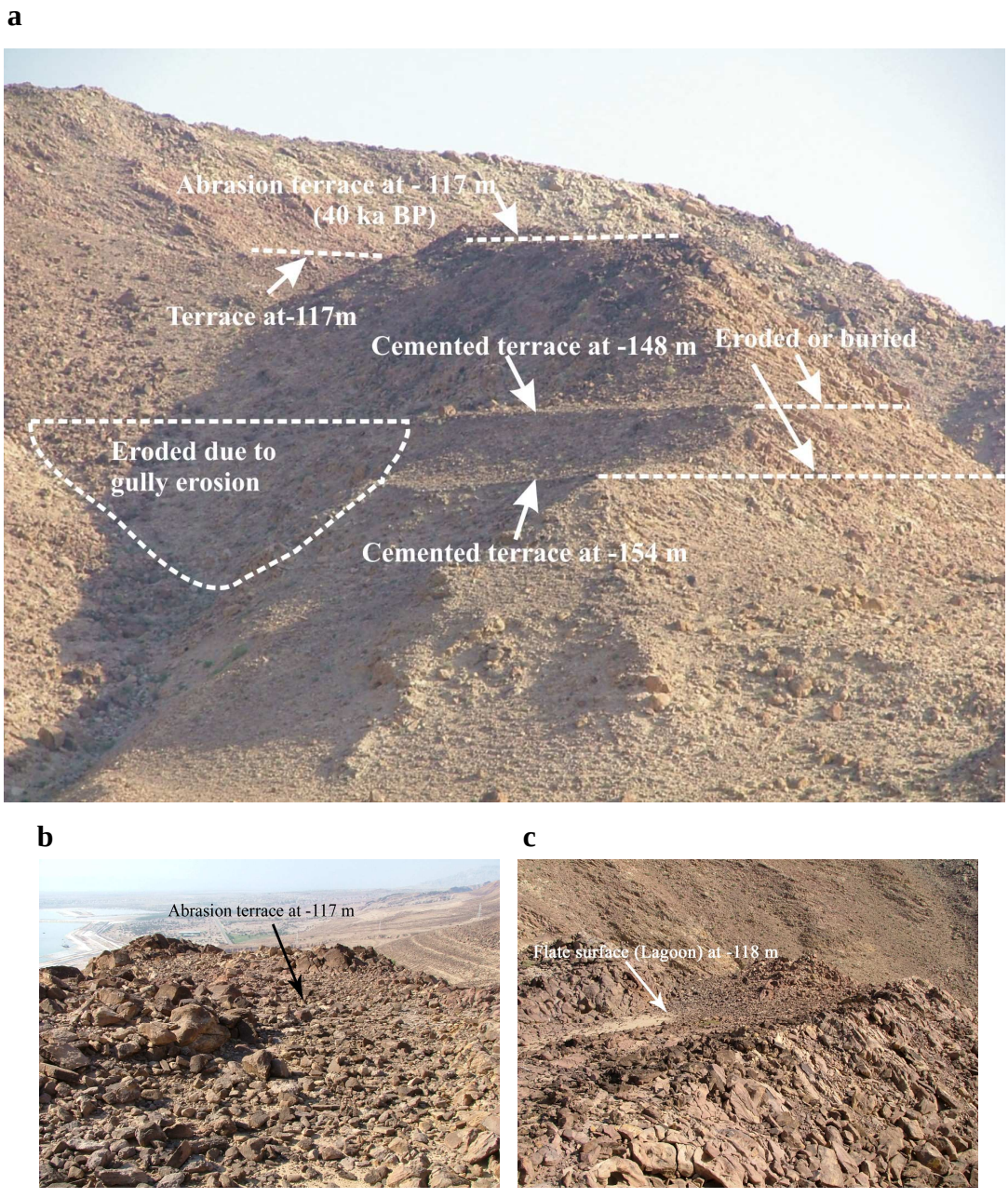

Fig. 4.7 a: The highest terraces in N4 at -159 to -148 m, b: The abrasion terrace on the top of the Cambrian sandstone mountain at -117 m, and c: The lagoon-like flat surface at -118 m.

Massive and grey-laminated stromatolites very similar to those found below were observed even at these high levels (Fig. 4.8 e). The joints and cavities of the dolomite played an important role in protecting stromatolites from waves and rain erosion. The abundance of stromatolites at -117 m and even much higher up to -56 m in N4 and the absence of such stromatolites at the same level in N2 suggest that this is caused by differences in the geology substrate acting as a shelter to minimise erosion.

However, thin red crusts of micro-laminated structure- similar to that of the lower stromatolites- were observed on the rock blocks covering these terraces. This difference could be attributed to: a) the Lake chemistry that was less alkaline at the high stand due to a high fresh water input. This is also indicated by the low Mg/Ca ratio of stromatolites at these levels and by the mineral composition of pure, primary calcite; and/or b) the wave action was stronger at the steep eastern shore of Lake Lisan in which these terraces were cut.The re-occurrence of the high level terraces (> -56 m) in two profile, and their appearance as one continuous sequence of terraces (Figs. 4.9 a, 4.10), in addition to the existence of red crust above and below -56 m, indicate that these highest terraces were derived from the same water body and that Lake Lisan stood most likely even up to 0 m.

4.5.2 Thin sections investigation

The thin sections of stromatolite samples taken from Lake Lisan terraces at -154 to -56 m show a typical lamination structure of stromatolites (Fig. 4.11 a-f). The micro- structure of stromatolites from -56 m to -58 m shows micro-laminated structures similar to those of the stromatolites from relatively lower levels (-154 to -148 m) (Fig. 4.11). This emphasises that all of these stromatolites were derived from the same lake and that the entire area up to -56 m was drowned by Lake Lisan. The lamination structure was slightly disturbed at the highest altitudes, indicating low water depth and sufficient wave energy. This is also indicated by a wavy lamination structure in the -58 m stromatolite (Fig. 4.11 e). The red stromatolite crust from -137 m exhibits also dome laminated structure (Fig. 4.11 c), demonstratig that both the red and the grey stromatolites were derived from Lake Lisan. Ooid structure was also recognised in these sections emphasizing that they were grown in agitated lake water.

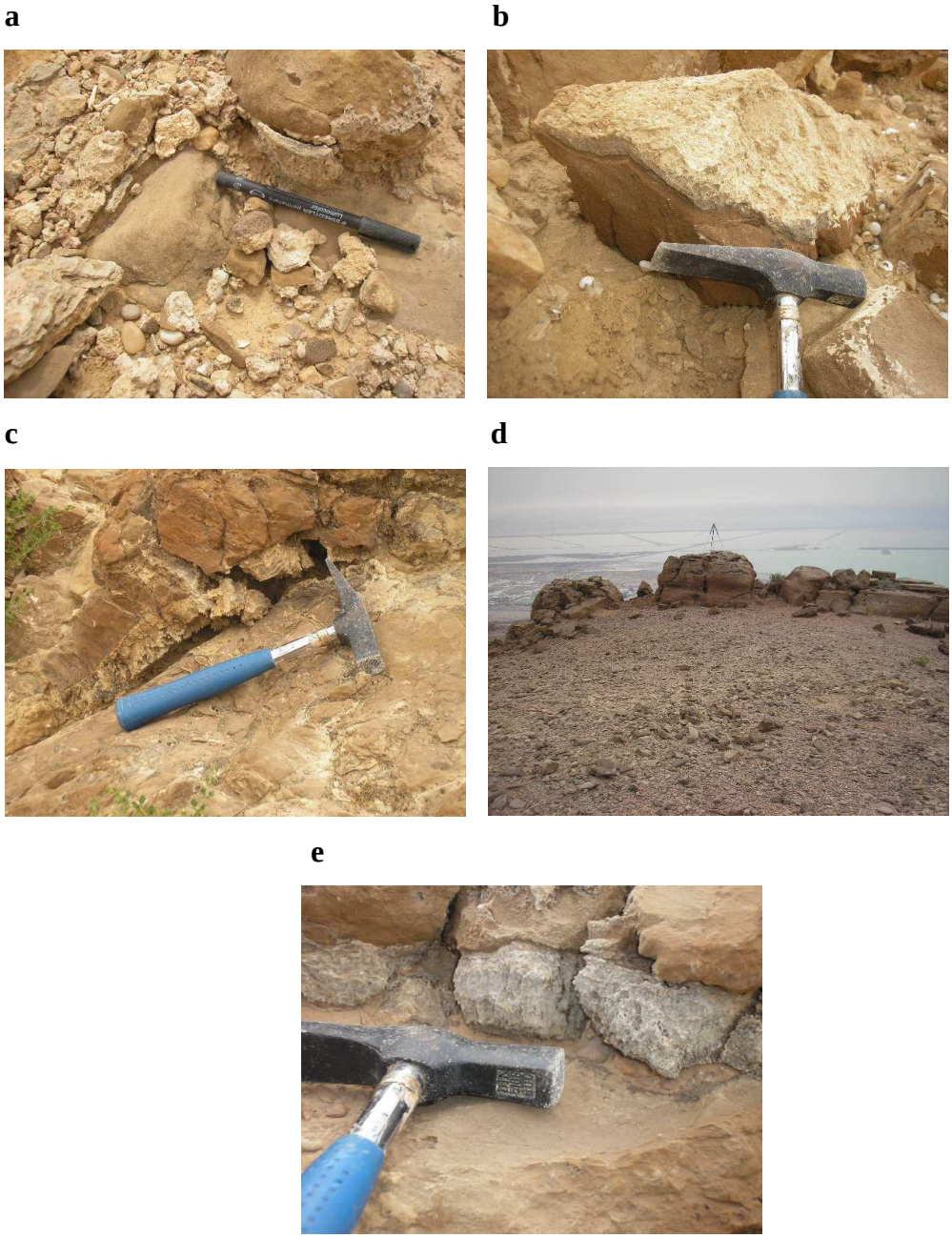

Fig. 4.8 a: Stromatolite crust cementing Cambrian dolomite cobbles and gravel on the patch reef of -138 m. b: Thick stromatolite crust overgrowing dolomite blocks at -117 m. c: Thick laminated stromatolites of Lake Lisan growing in the cavities and joints of Cambrian dolomite between -117 and -58 m. d: The abrasion terrace in N4 at -58 to -56 m. e: Lake Lisan stromatolites grew in the joints of dolomite at -56 m.

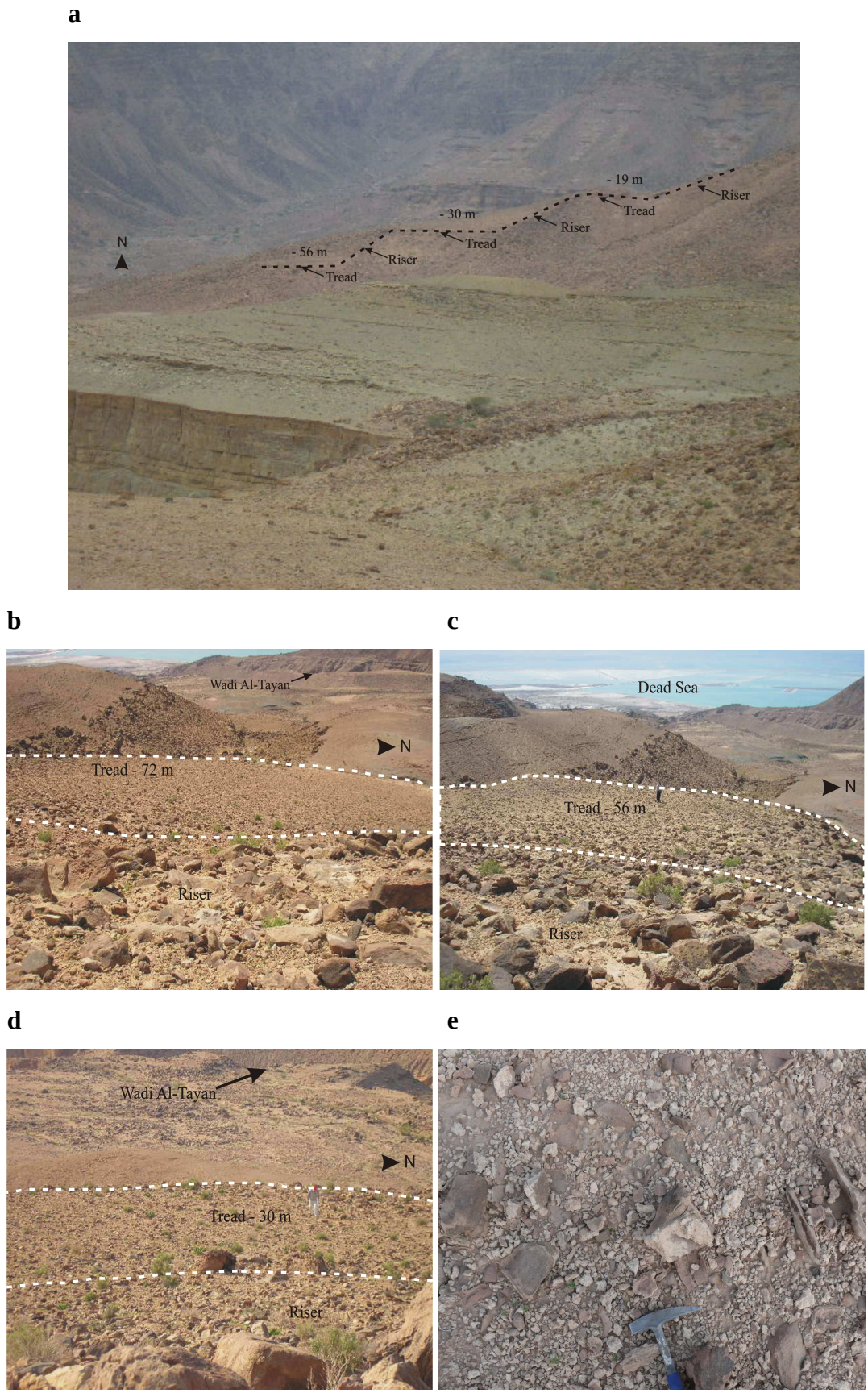

Fig. 4.9 a: Sequence of Lake Lisan terraces in T3 at -78 to -18 m. b, c, d: The first, second and third terrace in T3, note the two prominent parts of these terraces: Tread and riser. e: Beige stromatolite crust overgrowing the surface deposits of the terrace at -30 m.

Fig. 4.10: The terrace sequence up to zero m in Tayan 4 profile.

4.5.3 Stable isotopes

Based on the analysis of carbon and oxygen isotopes of primary carbonates from several lake basins, Talbot (1990) suggested that the isotopic covariance trend could be used to distinguish closed-lakes from open basins in ancient lacustrine records. The most common features of closed lake carbonates, in contrast to those from open lakes, are the large variations in both $\delta^{18}O$ and the high $\delta^{18}O$- $\delta^{13}C$ covariance with a strong positive correlation (r = > 0.7).

Talbot (1990) also suggested that the water balance is the most dominant factor that controls the isotopic evolution of closed lakes. Temperature effects on both the isotopic composition of rainfall and isotopic fractionation during carbonate precipitation are of secondary importance and are generally masked by evaporation and residence-related effects (Stuvier, 1970; Fontes and Gonfiantini, 1967; Gat, 1981; Gonfiantini, 1986; Fritz et al., 1987). The change from negative to positive $\delta^{13}C$ values could be due to the fact that the runoff in humid well-vegetated catchments is more influenced by the decomposition of isotopically-light plant material than those from drier, sparsely vegetated ones. Thus the former tends to produce runoff with more negative $\delta^{13}C$ values than the latter (Talbot, 1990; Salomons et al., 1978; Cerling, 1984; Quade et al., 1989). The shift to more positive $\delta^{13}C$ could be also attributed to preferential outgassing of ^{12}C-rich CO_2 during a period of increasing evaporation and to changes in primary productivity (McKenzie, 1985).

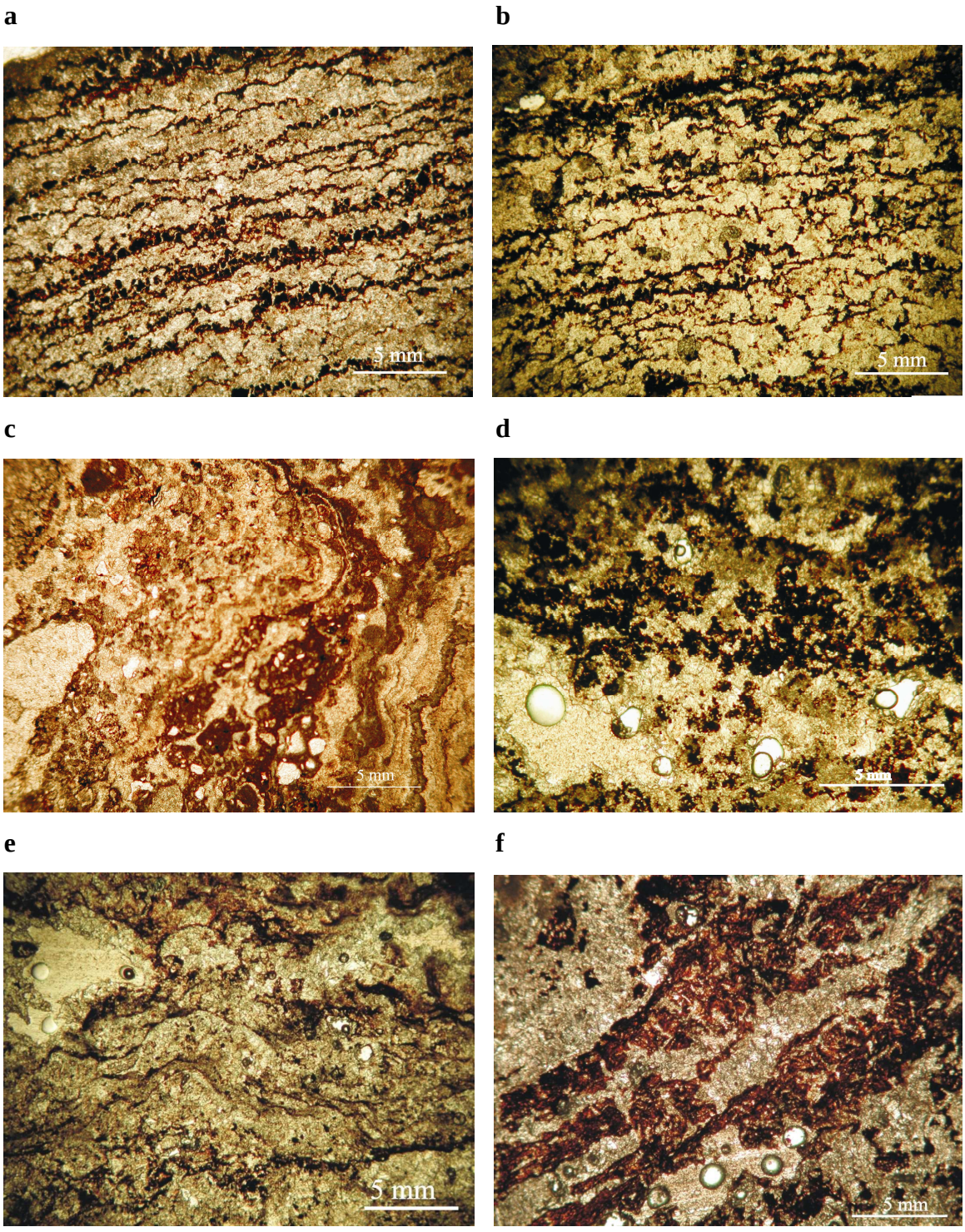

Fig. 4.11: Thin sections of the lake stromatolites in plain light showing the typical lamination structure build by cyanobacteria at -154 m and -148 m (a, b successively), at -117 and -137 m (c, d), at -58 m (e) and at -56 m (f). Note the wavy structure in the -58 m stromatolite caused by sufficient wave energy in shallow water environment.

4.5.3.1 Stable isotopes from Lake Lisan

Oxygen and carbon isotopic analyses were performed on 12 stromatolite samples from Lake Lisan terraces that range in altitude between -160 and -19 m, representing the time interval from ~ 80-19 ka BP according to our U/Th dating (Table 4.1). Since the stromatolites grow in shallow water, they are very sensitive to minor shifts in rainfall and evaporation and therefore a good tool to track the small changes in the hydrology, climate and paleoenvironmental conditions of the lake.

Oxygen and carbon isotopic compositions of these stromatolites show a linear covariant trend with a relatively strong positive correlation (r = 0.8; disregarding sample -160 m because of its anomalous high $\delta^{13}C$ and low $\delta^{18}O$ values) (Fig. 4.12) and large ranges (7.85 and 6.78‰, respectively). According to Talbot (1990), this trend is most typical of primary carbonates formed in closed lakes, implying that the mineral phases of Lisan stromatolites retain their original isotopic signature and that diagenetic alteration is very limited. Apparently, this is due to dry climatic conditions prevailing in the Lake Lisan basin after the last regression. In contrast**,** Kolodny et al. (2005) found that there is no $\delta^{18}O$- $\delta^{13}C$ covariance in most of the Lisan aragonite samples except in few cases, probably reflecting a period of "shut off" of the Jordan and mixing of the two water masses in the north and in the south.

4.5.3.2 Oxygen Isotopes

The oxygen isotopic composition of the stromatolites varies from -4.83 to +3.2 ‰ (range 7.85 ‰; average -0.6 ± 3.9 ‰). These values are less heavy and more varied than the $\delta^{18}O$ values of Lake Lisan aragonite (1.6-6.8 ‰) (1.5-7 ‰) reported by Kolodny et al. (2005) and Katz et al. (1977), respectively. The difference is most likely due to the fact that our stromatolite samples represent the highest stands of Lake Lisan (-160 to -19 m), thus reflecting relatively fresh-water conditions and low evaporation rates. In contrast, the aragonite samples were taken from the low stands of the lake (-267 to -307 m), implying relatively low water input and high evaporation. Talbot (1990) concluded that carbonates precipitated during periods of high lake level will plot toward the negative end of the covariant trend, while those precipitated during periods of low lake levels will plot toward the positive end.

Previous reconstructions of Lake Lisan history (Bartov et al., 2002; Machlus et al., 2000) show that the lake stabilised at -280 to -290 m for a long time period. This indicates small changes in the hydrological balance of the lake at these altitudes and thus small variations in the isotopic composition of the lake water. However, during the period of high lake levels, significant hydrological changes occurred, as indicated by our age data, causing large variations in the isotopic signal of the lake water.

The large range in the $\delta^{18}O$ values could be also due to the difference in the isotopic composition of precipitation in the Lake Lisan basin. It is known that most of the rain in the lake basin originates from East Mediterranean vapour. However, it was suggested by Abed and Yagan (2000) that monsoon rains reached the interior southern Levant during the late Pleistocene. Frumkin et al. (1999) and Matthew and Roberts (2008) pointed out that changes in precipitation isotope values can occur if the source area of precipitation alters, and thus the $\delta^{18}O$ of the lake carbonates varies accordingly. Charles et al. (1994) suggested that variability in moisture source leads to changes in the moisture paths, and thus ultimately to large, abrupt changes in $\delta^{18}O$. Kolodny et al. (2005) attributed the variations in $\delta^{18}O$ of Lake Lisan aragonite to the oscillations in $\delta^{18}O$ of the input water, which reflect climatic conditions in the basin such as drought years, rainy seasons and changing patterns of moisture supply from the sea.

The analysis of $\delta^{18}O$ values of Lisan stromatolites shows the following characteristics:

1. The $\delta^{18}O$ of stromatolites at -76 to -19 m display relatively low values of -1.25 to 1 ‰ with an average of 0.028 ± 0.94 ‰ and a relatively low range of ~ 2.3 ‰. This points to high water input and fresh water conditions of Lake Lisan associated with its highest stands. Fresh water conditions of the lake are also indicated by the fact that calcite is the main carbonate mineral of stromatolites at -76 to -19 m. The small variations in $\delta^{18}O$ most probably reflect minor oscillations in temperature and inflow-evaporation balance of the lake at these high levels.

2. At -103 to -119 m, the $\delta^{18}O$ of stromatolites show an excursion to lighter values (0.75 to -4.83 ‰) with an average of -1.7 ± 0.9 ‰ and a large range of ~ 5 ‰. This excursion is consistent with the sharp transgression of Lake Lisan from -350 m after 63 ka BP to higher than -137 m before 32 ka BP. Such a dramatic rise in the lake level requires an exceptional wet condition that seems unlikely to occur only

due to precipitation originating from the Mediterranean. Thus we agree with the conclusion of Abed and Yaghan (2000) that monsoon rain influenced Lake Lisan basin. These wet conditions are also indicated by the existence of calcite as the dominant mineral of stromatolites at these high stands.

3. Stromatolites from the -137 to -149 m terraces exhibit a shift to heavier positive values of +0.46 and +3.02 ‰ respectively, reflecting a change to relatively dry climatic conditions with low precipitation and more evaporation. This is clearly indicated by our U/Th dates that show a drop of the lake level from -137 m to -154 m. The existence of aragonite as the main or the second most important mineral in these stromatolites emphasizes the change to more dry conditions.

4. At -160 m the $\delta^{18}O$ returned to a low negative value of -3.7 ‰, suggesting a return to more wet conditions in Lake Lisan basin. This agrees with the sharp transgression of Lake Lisan from -200 m after 22 ka BP to -160 m at ~19 ka BP revealed by our U/Th dates. Robinson et al. (2006) reported that in spite of the arid conditions that prevailed during the LGM, Lake Lisan maintained a high level, possibly due to high water input from the melting snow of Mount Hermon.

4.5.3.3 Carbon isotopes

The $\delta^{13}C$ of Lisan stromatolites exhibits relatively low values ranging between -4.87 and +1.91 ‰ with an average of -2 ± 2.8 ‰ and a wide range of 6.78 ‰. These values are less heavy and less varied than those of the Lisan aragonite (-3.4 to +7.9 ‰) reported by Kolodny et al. (2005). This can be interpreted as climatically-induced flora changes in the lake basin between the period of the high-lake level stromatolites and that of the relatively low-lake level aragonites. It could be also attributed to the outgassing of ^{12}C by evaporation during the period of aragonite precipitation causing ^{13}C enrichment in the lake water.

In general the $\delta^{13}C$ values of the Lisan stromatolites show the following major features:

1. Low negative $\delta^{13}C$ values of the highest stromatolites at -19 to -76 m ranging between - 2.14 and -2.78 ‰. These values indicate very wet conditions and a positive water-balance of Lake Lisan during its early stage of ~ 80 to 67 ka BP. This agrees with the conclusion of Talbot (1990) and Tucker (1989) that the high input of organic-derived CO_2 from the humid and well-vegetated basin could

contribute to low $\delta^{13}C$ values. The constant $\delta^{13}C$ values of stromatolites at -76 to -19 m (~ -2 ‰) and the small variance of $\delta^{18}O$, combined with a low correlation between $\delta^{18}O$ and $\delta^{13}C$, reflect a relative long-term stability in the inflow composition and hydrological characteristics of the water body from which they were formed. This implies that both terraces higher and lower than -56 m were most likely derived from the same lake. According to Talbot (1990) these characteristics are most typical of fresh, open lake conditions. This implies that Lake Lisan has evolved from deep, diluted lake during its early stage (at ~ 80 ka BP) to a shallow and more alkaline water body later on. Although geomorphological evidence and U/Th ages indicate a lake-level drop at this time, the large water volume and depth of the lake at these high stands may have damped the changes inthe carbon isotopic signal. Moreover, increased groundwater inflow to the lake due to the level lowering could provide a buffer against the extreme effects of evaporation as reported by Talbot (1990). Thus the lake reacted less dramatically to changes in evaporation rates.

2. A change to more negative $\delta^{13}C$ values of stromatolites (-3 to -4.87 ‰) occurred at -103 to -119 m, indicating increased precipitation and decreased evaporation in the lake basin. This is supported by the sharp transgression of Lake Lisan to these high levels before 32 ka BP. A positive correlation between $\delta^{13}C$ and $\delta^{18}O$ is also recognised at these high altitudes (Table 4.1). The exception at -110 m displays relatively heavier $\delta^{18}O$ value with a negative correlation between $\delta^{13}C$ and $\delta^{18}O$. This could be explained by a short-term climatic change to more arid conditions possibly associated with an omission of the monsoon.

3. A shift to heavier positive values occurred at -137 to -160 m. The massive occurrence of stromatolites at these levels and the increase in evaporation rate as indicated by the lake level drop from -137 to -160 m caused a removal of isotopically light CO_2 from the lake water and $\delta^{13}C$ enrichment.

Table 4.1: Average oxygen and carbon isotopic values of Lake Lisan stromatolites from -160 to 0 m.

Altitude (m)	δ^{13}C ‰ (mean)	δ^{18}O ‰ (mean)	Description
-160	0.44	-3.70	laminated grey stromatolites
-149	1.91	3.02	laminated grey stromatolites
-137	0.75	0.74	laminated grey stromatolites
-119	-4.24	-0.38	grey stromatolites
-117	-4.87	-3.64	grey stromatolites
-110	-0.97	1.32	grey stromatolites
-105	-4.53	-4.83	grey to red stromatolites
-103	-3.01	-0.77	grey stromatolites
-76	-2.51	1.06	grey stromatolites
-64	-2.14	-0.36	laminated grey stromatolites
-30	-2.78	0.66	red crust
-19	-2.17	-1.25	red crust

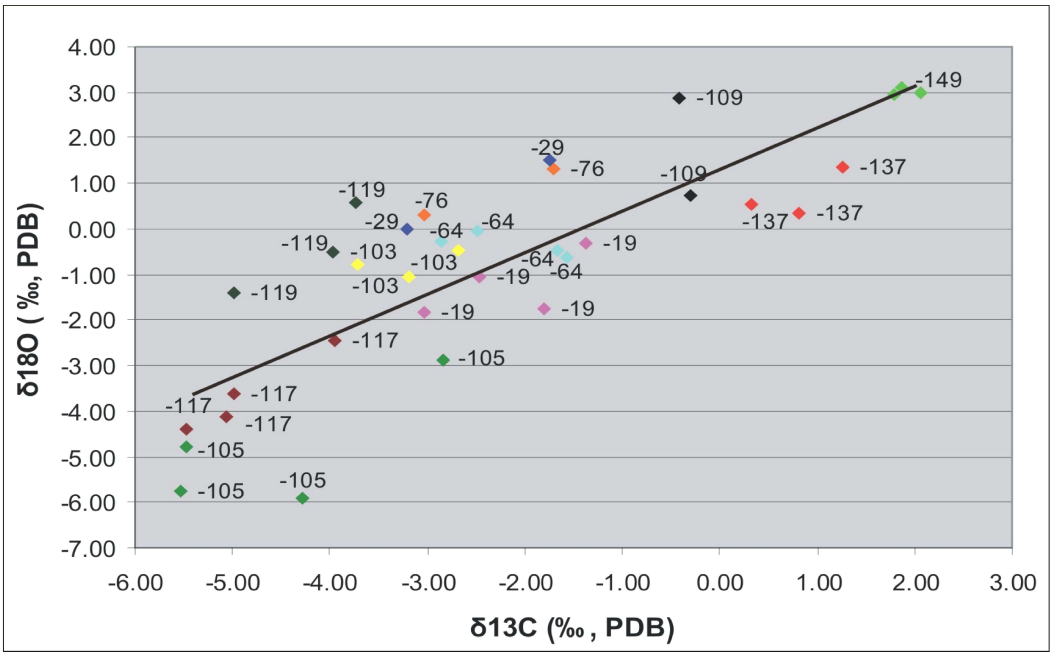

Fig. 4.12: Scatter plot of δ^{13}C versus δ^{18}O values for Lake Lisan stromatolites from -149 to 0 m showing high covariance trend with a strong correlation (r = 0.83, y = 0.8912x + 1.3191).

4.5.4 X-ray analysis and Mg/Ca ratio

X-ray diffraction analysis was applied to 19 samples of Lake Lisan stromatolites ranging in altitude between -350 and 0 m in order to identify their mineral composition (Table 4. 2). The formation of carbonate minerals such as aragonite, calcite, high-Mg calcite and dolomite is thought to be dependent on the Mg/Ca ratio of the lake water (Müller et al., 1972). Therefore, the stromatolite samples were further analysed using AAS in order to determine their Mg/Ca ratio (Table 4.2).

Long-term deposition of aragonite from lake water removes the Ca, while the Mg remains, resulting in a high Mg/Ca ratio. Müller et al. (1972) analysed water and carbonate sediments of several lakes from humid and arid regions and determined their Mg and Ca composition (Table 4.3). They classified the lakes in four groups according to the Mg/Ca ratio of the lake water, from which the minerals precipitated (Table 4.3). Müller et al. (1972) have also concluded that secondary carbonates are found only in lake sediments with high-Mg calcite as a primary mineral and a Mg/Ca ratio of the lake water of > 7. Therefore, they suggested that lakes in groups (a) and (d) have only primary carbonates, while those in (b) and (c) contain diagenetic minerals such as dolomite (Table 4.3).

The AAS analysis of the stromatolites at altitudes of 0 to -56 m (Table 4.2, Fig. 4.13) shows Mg/Ca ratios of 0.040 to 0.049. This suggests that the lake at these levels had Mg/Ca ratios of ~2, indicating high fresh water input to the lake during its highest stands. According to Müller et al. (1972), such Mg/Ca ratios associate mainly with precipitation of (low-Mg) calcite. This agrees well with our XRD analysis of these stromatolites (Table 4.2) that shows a mineral composition of pure calcite. However, the -56 m stromatolite shows a change in the mineralogical composition from calcite to aragonite as the main mineral phase. This could be due to a climatic change to drier conditions that caused a regression of the lake from its high stand at ~80 ka BP. Müller et al. (1972) suggested that lacustrine sediments with such Mg/Ca ratios and such mineral composition contain only primary carbonates without any diagenetic alteration.

The -58 m stromatolite is characterised by the highest Mg/Ca ratio (0.204) of all samples. It must have been precipitated under conditions of high evaporation and of a high Mg/Ca ratio of >7. Such conditions favour precipitation of high-Mg calcite that could be

transformed into dolomite under elevated Mg/Ca ratios. Therefore, we suggest that the abundance of dolomite in this sample is of a diagenetic origin and consequently its U/Th date can be excluded.

Intermediate Mg/Ca ratios of 0.044-0.135 were found in stromatolites at -76 to -117 m reflecting Mg/Ca ratios of the lake water ranging between 2 and 12. Such conditions favour precipitation of high Mg-calcite as a primary mineral in addition to some aragonite. This is supported by our XRD analysis that shows dominance of calcite in these stromatolites with only small amounts of aragonite. Although the Mg/Ca ratios of these stromatolites indicate increasing aridity causing a continuous drop of Lake Lisan after 76 ka BP, the light oxygen and carbon isotopic values and the existence of calcite as a pure mineral or as a main mineral phase implies high fresh water input to the lake. This agrees with the result of our dates that indicate a lake level transgression to these high levels before 32 ka BP. The existence of dolomite as the third mineral phase in some of these stromatoloites is most probably of diagenetic origin.

The lowest stromatolite at -350 m consists purely of aragonite reflecting a high Mg/Ca ratio of the lake water of >12. This implies extremely dry conditions and low water input associated with the lake lowering to this level at ~63 ka BP. Since the Mg/Ca ratio of the lacustrine sediments containing pure aragonite is expected to be close to zero (Müller et al., 1972), the sample displays a very low Mg/Ca ratio of 0.027.

XRD analysis (Table 4.2) of the stromatolites at -246 to -137 m shows that they consist mainly of calcite, reflecting high fresh water input and low evaporation. This implies that the lake level rose after 63 ka BP to higher than -137 m. However, the existence of aragonite in the stromatolites of -150 to -137 m implies a return to a negative water balance that caused a subsequent drop of the lake level. This is supported by our U/Th dates that suggest a lake level rise to higher than -137 m before 32 ka BP followed by a consequent drop from these high stands between 32 and 22 ka BP. The Mg/Ca ratios (0.014 to 0.032) of these stromatolites support the preceding interpretation. They suggest that the Mg/Ca ratio of the lake water was < 2 during the transgression allowing precipitation of low-Mg calcite. Subsequently, the Mg/Ca ratio of the lake water increased during the regression causing precipitation of aragonite.

The low Mg/Ca ratio and the mineral composition of these stromatolites suggest that the calcite has been precipitated primarily from the lake and that no diagenetic alteration occurred.

The dominance of calcite in the -160 m stromatolite without any aragonite, in addition to the low Mg/Ca ratio of 0.027 indicates that a high fresh water input and a low Mg/Ca ratio of the lake water was associated with the lake level rise during the LGM (~19 ka BP). Experience from the Dead Sea shows that calcitic marls were deposited with almost no aragonite during the mid-Holocene lake level rise (between 7.8 and 3.6 ka BP), while sequences of aragonitic laminae were deposited during the past 3000 years (Waldmann et al., 2007) associated with the lowering of the Dead Sea to its current level.

Table 4.2: Mg/Ca ratios and XRD analysis of Lake Lisan stromatolites, xxxx: abundant, xxx: common, xx: intermediate, x:low.

S.n.	Altitude (m)	Mg/Ca ratio	Aragonite	Calcite	Dolomite	Quartz
8	0	0.041		xx		xxxx
6	-19	0.040		xxxx		xxx
10	-30	0.049		xxxx		xx
14	-56	0.042	xxxx	xx		x
13	-58	0.204	xxx	xx	xxxx	x
12	-66	0.097		xxxx		xx
7a	-76	0.044		xxxx		x
7b	-76	0.090		xxxx		x
9a	-101	0.096	xx	xxxx	xx	x
9b	-101	0.135	-	-	-	-
11	-105	0.073		xxxx	xx	xx
42	-109	0.087	x	xxxx	xx	x
43	-116	-		xxxx		x
44	-117	0.087	xx	xxxx	xx	x
15	-137	0.014	xxx	xxxx		x
34	-148	0.027	xxxx	xxx		x
45	-150	0.028	xxx	xxxx		x
30	-154	0.032	xxx	xxxx		x
5	-160	0.027		xxxx		x
17	-175	0.042	x	xxxx		x
18	-264	0.026	x	xxxx		x
1	-350	0.027	xxxx			x

It is remarkable that the red stromatolite crust at 0 to -30 m display a Mg/Ca ratio similar to that of the grey stromatolites at -56 m and even similar to that at -175 m. This indicates that these stromatolites grew in similar water conditions providing additional evidence that the lacustrine terraces higher than -56 m and up to zero were derived from the same lake. Two stromatolite crusts from the same altitude of -76 m exhibit two different Mg/Ca ratios of 0.09 for the grey crust and 0.044 for the red crust. This implies that the red stromatolite grew during a period of transgression and wetter conditions while the grey stromatolites grew in a period of drier conditions and lake regression.

Table 4.3: Mg/Ca ratios of lake water and lacustrine carbonates according to Müller et al. (1972).

	Mineral	Mg/Ca of lake water	Mg/Ca of carbonates
a	(Low-Mg) calcite/or high- Mg calcite, (± additional aragonite).	< 2	0 - 0.042
b	High-Mg calcite, aragonite and dolomite	2-12	0.042 - 0.176
c	Dolomite (diagentic)	7-12	0.538 - 0.818
d	Aragonite	> 12	~ 0

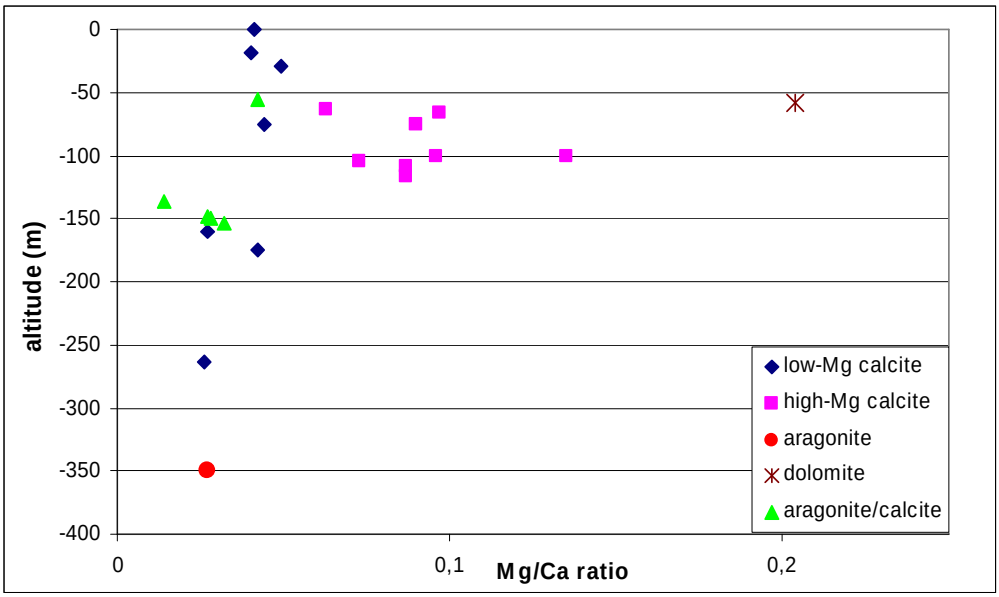

Fig. 4.13: The Mg/Ca ratio of Lisan stromatolites at altitudes of 0 to -350 m.

4.5.5 U/Th dating

Uranium-series dating can serve as an effective tool to obtain precise ages on Quaternary carbonates. However, most samples require a correction for Th in admixed detritus through the generation of U-Th isochrons (i.e., Kaufman et al., 1998; Schramm et al., 2000; Haase-Schramm et al., 2003).

In this study, twelve samples of stromatolites overgrowing Lisan terraces at -56 to -350 m were dated using U-series and corrected for the initial ^{230}Th (Table 4.4). The Mg/Ca ratios and the mineral composition of the dated stromatolite samples in addition to the covariance trend of their isotopic values suggest that they were deposited primarily from the lake water and that diagentic alteration is very limited. These characteristics, in addition to the good stratigraphic correlation between the U/Th dates and the shoreline terraces provide evidence as to the dating accuracy. Only the age of the -58 m sample was discarded because the stromatolite is composed of diagentic dolomite as the main mineral.

Our dates show that Lake Lisan had achieved its maximum stand of -56 to -66 m between 79.2±1.4 and 76.5±2.3 ka BP, implying that the highest level of Lake Lisan is about 100 m higher than the previously reconstructed level of -150 to -148 m. The ages of the high levels (-56 to -66 m) agree well with the transition period from Lake Samra to Lake Lisan at ~ 90 - 70 ka BP, as reported in the literature.

The transition between the Samra and Lisan Formation in the Dead Sea basin is marked by a depositional hiatus in the Perazim Valley at an altitude of ~ -305 m or by a structural unconformity exposed on the Lisan Peninsula (Waldmann et al., 2002). U-series ages of aragonite from below and above the unconformity suggest that this hiatus spans over ~ 10 ka (~80-70 ka BP) (Stein, 2001; Waldmann et al., 2002). This age corresponds well with our dates of the early regression of Lake Lisan from its highest stands (-56 to -66 m) at ~80 to 76 ka BP. However, the difference in the altitude results from the fact that our dates were derived from stromatolites overgrowing shore-line terraces, while the previous dates were based on the deep water deposits of aragonite. Similar difference was also detected from the U/Th dates of Lisan stromatolites along the western escarpment of the Dead Sea. These dates suggested a lake stand up to 80 m higher than the accepted level for most of the Lake Lisan time and up to 150 m for the interglacial-glacial transition (90-70 ka BP).

The difference in altitude was interpreted as a result of tectonic subsidence of ~2.2 m/ka of the DS depression fill compared to the relative stable escarpment (Lisker et al., 2009, 2010).

Stein (2001) reported that such a hiatus in the order of several thousand years in lacustrine sedimentation exists within the Lisan Formation. This led Stein (2001) to ask whether the determination of boundaries between the late Pleistocene lacustrine formations in the Dead Sea basin is arbitrary, or if it reflects a real change in the sedimentary and climatic conditions in the area.

Waldmann et al. (2002) described a 25 m-section of the Samra Formation at Perazim Valley that lies beneath the Samra-Lisan hiatus at an altitude of -330 m. The section consists of layered marl, intercalated with laminated calcite and silty detritus or with aragonite and detritus laminae. The Samra sequence is capped by gravels overlapping with travertine deposits. The U/Th ages of the aragonites below and above the pebbly-travertine unit show that the transition lies between ~ 89 and 80 ka BP. In the Mishmar section, the pebbly unit is covered by laminated calcitic marl dated between 80-75 ka BP (Waldmann et al., 2002). This indicates a low lake level at ~89 ka BP most likely when Lake Samra dried out and Lake Lisan began to fill. As soon as Lake Lisan was completely filled, it reached high levels of -56 to -66 m at ~ 80-76 ka BP as also indicated by the dates of calcitic marl in Mishmar section.

However, in the Massada and Mor sections there is no gravel or travertine in their upper parts, instead, layered calcitic marls intercalated with laminated aragonite similar to the Lisan Formation were found (Waldmann et al., 2007). The upper parts of the Massada and Mor sections have been dated between ~ 90-71 ka BP. The existence of thick calcite layers at the uppermost part of the Samra Formation was interpreted by Waldmann et al. (2002) as a result of increasing supply of fresh water to the lake. Stein (2001) suggested that the period of calcite precipitation (~90-71) could represent the initial filling time of Lake Lisan. Consequently, the transition between the Samra and Lisan Formations could be placed lower in the sedimentary section.

Table 4.4: U/Th dates of the terrace stromatolites.

Sample Nr.	δ U(corr.)	Error	238U	Error	232Th	Error	230Th	Error	Age (corr.)	Error	Age (uncorr.)	Altitude
	(‰)	(abso.)	(µg/g)	(abso.)	(ng/g)	(abso.)	(pg/g)	(abso.)	(ka)	(abso.)	(ka)	(m. b.s.l)
14	229.4	5.1	0.5878	0.0012	141.87	0.65	6.435	0.071	79.2	1.4	84.8	56
13	127.2	2.5	1.1663	0.0012	153.49	0.61	10.306	0.078	67.22	0.75	70.56	58
12	172.1	5.1	0.8243	0.0016	307.7	3.0	8.61	0.17	76.5	2.3	85.8	66
36	455.0	3.1	4.9387	0.0049	77.26	0.30	30.49	0.16	31.99	0.21	32.29	137
34	448.0	2.7	5.6871	0.0057	85.25	0.39	33.55	0.19	30.55	0.22	30.84	148
30	413.5	4.7	4.9091	0.0049	62.78	0.46	21.88	0.24	22.90	0.29	23.16	154
6	478.2	2.5	6.1241	0.0061	51.23	0.12	33.41	0.15	27.38	0.16	27.54	152
5	462.2	2.5	3.2032	0.0032	89.65	0.38	12.690	0.094	19.08	0.16	19.63	160
4	467.4	2.1	5.9032	0.0059	79.45	0.33	35.09	0.15	30.36	0.16	30.61	170
35	413.4	2.9	2.2757	0.0023	193.41	0.66	10.52	0.10	22.55	0.24	24.27	200
3	-	-	5.6231	0.0058	91.92	0.43	7.04	0.36	-	0.72	57.15	346.5
1	442.6	5.9	4.3376	0.0056	109.77	0.30	46.57	0.18	63.60	0.50	64.08	350

Our findings agree very well with this suggestion. The highest stands of -76 to 0 m found in N2, T3 and T4 represent a continuous series of terraces that must have been derived from the same lake. Since the terraces stromatolites at -56 to -66 m were dated to Lisan age (79-76 ka BP), the terraces higher than -56 m should be also derived from Lake Lisan. This is also supported from the morphology of these terraces (Fig. 4.9 a) that do not shows any erosion activity separating the terraces below and above -56 m. Apparently, these terraces represent a period of high fresh water input that led to the initial filling of the lake up to 0 m just before 79 ka BP. This emphasizes that the transition from Samra to Lisan was much older than 80 ka BP.

XRD analysis and Mg/Ca ratios (Table 4.2) of red stromatolite crusts from the terraces higher than -56 m shows that they consist purely of primary calcite, reflecting fresh water conditions of the lake. Moreover, the low negative values of carbon isotopes of stromatolites overgrowing these terraces indicate very wet conditions of the lake basin. These evidences lead us to correlate the highest terraces at -56 to 0 m with the calcite-rich layer on the top of the Samra Formation that represent the early wet stage of Lake Lisan. Although Lake Lisan has experienced its maximum high stands between ~79-76 ka BP, it is clear from the U/Th dates and from the erosional sequences of shore-line terraces that the lake was dropping. Thus, the lake dropped slightly from -56 m at 79 ka BP to -66 m at 76 ka BP, maintaining high stands for a long period. Then it continued to drop sharply until it reached -350 m at ~ 63 ka BP.

This drop is also indicated by the low level stromatolites of - 247 m found by Lisker et al. (2009) and dated to ~72 ka BP. The dramatic drop of Lake Lisan during this period was associated with the dry climate prevailed during H6 at ~ 63 ka BP. This early period of lake regression correlates well with the age of the lower member (LM) of the Lisan Formation (LF) (~70-56 ka BP). Landmann et al. (2002) concluded that the LM is characterised by a high gypsum/aragonite ratio and low lithogenic content, implying a regression of an initially high water level. They also suggested that the lake stand during the period of LM must have been higher than that associated with the middle member (MM), as indicated by the lowest residue content and the light colour.

After this regression period, Lake Lisan rose slightly to -346 m at ~ 57 ka BP, maintaining a low water level. Kaufman et al. (1992) reported that the clay and aragonite beds of the LF started to accumulate about 63 ka BP reflecting a rise in water level to at least -280 m. Although Machlus et al. (2000) suggested that Lake Lisan fluctuated at a low level of -280 to -290 m during most of the period 55-35 ka BP; the U/Th dates of this study show that Lake Lisan experienced a high stand of -137 m at 31.99 ± 0.21 ka BP. This implies that the lake must have been risen to higher than -137 m before 32 ka BP. The same conclusion was reached by Sheinkman (2002). He found high-level lacustrine sediments in Wadi Zin along the western coast of the Dead Sea at ~ -137 to -130 m dated to 30.4 ± 2 and 34.2 ± 2.4 ka BP respectively. The stromatolite ages from the western coast of the DS agree very well with those reported by this study. They showed a lake level transgression from -292 to -188 m between 55 and 35 ka BP. Lisker et al. (2009) assumed that most of these stromatolites have been down faulted and thus, they do not represent the original lake level which was even much higher. U-series ages of stromatolites from this study and from the western coast of the Dead Sea showed that this transgression period correlates well with the age of the MM. The low gypsum and high aragonite content as well as the high detrital sediment ratio found in the MM of the LF (Landmann et al., 2002) suggest more water input to the lake and a rise in the water level.

^{14}C dating of stromatolite at -105 m and OSL dating of Lisan sand at -117 m give ages of 45 and 40 ka BP, respectively. They suggest that Lake Lisan rose to higher than -105 just before 45 ka BP and then dropped from -105 m at 45 ka to -117 m at 40 ka BP correlating with the dry Heinrich events 5 and 4. In spite of the low organic carbon content in the ^{14}C sample and the unsuitable characteristics of quartz in the sand sample for OSL dating,

their ages seem to be reasonable since they agree well with U/Th dates of this study and with those reported from the western coast. They also allowed detecting the Heinrich events 5 and 4 (Figs. 4.14, 4.15).

The U/Th dating (Table 4.4, Figs. 4.14, 4.15) shows that Lake Lisan subsequently started a regression from its initial high level of -137 m at ~ 31.99 ± 0.21 ka BP consistent with the H3 event. It dropped to -148 m at 30.55 ± 0.22 ka BP and to -152 m at 27.38 ± 0.16 ka BP. Then the lake declined to -154 m at 22.9 ± 0.29 ka BP. These findings correlate well with the suggestion of Bartov et al. (2003) that Lake Lisan experienced a minimum drop of 20 m during the H3 event. Moreover, they agree with the conclusion of Landmann et al. (2002) that two regressions of Lake Lisan occurred at ~ 32 and ~ 24 ka BP marked by thick gypsum layers within the LF of the Lisan Peninsula. The lake continued to drop sharply until it reached -200 m at 22.5 ± 0.29 ka BP, associated with the dry event of H2.

Although such a drop of ~ 50 m in a short period of <1 ka sounds unreasonable, a significant regression of Lake Lisan at ~ 23 ka BP was well documented in the previous lake level reconstructions. Bartov et al. (2003) reported that Lake Lisan declined sharply to -220 m at ~23 ka BP with a total drop of ~ 50 m. Further more, Hazan et al. (2005) recorded a subsequent drop of Lake Tiberias to -208 m at the same time. Since stromatolites are able to grow within a water depth of 2-50 m, they represent the minimum level of the lake water. Therefore, we can not exclude the possibility that the -200 m stromatolite grew in a deep water environment while the lake level was at ~ -154 m. This is also evidenced from the existence of stromatolites at -148 and -170 m dated to the same age of ~ 30 ka BP, implying a water depth of > 20 m above the -170 m stromatolite. This period of lake level regression coincides very well with the age of the upper member (UM) of the LF (Fig. 4.15). Kaufman et al. (1992) concluded that at ~ 36 ka BP a period of enhanced chemical sedimentation of Lake Lisan began and the White Cliff Member was deposited.

After 23 ka BP Lake Lisan recovered again and reached a high level of -160 m at 19 ka BP, associated with the Last Glacial Maximum (LGM) (Fig. 4.15). Bartov et al. (2003) suggested a rise of the lake level to -190 m between 22 and 17 ka BP. According to Hazan et al. (2005) Lake Tiberias rose also to ~ -190 m between 22 and 19 ka BP.

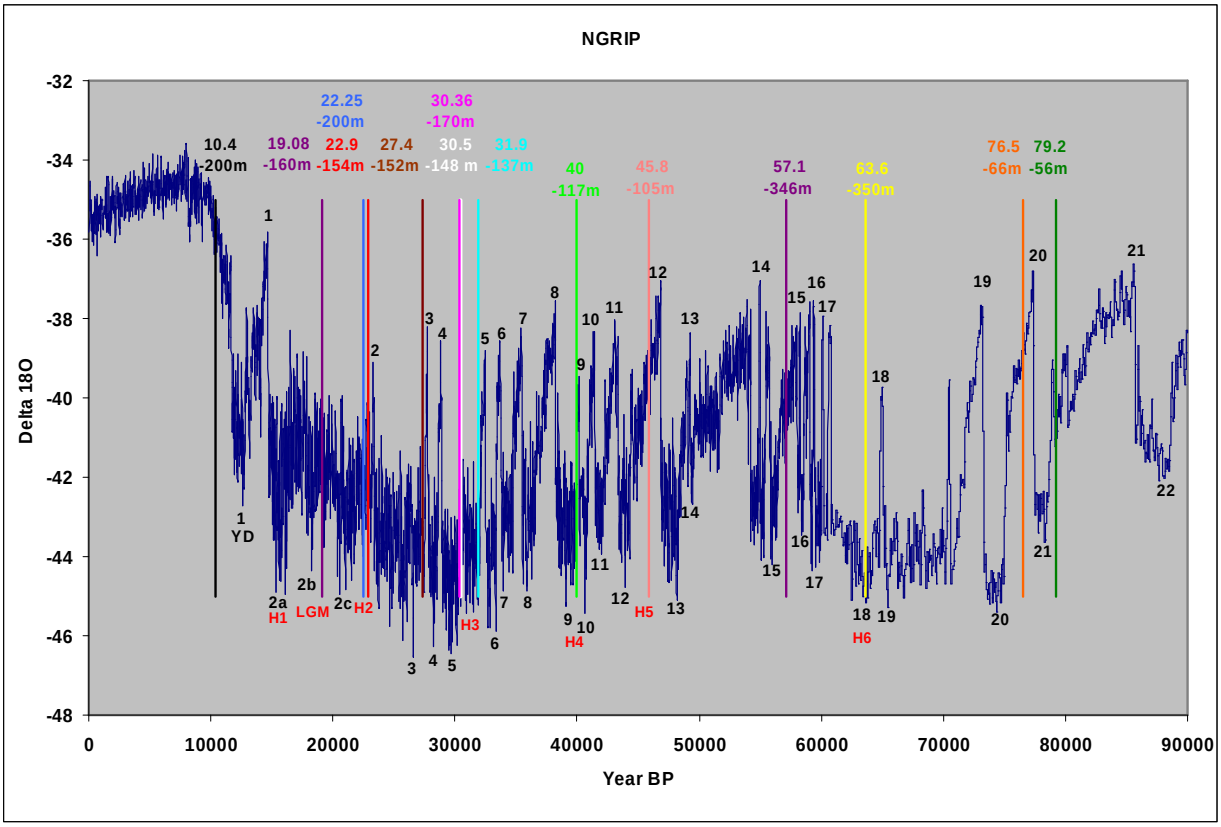

Fig. 4.14: The U/Th and OSL dates of Lake Lisan stromatolites and deposits superimposed on stadials (lower numbers), interstadials (upper numbers) and Heinrich events of the NGRIP during the Last Glacial (NGRIP dating group, 2008).

Therefore, both Lake Lisan and Lake Tiberias achieved a high stand during the LGM and merged to form one lake, while the maximum level occurred long time before. After the LGM, Lake Lisan dropped to ~ -300 m as indicated by the thick gypsum layers at the top of Lisan Formation (Bartov et al., 2002; 2003).

Landmann et al. (2002) suggested that the lake declined to a much lower level at 15.4 ka BP allowing growth of microbialites at -370 m. The OSL date of a sand layer within Lisan formation in Wadi Dahel suggest a dry condition and low lake level around 10±0.8 ka BP associated with the final glacial period of the Younger Dryas (YD). However, the existence of finely laminated Lisan deposits overlying the sand layer suggests a transgression of Lake Lisan after 10 ka BP associated with wet conditions prevailing in early Holocene (Abu Ghazleh and Kempe, 2009).

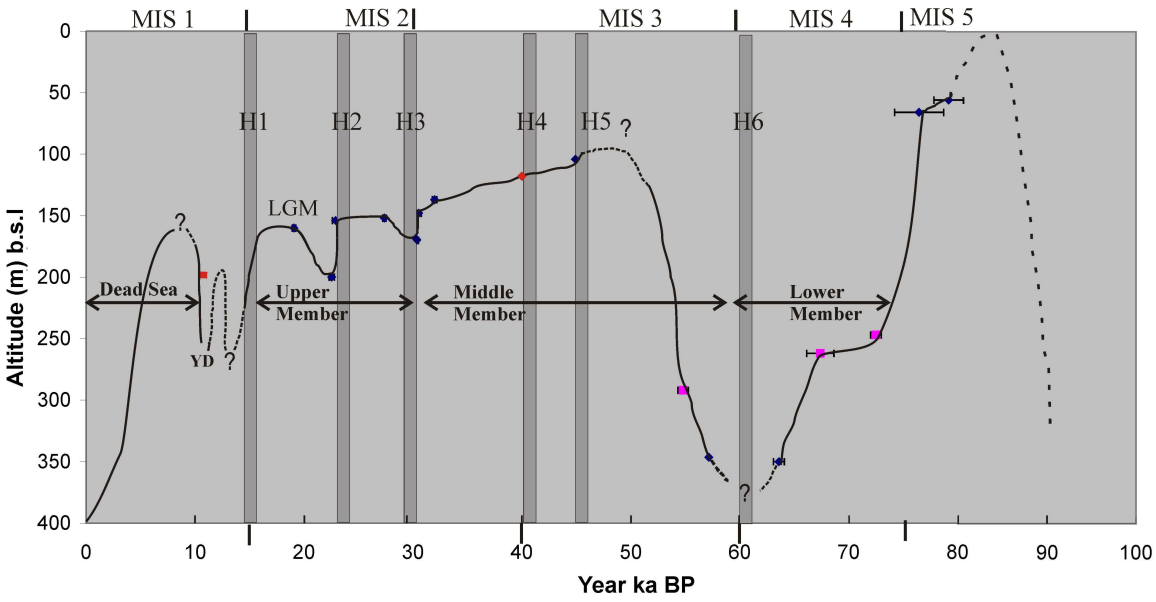

Fig. 4.15: Reconstruction of Lake Lisan level curve during the last 80 ka according to the U/Th and OSL dates of this study (blue and red points respectively). The pink points refer to U/Th ages of the lake stromatolites from the western coast reported by Lisker et al. (2009). Heinrich events according to Hemming (2004), Vidal et al. (1999) and (GISP2).

The U/Th dates of this study show that Lake Lisan experienced significant drops during the stadials of the last glacial period associated with Heinrich events 6, 5, 4, 3, 2 and YD. This suggests cold dry climate of the Levant during the stadials and Heinrich events and warm wet climate during the interstadials (Figs. 4.14, 4.15). However, the lake experienced a rise during the LGM, indicating indirect effects of the glaciations on the lake basin. Apparently, increasing precipitation that fed the glaciers during the LGM caused increasing runoff of the major rivers and streams draining Lake Lisan.

4.6 Conclusions

- Geomorphological investigations of shore line terraces of Lake Lisan, along with U/Th dating of their stromatolites, gave new results regarding the timing and altitudes of the highest lake stand and the transgression-regression phases. These results can not be obtained by sedimentary stratigraphy methods used in the previous lake level reconstructions. This is because these were based either on deep-water deposits that do not represent the actual lake level or on sedimentological indicators (sand and gravel layers) below -265 m (i.e., Machlus et al., 2000; Bartov et al., 2002).

- Based on the U series ages of the terrace stromatolites, a lake level curve of the last glacial period (MIS 4, MIS 3 and MIS 2) was established. Consequently, the following conclusions are drawn:

1. Lake Lisan experienced high stands of -56 to -66 m at ~ 79 to 76 ka BP, implying that the lake stood at least at 100 m higher than previously reconstructed. The existence of a sequence of shore line terraces at -80 to zero m, without any indication of erosional activity separating them, suggests that Lake Lisan stood even at sea level before 80 ka BP and that the maximal stand was reached ~50 ka earlier than suggested in previous studies. Thin section investigations, CNS, XRD and isotopic analysis of stromatolites from the terraces higher and lower than -56 m show similar characteristics, again suggesting that both sets of terraces were derived from Lake Lisan. However, more dating of the terraces > -56 m and more investigation of their sediments is required in the future.

2. The ages of the highest stands of Lake Lisan presented in this study correlates very well with those of stromatolites from the western escarpment of the Dead Sea reported by Lisker et al. (2009). They suggested a lake stand up to 80 m higher than the previously reconstructed level for most of the Lake Lisan time and ~150 m higher for the interglacial-glacial transition (90-70 ka BP). The difference in altitude was interpreted as a result of tectonic subsidence of ~2.2 m/ka of the DS depression fill compared to the relative stable escarpment (Lisker et al., 2009).

3. After the transgression of Lake Lisan to its maximal stand (before 80 ka BP), the lake level began to drop from -56 m at 79 ka BP to -66 m at 76 ka BP. Then, the lake receded sharply to -350 m at ~ 63 ka BP associated with the dry climatic conditions of H6. The lake fluctuated at low levels of -350 to -346 m for the time interval of 63 to 57 ka BP.

4. The stromatolite dates of this study remove the uncertainty of the lake level changes during its early stage (80-57 ka BP) and suggest a warm wet climate of the Levant during the end of MIS 5 that led to the filling of Lake Lisan followed by a cold dry climate of the MIS 4 that caused a sharp regression of the lake to -350 m or even lower.

5. Between 55 and 33 ka BP, the lake level rose sharply to higher than -137 m, implying warm and wet climatic condition of the Levant during MIS 3. This transgression is supported by the stromatolite dates from the western coast of the Dead Sea (Lisker et al., 2009) as well as by the ages of high-level lacustrine sediments in Wadi Zin (Sheinkman, 2002). This conclusion contradicts with the suggestions of Machlus et al. (2000) and Bartov et al. (2002, 2003) that the lake fluctuated at a low level of -280 to -290 m during most of MIS 3.

6. U/Th ages of stromatolites from a sequence of terraces at -137 to -160 m allowed resolving the lake level curve at a high resolution during MIS 2 (32-19 ka BP). In spite of the lake high stands during this period, the lake level dropped sub-sequently from -137 m to - 200 m between 32 and 22 ka BP, implying cold and dry climatic conditions of the Levant during MIS 2. This is in contradiction with the conclusion of Bartov et al. (2002, 2003) who suggested that Lake Lisan rose sharply to its maximum stand of -165 m between 27 and 23 ka BP.

7. During the LGM, Lake Lisan recovered again to a high level of -160 m at ~19 ka BP followed by a regression to -200 m or even lower at ~ 11 ka BP as indicated by the OSL dating of Lisan sand from Wadi Dahel (Abu Ghazleh and Kempe, 2009).

    - The stable isotope analyses of Lake Lisan stromatolites support the conclusions on the lake level changes during the Pleistocene. In general, they show low isotopic values of stromatolites from the highest stands at -76 m to -19 m, reflecting fresh water conditions of the lake at the last interglacial-glacial boundary. Lowest values were derived from stromatolites at -103 to -119 m associated with the transgression of the lake to these high stands between 55 and 33 ka BP. The heaviest values were derived from stromatolites at -137 to -160 m indicating a change to dry climatic conditions that caused a subsequent drop of the lake level during MIS 2.

    - The XRD analysis and Mg/Ca ratios of the stromatolites correlate also with transgression-regression phases of the lake. Dominance of calcite in

stromatolites at -76 to 0 m and inferred low Mg/Ca ratios of the lake water (i.e. ~2) imply a high fresh water input of the lake during the period of the highest stands. A high Mg/Ca ratio of the lake water of >7 inferred from stromatolite at -350 m and the existence of aragonite as the sole mineral in this sample reflect low fresh water input and high evaporation rates of the lake during its regression to this low level. Inferred low Mg/Ca ratios of stromatolites at -247 to -101 m and the existence of calcite as a main mineral phase indicate wet climatic conditions that caused a lake transgression to higher than -137 during MIS 3. The appearance of more aragonite in stromatolites at -137 to -154 m points to a return to dry climatic conditions that caused a regression of Lake Lisan between 32 to 22 ka BP (MIS 2). However, the change in the mineral composition to pure calcite at -160 m in addition to the low Mg/Ca ratio correlates well with the transgression of the lake to this level by the end of the LGM.

- Superimposing the dates of this study on the NGRIP curve (Fig. 4.14) shows that several drops of Lake Lisan occurred during the cold stadials of the Northern Hemisphere associated with Heinrich events 6, 5, 4, 3 and 2. This suggests a dry cold climate of the Levant during Heinrich events and stadial periods and a warm wet climate during interstadials. This is in contrast to our conclusion published earlier (Abu Ghazleh and Kempe, 2009) that were based only on two U/Th dates. More dating of Lake Lisan terraces in this study allowed a better understanding of the palaeoclimatic conditions of the lake basin.

Acknowledgements

We would like to thank Mohammad Abo Kazleh (Amman) for his exceptional assistannce in the field and help with DGPS data processing; Mohammad Nawasrah (NRA, Amman) and Horst-Volker Henschel (Darmstadt) for their support in the field; Günter Landmann for useful discussions; Augusto Mangini (Heidelberg University) for U/Th dating; Ingo Sass (TU, Darmstadt) for providing DGPS equipment; and BGR Hannover for providing aerial photos for Lake Lisan. This work was supported by grants from the DAAD and the DFG (Ke-287/28-1), Germany.

References

Abed, A.M., 1985. Geology of the Damya Formation. Dirasat 12, 99-108.

Abed, A.M., 2000. Geology of Jordan, its Environment and Water (in Arabic). Jordanian Geologist Association, Amman, 571 pp.

Abed, A.M., Yaghan, R., 2000. On the palaeoclimate of Jordan during the Last Glacial Maximum. Palaeogeography, Palaeoclimatology, Palaeoecology 160, 32-33.

Abu Ghazleh, S., Kempe S., 2009. Geomorphology of Lake Lisan terraces along the eastern coast of the Dead Sea, Jordan. Geomorphology 108, 246-263.

Abu Ghazleh, S., Hartmann, J., Jansen, N., Kempe, S., 2009a. Water input requirements of the rapidly shrinking Dead Sea. Naturwissenschaften 96, 637-643.

Abu Ghazleh, S., Jansen, N., Hartmann, J., Kempe, S., 2009b: Das Sterben des Toten Meeres. - Naturwissenschaftliche Rundschau 62(7), 368-370.

Abu Ghazleh, S., Kempe, S., Hartmann, J., Jansen, N., 2010. Rapidly shrinking Dead Sea urgently needs infusion of 0.9 km^3/a from planned Red-Sea Channel: Implication for renewable energy and sustainable development. - Jordan Journal of Mechanical and Industrial Engineering 4 (1), 211-216.

Abu Ghazleh, S., Abed, A.M., Kempe, S., 2011. The dramatic drop of the Dead Sea: background, rates, impacts and solutions. - In: Badescu, V. & Cathcart, R.B. (eds.), Macro-engineering Seawater in Unique Environments; Arid Lowlands and Water Bodies Rehabilitations; Springer, in press.

Allan, J.C., Kirk, R.M., 2000. Wind wave characteristics at Lake Dunstan, South Island, New Zealand. New Zealand Journal of Marine and Freshwater Research 34, 573-591.

Allan, J.C., Stephenson, W.J., Kirk, R.M., Taylor, A., 2002. Lacustrine shore platforms at Lake Waikaremoana, North Island, New Zealand. Earth Surface Processes and Landforms 27, 207-220.

Allen, B.D., 1991. Effect of climatic change on Estancia Valley, New Mexico, sedimentation and landscape evolution in a closed-drainage basin. In, Julian, B., Zidek, J., (eds), Field Guide to Geologic Excursions in New Mexico and Adjacent Areas of Texas and Colorado, New Mexico Bureau of Mines and Mineral Resources Bulletin, 137.

Allen, W., 1855. The Dead Sea, A New Route to India, with Other Fragments. London, Brown and Co., 374 pp.

Al-Weshah, R.A., 2000. The water balance of the Dead Sea, an integrated approach. Hydrological Processes 14, 145-154.

Al-Zoubi, A., 2001. Salt diapirs in the Dead Sea basin and their relationship to Quaternary extensional tectonics. Marine and Petroleum Geology 18 (7), 778-797.

Bar-Matthews, M., Ayalon, A., Gilmour, M., Matthews, A., Hawkesworth, C.J., 2003. Sea-land oxygen isotopic relationships from planktonic foraminifera and speleothems in the Eastern Mediterranean region and their implication for paleorainfall during interglacial intervals. Geochimica et Cosmochimica Acta 67, 3181-3199.

Bartov, Y., Sagy, A., 2003. Recent faulting in the Dead Sea-pull apart structure in the Lisan Formation. Israel Geological Society, field trip guidebook, Israel, Ein Boqeq, 1-16.

Bartov, Y., Goldstein, S.L., Stein, M., Enzel, Y., 2003. Catastrophic arid episodes in the Eastern Mediterraean linked with the North Atlantic Heinrich events. Geology 31 (5), 439-442.

Bartov, Y., Stein, M., Enzel, Y., Agnon, A., Reches, Z., 2002. Lake levels and sequence stratigraphy of Lake Lisan, the late Pleistocene precursor of the Dead Sea. Quaternary Research 57, 9-21.

Bar-Yosef, O., Goldberg, P., Leveson, T., 1974. Quaternary stratigraphy and prehistory in Wadi Fazael, Jordan Valley - A preliminary report. Paleorient 2, 415-428.

Begin, Z.B., 1975. The Geology of Jericho Sheet (1:10,000). Geological Survey of Israel, Bulletin 67, 35 pp.

Begin, Z.B., Ehrlich, A., Nathan, Y., 1974. Lake Lisan, the Pleistocene Precursor of the Dead Sea. Geological Survey of Israel, Jerusalem, Bulletin 63, 30 pp.

Begin, Z.B., Broecker, W., Buchbinder, B., Druckman, Y., Kaufman, A., Magaritz, M., Neev, D., 1985. Dead Sea and Lake Lisan levels in the last 30,000 years, a preliminary report. Israel Geological Survey Report 29/85, 1-18.

Ben-Avraham, Z., Niemi, T. M., Neev, D., Hall, J. K., Levy, Y., 1993. Distribution of Holocene sediments and neotectonics in the deep north basin of the Dead Sea. Marine Geology 113, 219-231.

Bender, F., 1968. Geologie von Jordanien. In, Martini, H. J., (ed) Beiträge zur Regionalen Geologie der Erde, Gebrüder Borntraeger, Berlin, Stuttgart, 227 pp.

Bender, F., 1974. Geology of Jordan. Borntraeger, Berlin.

Bentor, Y.K., Vroman, A.J., 1960. The Geological Map of Israel, 1:100,000, Sheet 16, Mount Sedom. Geological Survey of Israel, Jerusalem, 117 pp.

Bird, E.C.F., 1985. The study of coastal line changes. Zeitschrift für Geomorphologie Supplementband 57, 1-9.

Blankenhorn, M., 1912. Naturwissenschaftliche Studien am Toten Meer und im Jordantal. Friedlander, Berlin. 478 pp.

Bookman, (Ken-Tor), R., Enzel, Y., Agnon, A, Stein, M., 2004. Late Holocene lake levels of the Dead Sea. Geological Society of America, 116 (5/6), 555-571.

Bookman, (Ken-Tor), R., Bartov, Y., Enzel, Y., Stein, M., 2006. Quaternary lake levels in the Dead Sea basin, two centuries of researchs. In, Enzel, Y., Agnon, A., Stein, M., (eds), New Frontiers in Dead Sea Paleoenvironmental Research. Geological Society of America, 253 pp.

Bowman, D., 1971. Geomorphology of the shore terraces of the Late Pleistocene Lisan Lake, Israel. Palaeogeography, Palaeoclimatology, Palaeoecology 9, 183-209.

Bowman, D., Gross, T., 1992. The highest stand of Lake Lisan, ~150 meters below sea level. Israel Journal of Earth Science 41, 233-237.

Bowen, R., Jux, U., 1987. Afro-Arabian geology. Chapman and Hall, London.

Butzer, K.W., 1957. Late Glacial and postglacial climatic variation in the Near East. Erdkunde 11, 21-35.

Carter, L., Carter, R.M., 1986. Holocene evolution of the nearshore sand wedge, South Otago Continental Shelf, New Zealand. New Zealand Journal of Geology and Geophysics 29, 413-424.

Carter, R.M., Carter, L., Johnson, D.P., 1986. Submergent shorelines in the S.W. Pacific, evidence for an episodic post-glacial transgression. Sedimentology 33, 629-649.

Cerling, T.E., 1984. The stable isotopic composition of modern soil carbonate and its relationship to climate. Earth and Planetary Science Letter 71, 229-240.

Charles, C.D., Rind, D., Jouzel, J., Koster, R.D., Fairbanks, R.G., 1994, Glacial-interglacial changes in moisture sources for Greenland, influences on the ice core record of climate. Science 263, 508-511.

Clark, G.A., 1988. Some thoughts on the southern extent of the Lisan Lake as seen from the Jordan side. Bulletin of the American School of Oriental Research 272, 42-43.

Closson, D., Abou Karaki, N., Klinger, Y., Hussein, M.J., 2005. Subsidence and sinkhole hazard assessment in the southern Dead Sea area, Jordan. Pure Applied Geophysics 162, 221-248.

Cooke, R.V., Varren, A., 1973. Geomorphology in Deserts. Batsford, London, 374 pp.

Dead Sea Data Summary. International Lake Environment Committee Foundation, http,//www.ilec.or.jp/eg/index.html. Accessed 1 Jun 2008.

Druckman, Y., Mayritz, M., Sneh, A., 1987. The shrinkage of Lisan Lake as affected by the diagnoses of its marginal oolitic deposits. Israel Journal of Earth Science 36, 101-106.

Edwards, R.L., Gallup, C.D., Cheng, H., 2003. Uranium series dating of marine and lacustrine carbonates. In, Bourdon, B., Henderson, G.M., Lundstrom, C.C., Turner S.P., (eds), Uranium Series Chemistry, Mineralogical Society of America, Washington, U.S.A.

El-Isa, Z.H., Mustafa, H., 1986. Earthquake deformation in the Lisan deposits and seismotectonic implications. Geophysical Journal of the Royal Astronomical Society 86, 413-424.

Emeis, K.-C., Schulz, H.-M., Struck, U., Sakamoto, T., Doose, H., Erlenkeuser, H., Howell, M.W., Kroon, D., Paterne, M., 1998. Stable isotope and temperature records of sapropels from ODP Sites 964 and 967, constraining the physical environment of sapropel formation in the Eastern Mediterranean Sea. Proceedings of the Ocean Drilling Program, Scientific Results 160, 309-331.

Emeis, K.-C., Struck, U., Schulz, H.-M., Bernasconi, T., Sakamoto, S., Martinez-Ruiz, F., 2000. Temperature and salinity of Mediterranean Sea surface waters over the last 16,000 years, constraints on the physical environment of S1 sapropel formation based on stable oxygen isotopes and alkenone unsaturation ratios. Palaeogeography, Palaeoclimatology, Palaeoecology 158, 259-280.

Emeis, K.-C., Schulz, H., Struck, U., Rossignol-Strick, M., Erlenkeuser, H., Howell, M.W., Kroon, D., Mackensen, A., Ishizuka, S., Oba, T., Sakamoto, T., Koizumi, I., 2003. Eastern Mediterranean surface water temperatures and $\delta^{18}O$ composition during deposition of sapropels in the late Quaternary. Paleoceanography, 18.

ESRI, 2006, ESRI® Data and Maps 9.2, Global Imagery and Shaded Relief, Electronic resource.

Fleming, N.C., 1965. Form and relation to present sea level of Pleistocene marine erosion features. Journal of Geology 73, 799-811.

Fontes, J.C., Gonfiantini, R., 1967. Comportement isotopique au cours de l'évaporation de deux bassins sahariens. Earth and Planetary Science Letter 3, 258-266.

Freund, R., Garfunkel, Z.I., Goldberg, M., Weissbord, T., Derin, B., 1970. The shear along the Dead Sea Rift. Philosophical Transactions of the Royal Society of London, Series A, Mathematical and Physical Sciences 267, 107-130.

Fritz, P., Morgan, A.V., Eicher, U., McAndrews, J.H., 1987. Stable isotope, fossil Coleoptera and pollen stratigraphy in Late Quaternary sediments from Ontario and New York State. Palaeogeography, Palaeoclimatology, Palaeoecology 58, 183-202.

Frostick, L.E., Reid, I., 1989. Climatic versus tectonic control of fan sequences - Lessons from the Dead Sea, Israel. Journal of the Geological Society, London 146, 527-538.

Frumkin, A., Magaritz, M., Carmi, I., Zak, I., 1991. The Holocene climatic record of the salt caves of Mount Sedom, Israel. The Holocene 1(3), 191-200.

Frumkin, A., Ford, D.C., Schwarz, H.P., 1999. Continental oxygen isotopic record of the last 170,000 years in Jerusalem. Quaternary Research 51, 317–327.

Frumkin, A., Ford, D.C., Schwarz, H.P., 2000. Palaeoclimate and vegetation of the last glacial cycles in Jerusalem from a speleothem record. Global Biogeochemical Cycles 14, 863-870.

Fuchs, M., Wagner, G.A., 2003. Optical dating of sediments, recognition of insufficient bleaching by small aliquots of quartz for reconstructing soil erosion in Greece. Quaternary Science Reviews 22, 1161-1167.

Garfunkel, Z., Zak, I., Freund, R., 1981. Active faulting in the Dead Sea rift. Tectonophysics 80, 1-26.

Gat, J.R., 1981. Lakes. In Gat, J.R., Gonfatini R., (eds), Stable Isotope Hydrology, Deuterium and Oxygen-18 in the Water Cycle, I.A.E.A. Tech. Rep. 210, 203-221.

Gonfiantini, R., 1986. Environmental isotopes in lake studies. In, Fritz P., Fontes, J.C., (eds), Handbook of Environmental Isotope Geochemistry, Vol. 2, the Terrestrial Environment, Amsterdam, 113-168.

Gvirtzman, G., Wieder, M., 2001. Climate of the last 53,000 years in the Eastern Mediterranean based on soil-sequence stratigraphy in the coastal plain of Israel. Quaternary Science Reviews 20, 1827-1849.

Haase-Schramm, A., Goldstein, S.L., Stein, M., 2003. U-Th dating of Lake Lisan (late Pleistocene Dead Sea) aragonite and implications for glacial east Mediterranean climate change. Geochimica et Cosmochimica Acta 68, 985-1005.

Hall, J., 1993. The GSI digital terrain model (DTM) project completed. Geological Survey of Israel Current Research 8, 47-50.

Hassan, M., Klein, M., 2002. Fluvial adjustment of the lower Jordan River to a drop in the Dead Sea level. Geomorphology 45, 21-33.

Hazan, N., Stein, M., Agnon, A., Marco, S., Nadel, D., Negendank, J.F.W., Schwab, M.J., Neev, D., 2005. The late Quaternary limnological history of Lake Kinneret (Sea of Galilee), Israel. Quaternary Research 63, 60-77.

Hemming, S. R., 2004. Heinrich events: massive late Pleistocene detritus layers of the North Atlantic and their global imprint. Reviews of Geophysics 42, RG1005, 43 pp.

Horowitz, A., 1979. The Quaternary of Israel. Academic Press, New York, 394 pp.

Horowitz, A., 1992. Palynology of Arid Lands. Amsterdam, Elsevier, 546 pp.

Huinink, H.P., Pel, L., Kopinga, K., 2004. Simulating the growth of Tafoni. Earth Surface Processes and Landforms 29, 1225-1233.

Hunt, C.O., Elrishi, H.A., Gilbertson, D.D., Gratten, J., McLaren, S., Pyatt, F.B., Rushworth, G., Barker, G.W., 2004. Early Holocene environments in the Wadi Faynan, Jordan. The Holocene 14, 921-930.

Huntington, E., 1911. Palestina and its Transformation. HoughtMifflin, Boston, Mass., 443 pp.

International Centre for Tropical Agriculture (CIAT), 2004. Voidfilled seamless SRTM data V1. Available from the CGIAR-CSI SRTM 90 m Database, http,//srtm.csi.cgiar.org. Accessed on 22 April 2008.

Joffe, S., Garfunkel, Z., 1987. Plate kinematics of the circum Red Sea - a re-evaluation. Tectonophysics 141, 5-22.

Kadan, G., 1997. Evidence of Dead-Sea level fluctuations and neotectonic events in the Holocene fan-delta of Nahal Darga. M.Sc., Ben Gurion University of the Negev, 54 pp.

Katz, A., Kolodny, Y., Nissenbaum, A., 1977. The geochemical evolution of the Pleistocene Lake Lisan-Dead Sea system. Geochimica et Cosmochimica Acta 41, 1609-1626.

Kaufman, A., 1971. U-Series dating of Dead Sea basin carbonates. Geochimica et Cosmochimica Acta 35, 1269-1281.

Kaufman, A., Yechieli, Y., Gardosh, M., 1992. Reevaluation of the lake-sediment chronology in the Dead Sea basin, Israel, based on new U/Th dates. Quaternary Research 38, 292-304.

Kaufman, A., Wasserburg, G.J., Porcelli, D., Bar-Matthews, M., Ayalo, A., Halicz, L., 1998. U-Th isotope systematics from the Soreq Cave, Israel, and climatic correlation. Earth and Planetary Science Letters 156, 141-156.

Ken-Tor, R., Agnon, A., Enzel, Y., Marco, S., Negendank, J., Stein, M., 2001. High-resolution geological record of historical earthquakes in the Dead Sea. Journal of Geophysical Research 106, 2221-2234.

Kempe, S., Kazmierczak, J., 1990. Calcium carbonate supersaturation and the formation of in situ calcified stromatolites. In, Ittekkot V.A., Kempe, S., Michaelis, W., Spitzy, A., (eds), Facets of Modern Biogeochemistry, Festschrift for E.T. Degens on occasion of his 60th birthday. Springer-Verlag, New York, 255-278.

Kempe, S., Kazmierczak, J., 2007. Hydrochemical key to the genesis of calcareous nonlaminated and laminated cyanobacterial microbialites. In, Seckbach, J., (eds), Extremophilic Algae, Cyanobacteria and Non-photosynthetic Protists, from Procaryots to Astrobiology. COLE Series. Springer, Berlin, 241-264.

Kempe, S., Landmann, G., Müller, G., 2002. A floating varve chronology from the Last Glacial Maximum terrace of Lake Van/Turkey. Research in Mountains and Deserts of Africa and Central Asia. Zeitschrift für Geomorphologie Supplementband 126, 97-114.

Kingston, J.D., Deino, A.L., Edgar, R.K., Hill, A., 2007. Astronomically forced climate change in the Kenyan Rift Valley 2.7-2.55 Ma, implications for the evolution of early hominin ecosystems. Journal of Human Evolution 53, 487-503.

Klein, C., 1986. Fluctuations of the level of the Dead Sea and climatic fluctuations during historical times. Ph.D. Dissertation, Hebrew University, Jerusalem. (in Hebrew, English abstract).

Klinger, Y., 1999. Sismotectonique De La Faille Du Levant. These De Doctorat, Universite Louis Pasteur - Strasbourg I, 238 pp.

Klinger, Y., Avouac, J., Abou Karaki, N., Dorbath, L., Bourles, D., Reyss, J., 2000. Slip rate on the Dead Sea transform fault in northern Araba valley, Jordan. Geophysical Journal International 142, 755-768.

Klinger, Y., Avouac, J.P., Bourles, D., Tisnerat, N., 2003. Alluvial deposition and lake-level fluctuations forced by Late Quaternary climatic changes, the Dead Sea case example. Sedimentary Geology 162, 119-139.

Kolodny, Y., Stein, M., Machlus, M., 2005. Sea-rain-lake relation in the Last Glacial East Mediterranean revealed by $\delta^{18}O$- $\delta^{13}C$ in Lake Lisan aragonites. Geochimica et Cosmochimica Acta 69 (16), 4045-4060.

Landmann, G., Reimer, A., Lemcke, G., Kempe, S., 1996a. Dating Late Glacial abrupt climate changes in the 14,570 yr long continuous varve record of Lake Van, Turkey. Palaeogeography, Palaeoclimatology, Palaeoecology 122, 107-118.

Landmann, G., Reimer, A., Kempe, S., 1996b. Climatically induced lake level changes at Lake Van, Turkey, during the Pleistocene/Holocene transition. Global Biogeochemical Cycles 10 (4), 797-808.

Landmann, G., Abu Qudaira, G.M., Shawabkeh, K., Wrede, V., Kempe, S., 2002. Geochemistry of the Lisan and Damya Formations in Jordan, and Implications for palaeoclimate. Quaternary International 89, 45-57.

Langozky, Y., 1961. Remarks on the petrography and geochemistry of the Lisan marl Formation. Unpublished Msc thesis, The Hebrew University, Jerusalem, Israel.

Langozky Y., 1963. High-level lacustrine sediments in the Rift Valley at Sedom. Israel Journal of Earth Science 12, 17-25.

Lartet, L.M., 1869. Essai sur la geologie de la Palestine et des contrees avoisinantes, telles que l'Egypte et l'Arabie: Comprenant les observations recueillian dans le course de l'expédition du Duc de Luynes a la Mer Morte: Paris, Masson, 292 pp.

Lisker, S., Vaks, A., Bar-Matthews, M., Porat, R. Frumkin, A., 2009. Stromatolites in caves of the Dead Sea Fault escarpment, implications to latest Pleistocene lake levels and tectonic subsidence. Quaternary Science Reviews 28 (1-2), 80-92.

Lisker, S., Vaks, A., Bar-Matthews, M., Porat, R., Frumkin, A., 2010. Late Pleistocene palaeoclimatic and palaeoenvironmental reconstruction of the Dead Sea area (Israel) based on speleothems and cave stromatolites. Quaternary Science Reviews 29, 1201-1211.

Lynch, W.F., 1854. Narrative of the United States' Expedition to the River Jordan and the Dead Sea. 9th ed. Blanchard and Lea, Philadelphia, 509 pp.

Machlus, M., Enzel, Y., Goldstein S.L., Marco, S., Stein, M., 2000. Reconstructing low-levels of Lake Lisan by correlating fan-delta and lacustrine deposits. Quaternary International 73/74, 127-144.

Macumber, P.G., Head, M.J., 1991. Implication of the Wadi al-Hammeh sequences for the terminal drying of Lake Lisan, Jordan. Palaeogeography, Palaeoclimatology, Palaeoecology 84, 163-173.

Manspeizer, W., 1985. The Dead Sea rift, Impact of climate and tectonism on Pleistocene and Holocene sedimentation. In, Biddle, K.T., Christie-Blick, N., (eds), Strike- slip Deformation, Basin Formation and Sedimentation, Society of Economic Paleontologists and Mineralogists Special Publication 37, 143-158.

Marco, S., Agnon, A., 1995. Prehistoric earthquake deformation near Masada, Dead-Sea graben. Geology 23, 695-698.

Marco, S., Stein, M., Agnon, A., Ron, H., 1996. Long-term earthquake clustering, a 50,000-year paleoseismic record in the Dead Sea Graben. Journal of Geophysical Research 101, 6179-6191.

Martrat, B., Grimalt, O.J., Lopez-Martinez, C., Cacho, M., Curtis, J.H., Hodell, D.A., 2004. Abrupt temperature changes in the western Mediterranean over the past 250,000 years. Science 306, 1762-1765.

Matmon, A., Crouvi, O., Enzel, Y., Bierman, P., Larsen, J., Porat, N., Amit, R., Caffee, M., 2003. Complex exposure histories of chert clasts in the Late Pleistocene shorelines of Lake Lisan, southern Israel. Earth Surface Process and Landforms 28, 493-506.

Matthew, D.J., Roberts, C.N., 2008. Interpreting lake isotope records of Holocene environmental change in the Eastern Mediterranean. Quaternary International 181 (1), 32-38.

McCullagh, P., 1985. Modern Concepts in Geomorphology. Oxford University Press, Oxford, 128 pp.

McKenzie, J.A., 1985. Carbon isotopes and productivity in the lacustrine and marine environment. In, Stumm, W., (ed) Chemical Processes in Lakes, Wiley, New York, 99-118.

McLaren, S.J., Gilbertson, D.D., Gratten, J.P., Hunt, C.O., Duller, G.A.T., Barker, G.A., 2004. Quaternary palaeogeomorphologic evolution of the Wadi Faynan area, southern Jordan. Palaeogeography, Palaeoclimatology, Palaeoecology 205, 131-154.

Migowski, C., Agnon, A., Bookman, R., Negendank, J.F.W., Stein, M., 2004 Recurrence pattern of Holocene earthquakes along the Dead Sea transform revealed by varve-counting and radiocarbon dating of lacustrine sediments. Earth and Planetary Science Letter 222, 301-314.

Migowski, C., Stein, M., Prasad, S., Negendank, J.F.W., Agnon, A., 2006. Holocene climate variability and cultural evolution in the Near East from the Dead Sea sedimentary record. Quaternary Research 66, 421-431.

Müller, G., Irion, G., Förstner, U., 1972. Formation and diagenesis of inorganic Ca-Mg carbonates in the lacustrine environment. Naturwissenschaften 59/4, 158-164.

Murray, A., Wintle, A., 2000. Luminescence dating of quartz using an improved single-aliquot regenerative-dose protocol. Radiation Measurements 32, 57-73.

Neev, D., Emery K.O., 1967. The Dead Sea, depositional processes and environments of evaporates. Geological Survey of Israel, Bulletin 41, 147 pp.

Neev, D., Emery, K.O., 1995. The Destruction of Sodom, Gomorrah, and Jericho. Oxford University Press, Oxford, 175 pp.

Neev, D., Hall, J.K., 1976. The Dead Sea Geophysical Survey. Final report No. 2., Geological Survey of Israel, Report MG/6/76, 21 pp.

Neev, D., Hall, J.K., 1977. Climatic fluctuations during the Holocene as reflected by the Dead Sea levels. In, Greer, D.C., (ed), Terminal Lakes, Proceedings from International Conference on Desertic Terminal Lakes, Ogden, Utah, 53-60.

Neev, D., Hall, J.K., 1979. Geophysical investigations in the Dead Sea. Sedimentary Geology 23, 209-238.

NGRIP dating group, 2008. IGBP PAGES/World Data Center for Palaeoclimatology Data Contribution Series # 2008-034 NOAA/NCDC Palaeoclimatology Program, Boulder CO, USA.

Niemi, T.M., 1997. Quaternary history of the lake and its environment. In, Niemi T.M., Ben-Avraham, Z., Gat, J., (eds.), The Dead Sea, the Lake and its Setting. Oxford Monographs on Geology and Geophysics, Oxford Univ. Press, Oxford, 36, 226-248.

Niemi, T.M., Ben-Avraham, Z., 1993. Neotectonics and Late Quaternary Palaeoclimate of the Dead Sea. Geological Society of America 25, 391 pp.

Nir, Y., 1967. Some observations on the morphology of the Dead Sea Wadis. Israel Journal of Earth Sciences 16, 97-103.

Phillips, F.M., Campbell, A.R., Kruger, C., Johnson, P., Roberts, R., Keyes, E., 1992. A reconstruction of the response of the water balance in western United States lake basins to climatic change, New Mexico. Water Resources Research Institute Report n. 269, (259) pp.

Picard, L., 1943. Structures and evolution of Palestine with comparative notes on neighboring countries. Jerusalem, Hebrew University, Department of Geology, Bulletin 4, 134 pp.

Powell, J., 1988. The Geology of the Karak Area. Amman, Natural Resource Authority, Bulletin 8, 172 pp.

Prasad, S., Voss, H., Negendank, J.F.W., Waldmann, N., Goldstein, S., Stein, M., 2004. Evidence from Lake Lisan of solar influence on decadal to centennial-scale climate variability during marine oxygen isotope stage 2. Geological Society of America 32, 581-584.

Quade, J., Cerling T.E., Bowman, J.R., 1989. Systematic variations in the carbon and oxygen isotopic composition of pedogenic carbonate along elevation transects in the southern Great Basin, United State: Geological Society of America Bulletin 101, 464-475.

Quennell, A.M., 1956. The structure and geomorphic evolution of the Dead Sea rift. Quarterly Journal 14, 1-24.

Quennell, A.M., 1958. The structures and geomorphic evolution of the Dead Sea rift, Journal of the Royal Geographical Society of London 14, 1-24.

Richard, A., Davis, J.R., 1985. Coastal Sedimentary Environments. 2nd ed. Springer, New York, 716 pp.

Robinson, S., Black, S., Sellwood, B.W., Valdes, P.J., 2006. A review of palaeoclimates and palaeoenvironments in the Levant and Eastern Mediterranean from 25,000 to 5000 years BP, setting the environmental background for the evolution of human civilisation. Quaternary Science Reviews 25, 1517-1541.

Rossignol-Strick, M., 1995. Sea-land correlation of pollen records in the Eastern Mediterranean for the glacial-interglacial transition, biostratigraphy versus radiometric time-scale. Quaternary Science Reviews 14, 893-915.

Rossignol-Strick, M., 1999. The Holocene climatic optimum and pollen records of sapropel 1 in the Eastern Mediterranean, 9000-6000 BP. Quaternary Science Reviews 18, 515-530.

Salameh, E., El-Naser, H., 1999. Does the actual drop in Dead Sea level reflect the development of water sources within its drainage basin? Acta Hydrochimica Hydrobiologica 27, 5-11.

Salameh, E., El-Naser, H., 2000. Changes in the Dead Sea level and their impacts on the surrounding groundwater bodies. Acta Hydrochimica Hydrobiologica 28, 24-33.

Salomons, W., Goudie, A., Mook, W.G., 1978. Isotopic composition of calcrete deposits from Europe, Africa and India. Earth Surface Processes 3, 43-57.

Schramm, A., 1997. Uranium series and ^{14}C dating of Lake Lisan (Paleo-Dead Sea) sediments, implication for ^{14}C time scale calibration and relation to global palaeoclimate. Ph.D. Thesis, Faculty of Mathematic and Natural Science, University of Göttingen, Germany, Göttingen, 115 pp.

Schramm, A., Stein, M., Goldstein, S.L., 2000. Calibration of the ^{14}C time scale to 50 kyr by ^{234}U–^{230}Th dating of sediments from Lake Lisan (the paleo-Dead Sea). Earth and Planetary Science Letters 175, 27-40.

Seiders, V.M., Briggs, R.P., Glover III, L., 1970. Geology of Isla Desecheo, Puerto Rico, with notes on the Great Southern Puerto Rico fault zone and Quaternary stillstands of the sea. U.S., Geological Survey Professional Paper 739, 22 pp.

Shanahan, T.M., 2000. Development of a ^{36}Cl chronology of glaciations in tropical east Africa. Master Thesis, The University of Arizona, 42 pp.

Sheinkman, V.S., 2002. Late Pleistocene invasion of Palaeo-Dead Sea into the lower Zin Valley, the Negev Highlands, Israel. EGU Stephan Mueller Special Publication Series 2, 113-122.

Sneh, A., 1982. Quaternary of the northwestern Arava. Israel Journal of Earth Sciences 31, 9-16.

Stein, M., 2000. The Late Pleistocene sediments and tectonics of the Dead Sea Basin. In, Professional field trip guide book, The First Stephan Mueller Conference of the European Geophysical Society, 41-85.

Stein, M., 2001. The sedimentary and geochemical record of Neogene-Quaternary water bodies in the Dead Sea basin-inferences for the regional palaeoclimatic history. Journal of Paleolimnology 26, 271-282.

Stein, M., Goldstein, S.L., Ron, H., Marko, S., 1992. Precise TIMS $^{230}Th/^{234}U$ ages and magnetostratigraphy of Lake Lisan sediments (paleo Dead Sea). EOS, Transactions American Geophysical Union 73, p.155.

Stein, M., Starinsky, A., Katz, A., Goldstein, L.S., Machlus, M., Schramm, A., 1997. Strontium isotopic, chemical, and sedimentological evidence for the evolution of Lake Lisan and Dead Sea. Geochimica Cosmochimica Acta 61 (18), 3975-3992.

Stein, M., Enzel, Y., Machlus, M., Goldstein, S., Marco, S., 1999. Chronology of low lake levels for Lake Lisan (paleo-Dead Sea, Israel). Terra. Nostra 99/10, 4th ELDP Workshop, Lund, 94-101.

Stephenson, W.J., Kirk, R., 2000. Development of shore platforms on Kaikoura Peninsula, South Island, New Zealand, part one, the role of waves. Geomorphology 32, 21-41.

Stuvier, M., 1970. Oxygen and carbon isotope ratios of freshwater carbonates as climatic indicators. Journal of Geophysical Research 75, 5247-5257.

Sunamura, T., 1992. Geomorphology of Rocky Coasts. Wiley, New York, 302 pp.

Svensson, A., Andersen, K.K., Bigler, M., Clausen, H.B., Dahl-Jensen, D., Davies, S.M., Johnsen, S.J., Muscheler, R., Parrenin, F., Rasmussen, S.O., Röthlisberger, R., Seierstad, I., Steffensen, J.P., Vinther, B.M., 2008. A 60,000 year Greenland stratigraphic ice core chronology. Climate of the Past 4, 47-57.

Talbot, M.R., 1990. A review of the paleohydrological interpretation of carbon and oxygen isotopic ratios in primary lacustrine carbonates. Chemical Geology 80, 261-279.

The Harza JRV Group, 1996. Red Sea-Dead Sea Canal Project, Draft Prefeasibility Report, Main Report. Jordan Rift Valley Steering Committee of the Trilateral Economic Committee.

Trenhaile, A.S., 2000. Modeling the development of wave-cut shore platforms. Marine Geology 166, 163-178.

Trenhaile, A.S., 2001a. Modeling the effect of weathering on the evolution and morphology of shore platforms. Journal of Coastal Research 17, 398-406.

Trenhaile, A.S., 2002. Rock coasts, with particular emphasis on shore platforms. Geomorphology 48, 7-22.

Trenhaile, A.S., Layzell, M.G.J., 1981. Shore platform morphology and the tidal duration factor. Transactions of the Institute of British Geographers 6, 82-102.

Tucker, M., 1989. Carbon isotopes and Precambrian-Cambrian boundary geology, South Australia, ocean basin formation, seawater chemistry and organic evolution. Terra Nova 1, 573-582.

Vidal, L., Schneider, R.R., Marchal, O., Bickert, T., Stocker, T.F., Wefer, G., 1999. Link between the North and South Atlantic during the Heinrich events of the last glacial period. Climate Dynamics 15 (12), 909-919.

Vogel, J.C., Waterbolk, H.T., 1972. Groningen radiocarbon dates-Geological samples Dead Sea series (Lisan). Radiocarbon 14, 46-47.

Waldmann, N., 2002. The Geology of the Samra Formation of the Dead Sea basin. MSc. Thesis, The Hebrew University of Jerusalem, Jerusalem, English abstract (in Hebrew).

Waldmann, N., Starinsky, A., Stein, M., 2007. Primary carbonates and Ca-chloride brines as monitors of a paleo-hydrological regime in the Dead Sea basin. Quaternary Science Reviews 26, 2219-2228.

Wilgus, C.K., Hastings, B.S., Posamentier, H., Wagoner, J. Van., Ross, C.A., Kendall, C.G.S.C., 1988. Sea-level changes, an integrated approach. Special Publication–Society of Economic Paleontologists and Mineralogists 42, 407 pp.

Wilkins, D.E., Currey, D.R., 1997. Timing and extent of Late Quaternary paleolakes in the Trans-Pecos closed basin, West Texas and South-Central New Mexico. Quaternary Research 47, 306-315.

Yechieli, Y., Magaritz, M., Levy, Y., Weber, U., Kafri, U., Woelfli, W., Bonani, G., 1993. Late Quaternary geological history of the Dead Sea area, Israel. Quaternary Research 39, 59-67.

Yechieli, Y., Wachs, D., Abelson, M., Crouvi, O., Shtivelman, V., Raz, E., Baer, G., 2002. Formation of sinkholes along the shore of the Dead Sea-summary of the first stage of investigation. In, Beck, B.F., (ed), Sinkholes and the Engineering and Environmental Impacts of Karst, Huntsville, Alabama, 184-194.

Yechieli, Y., Abelson, M., Bein, A., Shtivelman, V., Crouvi, O., Wachs, D., Baer, G., Calvo, R., Lyakhovsky, V., 2004. Formation of Sinkholes Along the Shore of the Dead Sea. Geological Survey of Israel, GSI/21/2004, 34 pp.

Zak, I., Freund, R., 1966. Recent strike-slip movements along the Dead Sea Rift. Israel Journal of Earth Science 15, 33-37.

Erklärung

Hiermit versichere ich, die vorliegende Dissertation ohne Hilfe Dritter nur mit den angegebene Quellen und Hilfsmitteln angefertigt zu haben. Alle Stellen, die aus Quellen entnommen wurden, sind als solche kenntlich gemacht. Diese Arbeit hat in gleicher oder ähnlicher Form noch keiner Prüfungsbehörde vorgelegen.

Darmstadt, den 13.12.2010

Shahrazad Abu Ghazleh

CURRICULUM VITAE

Personal data

Name: Shahrazad Abu Ghazleh

Place of Birth: Amman, Jordan

Nationality: Jordanian

Working experience

2008-2011 **Research assistant,** Department of Physical Geology and Global Cycles, Darmstadt University of Technology.

2002-2004 **Teacher,** International High School (Adni). Kuala Lumpur-Malaysia-Cambridge Curriculum.

1998-2000 **Teacher,** Secondary School, Jerash, Al-Ruwayshid, Jordan.

Academic education

1993 **Secondary school**, Kufurkhal, Jerash, Jordan

1994-1997 **Bachelor, Geography,** The University of Jordan, Amman.

1998-2000 **Master, Geography/Geomorphology,** The University of Jordan. Thesis title: "Geomorphological Changes in the Eastern Coast of the Dead Sea".

2004-2010 **PhD, Physical Geology and Global Cycles,** Institute for Applied Geosciences, Darmstadt University of Technology, Germany.

Appendix 1: List of Figures

Appendix 2: List of Tables

Appendix 3: Coordinates and altitudes of the studied samples

Sample	Altitude (m)	Northing	Easting	Analyses type
8	0	31° 08' 43.15509"	35° 33' 12.45494"	XRD, AAS
6	-19	31° 09' 00.31605"	35° 33' 21.45288"	XRD, AAS,
10	-30	31° 09' 01.00221"	35° 33' 20.30376"	XRD, AAS, $\delta^{13}C$, $\delta^{18}O$
14	-56	31° 08' 46.54750"	35° 32' 46.58124"	U/Th dating, XRD, AAS
13	-58	31° 08' 46.84878"	35° 32' 46.71225"	U/Th dating, XRD, AAS
2	-64	31° 09' 03.08803"	35° 33' 16.73866"	$\delta^{13}C$, $\delta^{18}O$
12	-66	31° 08' 47.38365"	35° 32' 46.89809"	U/Th dating, XRD, AAS
7	-76	31° 09' 03.06348"	35° 33' 15.03193"	XRD, AAS, $\delta^{13}C$, $\delta^{18}O$
9	-101	31° 09' 02.21970"	35° 33' 09.16708"	XRD, AAS
41	-103	31° 08' 44.35938"	35° 32' 40.98084"	$\delta^{13}C$, $\delta^{18}O$
11	-105	31° 08' 49.03424"	35° 32' 45.51726"	XRD, AAS, $\delta^{13}C$, $\delta^{18}O$
42	-109	31° 08' 49.07821"	35° 32' 45.51443"	XRD, AAS
30	-110	31° 08' 52.91106"	35° 32' 51.62504"	$\delta^{13}C$, $\delta^{18}O$
43	-116	30° 51' 40.37650"	35° 26' 02.41174"	XRD
44	-117	31° 08' 49.52693"	35° 32' 44.76056"	OSL dating, XRD, AAS, $\delta^{13}C$, $\delta^{18}O$
19	-119	31° 09' 32.37000"	35° 32' 30.86369"	$\delta^{13}C$, $\delta^{18}O$
15	-137	31° 09' 09.70328"	35° 32' 56.58441"	U/Th dating, XRD, AAS, $\delta^{13}C$, $\delta^{18}O$
34	-148	31° 09' 09.81322"	35° 32' 57.90075"	U/Th dating, XRD, AAS
16	-149	31° 09' 09.47531"	35° 32' 57.47531"	$\delta^{13}C$, $\delta^{18}O$
45	-150	31° 09' 09.47531"	35° 32' 38.45731"	XRD, AAS
30	-154	31° 09' 08.18131"	35° 32' 56.96841"	U/Th dating, XRD, AAS
5	-160	31° 09' 07.77574"	35° 32' 55.99328"	U/Th dating, XRD, AAS
4	-170	31° 08' 48.68091"	35° 32' 35.30859"	U/Th dating,
17	-175	31° 08' 48.49336"	35° 32' 33.89025"	XRD, AAS
35	-200	31° 10' 05.91515"	35° 32' 33.93513"	U/Th dating
20	-200	30° 50' 33.95108"	35° 23' 35.15325"	OSL dating
18	-264	31° 44' 05.66101"	35° 36' 11.41462"	XRD, AAS
3	-346	31° 10' 07.44543"	35° 32' 10.78392"	U/Th dating
1	-350	31° 44' 05.66101"	31° 44' 05.66101"	U/Th dating, XRD, AAS

Appendix 4: Surface area and water volume of the Dead Sea calculated from SRTM

Height (m)	Surface area (km^2)	Area difference (km^2)	Remaining water volume (km^3)	Volume difference (km^3)
-389	1081.97	0	166.71	0
-390	1028.86	53.11	165.68	1.03
-391	1016.23	12.63	164.65	1.03
-392	1003.83	12.40	163.64	1.01
-393	988.21	15.62	162.65	0.99
-394	951.96	36.25	161.67	0.98
-395	864.95	87.01	160.80	0.87
-396	840.24	24.71	159.95	0.85
-397	764.25	75.99	159.18	0.77
-398	739.40	24.85	158.43	0.75
-399	729.46	9.94	157.70	0.73
-400	717.05	12.41	156.98	0.72
-401	704.43	12.62	156.27	0.71
-402	696.78	7.65	155.57	0.70
-403	689.53	7.25	154.88	0.69
-404	682.96	6.57	154.19	0.69
-405	677.74	5.22	153.51	0.68
-406	673.18	4.56	152.84	0.67
-407	668.98	4.20	152.17	0.67
-408	664.87	4.11	151.50	0.67
-409	660.70	4.17	150.84	0.66
-410	655.97	4.73	150.18	0.66
-411	651.33	4.64	149.53	0.65
-412	646.38	4.95	148.88	0.65
-413	641.77	4.61	148.24	0.64
-414	636.71	5.06	147.59	0.65
-415	631.93	4.78	147.00	0.59

Appendix 5: Abbreviations

AAS: Atomic Absorption Spectrometry.

PDB: Pee Dee Belemnite is the standard established for ^{13}C and was based on a Cretaceous marine fossil called *Belemnitella americana.* It had an anomalously high ^{13}C:^{12}C ratio (0.0112372), and was established as a delta ^{13}C value of zero giving almost all other naturally-occurring samples negative delta values. http://www.uga.edu/sisbl/stable.html#calib).

BP: before present.

b.s.l: below sea level.

CIAT: International Centre for Tropical Agriculture.

C3 vegetation: plants that survive solely on C_3 fixation. They thrive in areas where temperature is moderate, CO_2 concentration is high (~ 200 ppm), and water is plentiful. The C_3 plants, originating during Mesozoic and Paleozoic eras, predate the C_4 plant and still represent ~ 85% of Earth's plant biomass (Raven and Edwards, 2001).

DGPS: Differential Global Positioning System.

DS: Dead Sea.

DSTF: Dead Sea Transform Fault.

GISP2: Greenland Ice Sheet Project 2.

GPS: Global Positioning System.

ka: 1000 years.

LGM: Last Glacial Maximum.

LGO: Leica Geo Office.

MDSC: Mediterranean-Dead Sea Channel.

MIS: Marine Isotope Stage.

NGRIP: North Greenland Ice Core Project.

ng/g: nanogram 1/1000,000,000.

µg/g: microgram 1/1000, 000.

pg/g: picogram 1/1000,000,000,000.

OSL: Optically stimulated luminescence dating relies on the optical properties of quartz and feldspar minerals found in sediments such as sand and silt in order to calculate the date that this sediment was last exposed to sunlight before it was buried by new layers of sediment. Under natural conditions quartz and feldspar absorb ionizing radiation

(Uranium, Thorium and Potassium) at a constant rate. The exposure of these deposits to sunlight releases the electrons and the radiation "clock" is reset to zero. The age is calculated based on the amount of radiation that was absorbed between the time of initial sediment burial and the subsequent exposure of this sediment to light under laboratory conditions. http://www.uga.edu/osl/applications.html.

RSDSC: Red Sea-Dead Sea Channel.

SRTM: Shuttle Radar Topography Mission.

U/Th: Uranium-Thorium dating is based on the detection by mass spectrometry of both parent ^{234}U and daughter ^{230}Th products of decay, through the emission of an alpha particle. The initial ratio of $^{230}Th/^{234}U$ at the time of sample formation must be known or calculated. By the time, ^{230}Th accumulates in the sample through radiometric decay. The sample age is calculated based on the difference between the initial ratio of $^{230}Th/^{234}U$ and the one in the sample being dated. http://www.geo.arizona.edu/Antevs/ecol438/uthdating.html.

WGS: World Geodetic System.